LOSS OF HETEROZYGOSITY OF THE H4833Y MUTATION ON *RYR1* GENE CAUSING MALIGNANT HYPERTHERMIA

A thesis presented in partial fulfilment of the requirements for the degree of Master of Science in Genetics at Massey University, Palmerston North.

Diana Balasubramanain

March 2010

ACKNOWLEDGEMENTS

I would first of all thank the almighty for always being my strength in times good and bad.

I would like to extend my sincere gratitude to my supervisor, Assoc. Prof. Kathryn Stowell for her guidance and support, her encouragement and reassurance throughout the one year that I spent at Massey. Thank you also, Kathryn, for your tremendous patience during my thesis writing.

I would forever be grateful to you for the opportunities you provided me with, in the one year that I've been here as well as for the future. I can only promise you I will never forget anything I learnt from you in the past year.

I would also like to thank everyone at the Twilite Zone for all their help and advice and the great times at the lab. You all made sure my stay in Palmerston North was a memorable one. Thank you Robyn for always lending an ear to my problems and for all your help.

I would especially like to thank Hilbert Grievink, whose observations my project was based on, for introducing me to the various techniques and for all the help and guidance in my first few weeks at the lab.

Finally and most importantly I would like to thank my mom and dad, and my brother, for always being there, for all the love and support. And for always backing me in whatever I wish to do in life. All the pampering though made it a bit harder for me to deal with the harsh realities of life on my own!

ABSTRACT

Malignant hyperthermia is a potentially fatal pharmacological disorder and is triggered by volatile anaesthetics in predisposed individuals. Mutations in the *RYR1* gene, encoding the skeletal muscle calcium receptor channel have been linked to MH susceptibility. Over 200 point mutations have been have been found to date in the *RYR1* gene linked to MHS worldwide.

EBV-immortalization is regularly used worldwide as an effective procedure for inducing long-term growth of human B lymphocytes. In the current study, it was observed that immortalized lymphocytes from MHS patients heterozygous for the missense mutation H4833Y when initially cultured expressed both wild type and mutant allele but after a few weeks of culture they seemed to lose the mutant allele. High resolution melting assays and hybridization probe assays showed the loss of heterozygosity and this was confirmed using DNA sequencing. Genotyping and haplotype analysis using three intragenic RFLPs and two $(CA)_n$ repeat microsatellite markers tightly linked to the *RYR1* gene showed a definite change in the haplotype, suggesting more widespread changes in the genome upon short-term culture of EBV-immortalized B-lymphocytes.

ABBREVIATIONS

4-C*m*C	4-Chloro-*m*-cresol
°C	Degree Celcius
6-FAM	6-Carboxyfluorescence
aCGH	Array comparative genomic hybridization
AM	Acetoxymethyl
ARVD2	Arrhythmogenic right ventricular dysplasia
ATP	Adenosine tri-phosphate
BSS	Balanced salt solution
bp	Basepairs
CaM	Calmodulin
CCD	Central core disease
CHCT	Caffeine halothane contracture test
CPVT	Catecholaminergic polymorphic ventricular tachycardia
DIC	Disseminated intravascular coagulation
DHPR	Dihydropyridine receptor
DMSO	Dimethylsulfoxide
DNA	Deoxyribonucleic acid
dNTPs	Dinucleotide triphosphates
dsDNA	Double-stranded DNA
ECC	Excitation-contraction coupling
EDTA	Ethylene diamine tetra-acetate
EMHG	European malignant hyperthermia group
ER	Endoplasmic reticulum
FCS	Fetal calf serum

FKBP	FK-506 binding proteins
FRET	Fluorescence resonance energy transfer
gDNA	Genomic DNA
HRM	High resolution melting
HybProbe	Hybridization probe (assay)
IVCT	*In vitro* contracture test
Kb	Kilobasepairs
LCL	Lymphoblasboid cell line
M	Molar (mol/L)
µM	Micromolar
MH	Malignant hyperthermia
MHE	Malignant hyperthermia equivocal
MHN	Malignant hyperthermia negative
MHS	Malignant hyperthermia susceptible
Min	Minute(s)
MmD	Multi-minicore disease
MQ	Milli-Q (deionized) water
mRNA	Messenger RNA
Mt	Mutant
nm	Nanomolar
NAMHG	North American malignant hyperthermia group
NTC	Non-template control
PSS	Porcine stress syndrome
RFLP	Restriction fragment length polymorphisms
RMH	Royal Melbourne hospital
RNA	Ribonucleic acids
RT	Room temperature

RyR	Ryanodine receptor protein
RYR1	Ryanodine receptor gene
RyR1	Ryanodine receptor type 1
RyR2	Ryanodine receptor type 2
RyR3	Ryanodine receptor type 3
Sec	Second(s)
SERCA	Sarco/endoplasmic reticulum Ca^{2+}-ATPase
SNP	Single nucleotide polymorphisms
SR	Sarcoplasmic reticulum
TAE	Tris-acetate-EDTA-buffer
Taq	*Thermus aquaticus*
Taq polymerase	*Thermus aquaticus* DNA polymerase
T_m	Melting temperature
T-tubule	Transverse tubule
Wt	Wildtype

LIST OF FIGURES

LIST OF TABLES

TABLE OF CONTENTS

1. INTRODUCTION

1.1 Malignant Hyperthermia

Malignant hyperthermia (MH) is an autosomal, dominantly inherited, potentially fatal pharmacogenetic disorder of skeletal muscle. It is triggered by volatile or inhalational anaesthetics like halothane and depolarizing muscle relaxants like succinylcholine (reviewed in [1], [2, 3]. In rare cases an MH reaction can also be triggered by exercise and/or excessive heat in some susceptible individuals [4], [5].

MH is a heterogeneous disorder and exhibits both allelic and locus heterogeneity. Over 200 different mutations have been reported in the *RYR1* gene and mutations in other genes have been reported to be linked to MH [6].

The incidence of MH worldwide is about 1 in 15,000 in children undergoing anaesthesia and 1 in 50,000 anaesthetics in adults [7]. Some researchers have suggested that the actual incidence of mutations causing MH could be as high as 1 in 2000 individuals in certain regions [8, 9]. The incidence of MH in the lower North Island of NZ is much higher than the worldwide average due to the presence of a large MH susceptible Maori pedigree [10]. The Palmerston North Hospital, which is the only National Testing Centre for malignant hyperthermia in New Zealand, encounters potential MHS individuals at a rate of ~1:120 general anaesthetics (Neil Pollock, personal communication).

Apart from humans MH has also been reported in other species such as swine, horses and dogs [11], [12]. MH in swine has been extensively studied and shows autosomal recessive inheritance. It can also be triggered by stress and is known as porcine stress syndrome (PSS) [3].

1.1.1 History

Malignant hyperthermia was first described in 1960 by Dr. Michael Denborough, a physician at the Royal Melbourne Hospital (RMH), Melbourne, Australia. A 21-year old student in Melbourne was admitted to the RMH in April, 1960 with multiple fractures and his family expressed reservations about him being administered general anaesthesia as some of his relatives had died when they were administered general anaesthetics for minor surgical procedures. On being administered anaesthesia the patient began showing the classical symptoms of what is now known as malignant hyperthermia. He survived, however, and was the first recorded patient to survive an MH reaction [13-15]. Denborough and his colleagues at the RMH also determined the autosomal dominant inheritance of the condition [16].

The first case of MH in New Zealand was noted in 1968 when a 20-year-old male died during an operation to his jaw at Palmerston North Hospital. He was subsequently found to be a member of a very large susceptible family based in the Manawatu-Horowhenua region of the lower North Island (www.midcentraldhb.govt.nz).

1.1.2 Clinical symptoms

An MH reaction can occur either during anaesthesia or during the post-operative period. Early symptoms include tachycardia, a rise in end-expiratory CO_2 concentration, and muscle rigidity (reviewed in [2]).

Further symptoms including an increase in blood pressure, hyperventilation, cyanosis, increasing arterial carbon dioxide tension, lactic acidosis and fever have also been observed [17]. The rise in body temperature (hyperthermia) develops slowly but can be dramatic and is considered as a confirmatory sign of an MH reaction (reviewed in [2]). In a fulminant crisis the rate of rise in body temperature is ~1°C / 5 min. Hyperthermia leads to increased consumption of oxygen and production of CO_2, multiple organ dysfunction and disseminated intravascular coagulation (DIC) [18].

Other life-threatening complications involving various organ systems may arise including pulmonary edema, renal failure due to myoglobinuria, congestive heart

failure, bowel ischemia and cerebral edema [19]. If left untreated death can occur due to ventricular fibrillation within minutes or pulmonary edema within hours. Once the temperature rises to over 40°C DIC is the most usual cause of death. During the post-operative period death can also occur due to neurological damage or renal failure (reviewed in [17]).

1.1.3 Treatment

The first step in therapy is to stop the administration of the triggering inhalational anaesthetic immediately. Ventilation with 100% oxygen at a flow rate of 10 $Lmin^{-1}$ should be started immediately. Dantrolene at a starting dose of 2.5 mg kg^{-1} body weight must be administered and the dosage can be increased to about 10 mg kg^{-1} body weight until the hypermetabolism has been overcome completely. It can be administered at 1 mg/kg body weight every 4–8 hours for about 24–48 hours (reviewed in [2]).

Dantrolene, being a hydantoin derivative, is highly lipophilic and thus poorly soluble in water. For clinical use it is available as an intravenous preparation in vials containing 20 mg lyophilized dantrolene sodium with 3 g mannitol to improve water solubility. The rise in the body temperature can also be controlled by surface cooling using ice-packs and cold infusions or lavages with ice-cold water.

1.1.3.1 Dantrolene

Dantrolene sodium is a muscle relaxant and is the only clinically available agent for treatment of an MH reaction. It acts primarily by affecting calcium release across the sarcoplasmic reticulum of skeletal muscle. Since its introduction in 1979 as a treatment for MH reactions it has led to a dramatic decrease in the mortality of MH from about 80% to less than 10% (reviewed in [20]).

Dantrolene inhibits release of Ca^{2+} from the sarcoplasmic reticulum without affecting its re-uptake. It also helps to reduce the resting intracellular Ca^{2+} concentration, thus aiding muscle relaxation (reviewed in [21]). Although it can block skeletal muscle contraction by about 75%, no similar effects of therapeutic amounts of dantrolene have been noted on cardiac or smooth muscle contractility [22].

Several studies have established at least two different binding sites for dantrolene in the skeletal muscle SR membranes [23], [24]. More recently, Paul-Pletzer (2002) identified the binding site of dantrolene in the the RyR1 protein between aminoacids Leu^{590} and Cys^{609}, which is the region of the RyR1 domain peptide 1 (DP1) [25]. DP1, along with DP4, has been reported to be involved in both activation of the calcium release channel and its hypersensitization to agonists [26].

1.1.4 Molecular genetics

1.1.4.1 Introduction

The *RYR1* gene was mapped and cloned in 1990 and contains 106 exons spanning about 158 kb and is one of the most complex genes characterized. It encodes a ~15.3 kb mRNA [27].

Genetic linkage studies have mapped the first susceptibility locus of MH to chromosome 19q13.1-13.2, which is the position of the gene encoding the skeletal muscle ryanodine receptor *RYR1* [7, 28]. This locus was designated MHS1 and more than 200 mutations have been identified in the *RYR1* gene thus far (reviewed in [1]).

1.1.4.2 Mutations

The majority of mutations thus far detected in the *RYR1* gene are missense mutations, with approximately 40% occurring in C_pG dinucleotide sequences (reviewed in [3]). Also, almost all of the mutations occur in the heterozygous state with homozygotes being reported very rarely [29]. The majority of mutations appear to be clustered between exons 2 and 17 encoding amino acid residues from 35 and 614 (MH/CCD region 1) and between exons 39 and 46 encoding amino acid residues from 2163 to 2458 (MH/CCD region 2) [30]. A third region in the 3' end of the gene (between exons 90 and 106) encoding amino acid residues from 4668 to 4906 has been reported more recently [10] (Figure 1).

It is of note that due to the large size of the *RYR1* gene, mutation screening has been performed over the years only in the regions where most of the mutations were known to be clustered thus limiting the identification of additional regions on the *RYR1* gene where novel mutations might exist. There have been a few studies

involving Complete sequence analysis of the *RYR1* gene in MHS individuals and these have reported increased mutation detection rates [8], [31, 32]. Galli (2002) analysed the entire coding region of RYR1 in 50 Italian MHS patients and found 31 mutations (16 novel mutations) with a mutation detection rate of 86% [33].

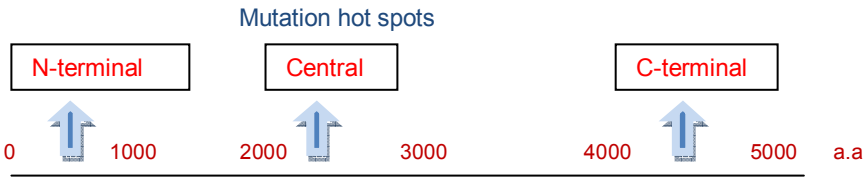

Figure 1. The mutational hot spot regions on the RyR1 protein

Linear representation of the RyR1 protein of ~5000 aminoacids showing the three mutation hotspot regions at the N-terminal, C-terminal and central regions of the protein

1.1.4.3 Other loci associated with MH

Linkage analyses have established up to six different loci to be linked to MH and two different genes with causative mutations have been identified. Extensive mutation screening in different populations across the globe has established that mutations in the *RYR1* gene account for about 50% of the cases of MH. Another gene identified to be linked to MH is the *CACNA1S* (or *CACNL1A3*) gene, encoding the alpha-1 subunit of the dihydropyridine receptor (DHPR) and is located on chromosome 1_q32 [34]. Carpenter et al. (2002) studied the *CACNAIS* gene in 50 MH patients and identified novel variant (Arg174Trp), potentially influencing MH susceptibility [35].

1.1.5 Pathophysiology of MH

1.1.5.1 Calcium homeostasis

The basic physiological consequence of MH is disruption of intracellular skeletal muscle calcium homeostasis. The intracellular calcium ion concentration $(Ca^{2+})_i$ is tightly regulated and plays a major role in normal physiology of higher organisms. In its soluble form Ca^{2+} plays important roles in various cellular processes like energy metabolism and muscle contraction. It acts as a membrane stabilizer, cofactor for proteins and diffusible intracellular carrier [36]. The total Ca^{2+} concentration in blood ranges from 1.6-2 mM. Almost 50% of the extracellular calcium is bound to proteins. Ca^{2+} is transported across the plasma membrane into cells through various calcium channels which can be receptor-mediated, voltage-gated or store-operated channels. Ca^{2+} can also enter the cells through the sodium-calcium exchanger pumps located on the plasma membrane [37]. Within cells intracellular calcium binding proteins like calmodulin act as Ca^{2+} receptors. Other proteins like calsequestrin (CSQ), present in the lumen of the SR, help in intracellular storage of calcium [38]. The largest intracellular store of Ca^{2+} is the endoplasmic reticulum (ER), especially the skeletal muscle sarcoplasmic reticulum (the ER of the muscle cell) (reviewed in [39]). The sarcoplasmic reticulum (SR) is thus a major regulator of Ca^{2+} concentrations [12]. The sarco-endoplasmic reticulum Ca^{2+}-ATPase pumps (SERCAs) play a vital role in transporting Ca^{2+} from the cytosol into the SR thus increasing the levels of Ca^{2+} within the SR. SERCA pumps act in two different ways in calcium homeostasis. They lower the cytosolic Ca^{2+} levels hence leading to muscle relaxation and replenish SR Ca2+ stores, which are necessary for muscle contraction [40]. The release of calcium from the SR is regulated predominantly by two adjacent calcium channels: the L-type voltage-gated channel DHPR in the membrane of the T-tubule and the calcium release channel, RyR1, located at the terminal cisternae of the SR (Figure 2) [12, 41].

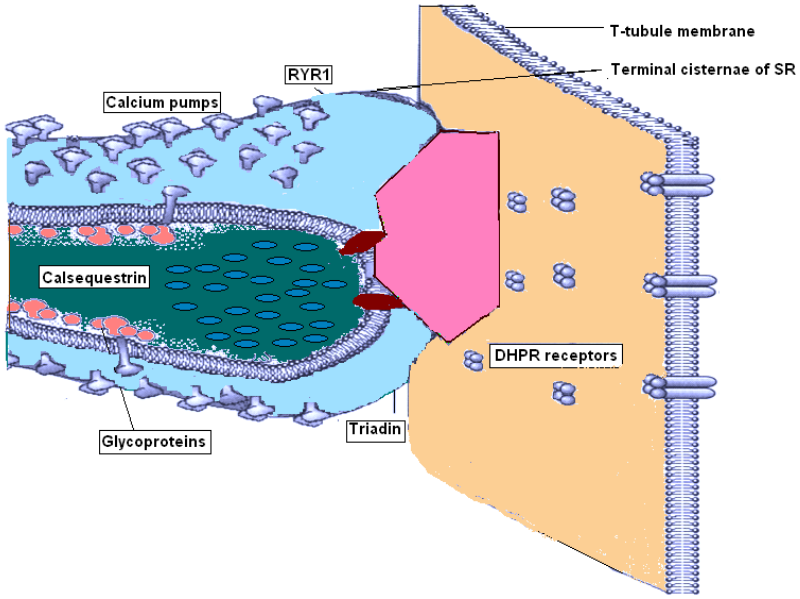

Figure 2. Arrangement of the RyR1, DHPR and associated proteins involved in SR calcium release

The terminal cisternae of the SR and the adjacent T-tubule membrane showing the RyR1 as a polygonal structure at the junction between the terminal cisternae and the T-tubule membrane. DHPRs are shown as tetrad complexes on the T-tubule membrane. Calsequestrins are shown as elongated (deep blue) structures within the SR lumen. Glycoproteins (pink globular structures) and triadin (red oblique) are seen attached to the membrane of the terminal cisternae (Figure adapted from [12]).

1.1.5.2 Excitation-Contraction coupling

Excitation contraction coupling (E-C coupling) is a term coined by Sandow in 1952 to describe the mechanism by which an electrical stimulus is converted into a mechanical response. Sandow observed that when a muscle is electrically stimulated the first response is excitation, set up in the membrane of the muscle fibres and is followed by contraction of the muscle fibres [42].

In skeletal muscles the ECC involves close interactions between the RyR1 located on the terminal cisternae of the SR and the alpha-1 subunit of the DHPRs (Figure 3) [41].

Once there is an electrical stimulus or depolarization of the sarcolemma, the action potential generated travels through the T-tubule membrane. The voltage-gated DHPRs are located on the T-tubule and have voltage sensors that can sense the depolarization and lead to conformational changes of the DHPR which in turn result

in activation of RyR1 and a subsequent release of SR calcium (orthograde coupling) [43], [44]. RyRs also enhance the capability of DHPRs to function properly as Ca^{2+} channels (retrograde coupling) [45].

The calcium released from the RyR1 channel leads to a rapid rise in the cytoplasmic levels of Ca2+, which binds to the Ca2+ binding protein troponin C, a subunit of the troponin complex, present in the thin filament of striated muscles [46]. This results in the formation of cross bridges between actin and myosin filaments and shortening of the sarcomere, which results in muscle contraction (reviewed in [47]).

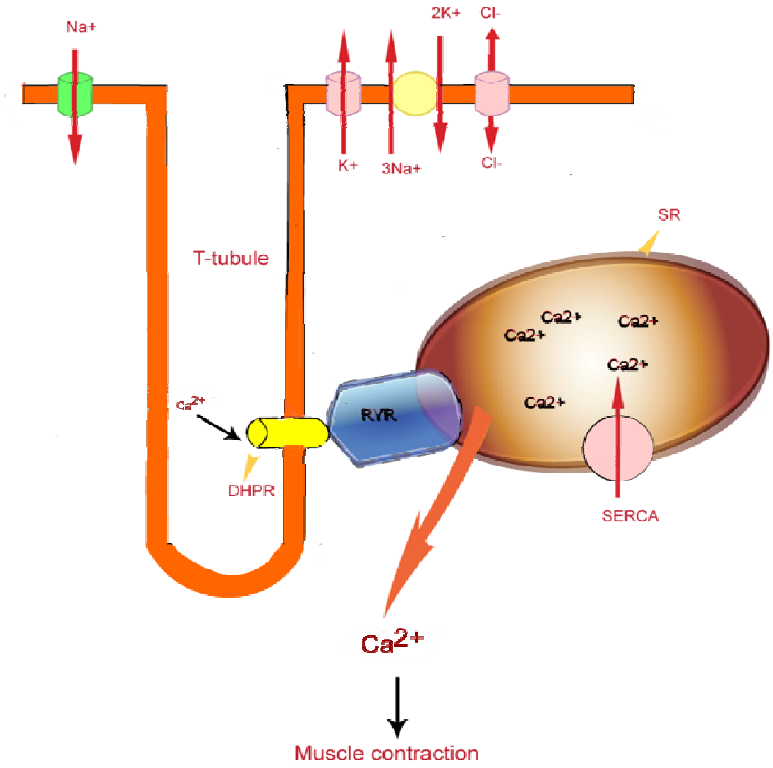

Figure 3. E-C coupling of the skeletal muscle

An action potential generated by the excited muscle fibre spreads down the T-tubule membrane. The voltage-gated DHPR senses the membrane depolarization and alters its conformation activating the adjacent RyR1 which in turn releases Ca^{2+} from the SR. Increased Ca^{2+} in the cytosol leads to muscle contraction (Figure adapted from [44]).

1.1.6 Diagnostic Testing

1.1.6.1 In Vitro Contracture Testing

The *in vitro* contracture test (IVCT), based on the contracture of muscle fibres in the presence of halothane or caffeine, is currently accepted as the 'gold standard' for the diagnosis of MH. There are two forms of the IVCT used worldwide: the Caffeine Halothane Contracture Test (CHCT) developed by the North American Malignant Hyperthermia (MH) Group (NAMHG) and the *In Vitro* Contracture Test (IVCT) developed by the European MH Group (EMHG) [48, 49].

For the IVCT a skeletal muscle specimen from the *quadriceps femoris* muscle is surgically removed and split into bundles of fibres and spread between two electrodes. The samples are stimulated electrically and viable muscle preparations (twitch response ≥10 mN) are used for the test. After equilibration, halothane is introduced in increasing concentrations using a vaporizer. On a separate muscle sample caffeine is introduced similarly in increasing concentrations. Pathological contracture of muscles after administration of the two agents leads to diagnosis of MH susceptibility. Absence of contracture leads to diagnosis of MHN [21],[50].

The two protocols mentioned above were developed independently and thus differ slightly in the test procedure and significantly in the interpretation of the results. In the protocol developed by NAMHG the person tested is considered MH Susceptible (MH+) if the muscle strips show a positive response when exposed to either halothane or caffeine and MH negative (MH-) when the response to both caffeine and halothane is negative. On the other hand, the protocol developed by the EMHG requires a positive response with both caffeine and halothane for the individual to be considered as MH susceptible (MHS). If the muscle strips show a positive response with either halothane or caffeine then the individual is considered to be MH equivocal or (MHE) and the individual is considered MHN when a negative response with both halothane and caffeine is seen [19]. In practice, however, all individuals classified as either MHE or MHS by the IVCT are considered to be clinically susceptible to MH.

1.1.6.2 Limitations of IVCT

IVCT is expensive, invasive as it requires a large muscle biopsy, time-consuming as well as labour-intensive. It requires a surgical procedure and is thus confined to certain medical centres (reviewed [2]). Also the invasive nature of the test means that only about 10% of the people showing a response indicative of an MH-reaction during anaesthesia, choose to undergo the IVCT [51].

1.1.6.3 Functional assays

A number of functional assays have been developed and used successfully to study the effect of the mutations in the *RYR1* gene on calcium release from the SR/ER. *RYR1* has been expressed in a number of heterologous non-muscle expression systems like COS-7 and HEK293 cells by transfecting them with mutant cDNA [52, 53]. Immortalized B-lymphocytes isolated from MHS individuals have also been used for functional assays [54, 55]. Myotubes isolated from the muscle biopsy tissue have also been used to assess the role of *RYR1* mutations in calcium release [56]. Yang et al. (2003) used 1B5 skeletal myotubes to functionally characterize six different *RYR1* mutations [57]. These myotubes express triadic proteins, such as triadin, calsequestrin, the FK-506 binding protein-12 (FKBP-12), sarcoplasmic reticulum Ca^{2+}-ATPase1, and alpha1s-DHPR, but do not constitutively express any RyR protein isoform. Calcium release has been monitored in these assays by using fluorescent indicators like Fura-2 and Fura-4, [^{3}H] ryanodine binding assays and also indirectly by proton release [58].

1.1.6.4 Genetic testing

Genetic analysis offers a safe and reliable alternative to the IVCT. It is relatively non-invasive as it only requires a blood sample. DNA testing was first suggested in 1990 by McCarthy et al. after linkage studies suggested that the *RYR1* gene was a likely candidate gene for MHS in humans [28]. Since then over 200 mutations have been identified within the *RyR1* gene which have been associated with MH susceptibility [2]. MH is a heterogeneous disorder, however, with at least six different susceptible loci identified, thus limiting the use of DNA-based diagnosis to genetically characterize many families. Because of heterogeneity DNA analysis

can only diagnose MHS cases and not MHN [59]. Also, discordance between genotype and phenotype has been reported [6, 10, 60, 61].

1.2 Ryanodine receptors

Ryanodine receptors are homotetrameric proteins that act as calcium release channels and regulate the release of calcium from the intracellular stores in the endo/sarcoplasmic reticulum [62].

Molecular cloning studies have defined three different RyR isoforms, namely, RyR1, RyR2 and RyR3, in fish, amphibians, birds, and mammals [63-65] Although the three isoforms are identical in about 65% of the aminoacids, three regions of diversity have been identified (Figure 4) and these are designated as D1, D2 and D3 [66].

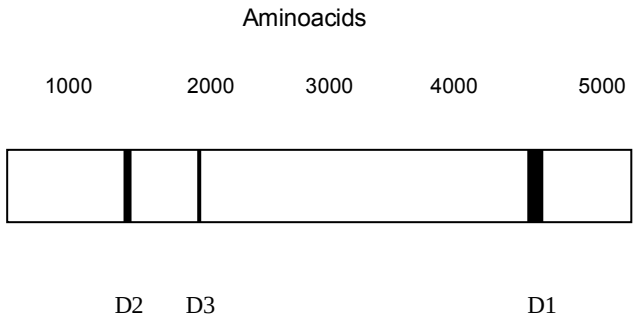

Figure 4. Regions of divergence between RyR1 and RyR2

The three regions of divergence between the three RYRs are depicted as D1, D2 and D3 (figure adapted from [67].

The three isoforms are present in different tissues. While RyR1 is found predominantly in the skeletal muscle and in lower levels in B-lymphocytes and the Purkinje cells of cerebellum [55]. RyR2 is present in cardiac muscles [68] and RyR3 is found in low levels in various tissues like the brain, diaphragm and smooth muscles in non-mammalian vertebrates [69], [70].

A number of mutations in the *RYR1* gene have been linked to cases of MH and central core disease and multi-minicore disease. Mutations in the cardiac ryanodine receptor (RyR2) have been linked to catecholaminergic polymorphic ventricular tachycardia (CPVT) and arrhythmogenic right ventricular dysplasia (ARVD2) [67].

In both RyR1 and RyR2 isoforms the mutations identified thus far cluster in the three hotspot regions mentioned in section 1.1.4.2.

1.2.1 RyR1

The ryanodine receptor that acts as the skeletal muscle calcium release channel is a tetrameric protein with a mass of about ~2,250 kDa and is one of the largest known proteins (reviewed in [3]). Each monomer consists of a N-terminal region forming the cytoplasmic 'foot' region and the C-terminal region forming the transmembrane channel [71]. The protein is situated at the interface between the sarcoplasmic reticulum and the cytosolic T-tubule. The protein consists of two main domains, the larger cytosolic domain and the smaller transmembrane assembly (Figure 5). It is the cytosolic part of RyR1 that contains binding sites for a number of activating ligands like calmodulin, calcium (μM), ATP, caffeine and ryanodine (nM) and inactivating agents like ryanodine (>100 μM) and calcium (>100 μM) (reviewed in [72]). Release of calcium from the sarcoplasmic reticulum into the cytosol is regulated through the calcium release channel in conjunction with the adjacent DHPR (situated at the T-tubule membrane).

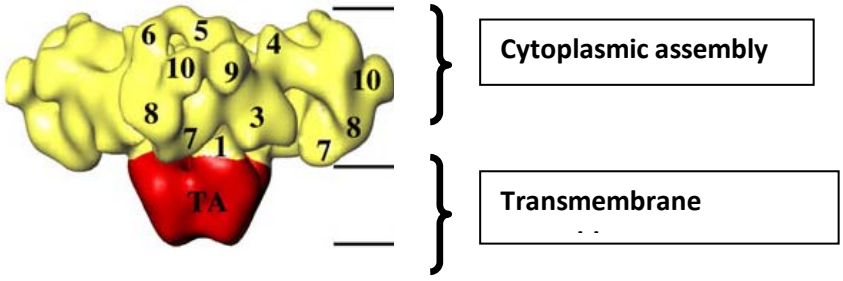

Figure 5. Side view of the surface representation of the RyR1 protein

Proposed three-dimensional structure of the RyR1 showing a side view. The cytoplasmic domain is shown in yellow and the transmembrane assembly (TA) is shown in red. The different RyR1 domains are numbered 1-10 (Figure adapted from [73]).

Three-dimensional models of all the three isoforms have been proposed (Figure 6) but X-ray crystallographic structures of the proteins have not been obtained thus far. This is because of the complex nature of the RYR proteins coupled with the fact

that they are integral membrane proteins which generally tend to be difficult to analyze by X-ray crystallography. Cryo-electron microscopy has been used to create 3D models of proteins with moderate resolutions of about 30-40 Å [74-76]. Ludtke et al. (2005) used single particle cryo-electron microscopy to resolve the 3D structure of RyR1 in a closed conformation at a resolution of 9.6 Å [77].

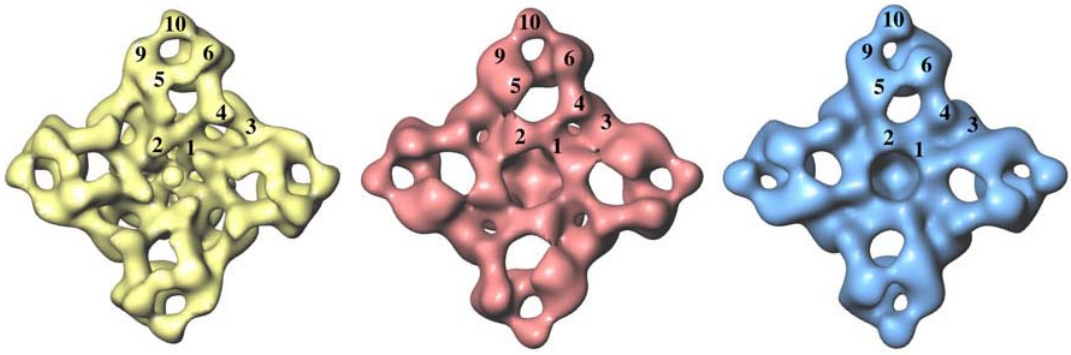

Figure 6. Solid body representations of the three isoforms of the ryanodine receptor

The three receptors, RyR1 (yellow), RyR2 (red), RyR3 (blue), are shown as viewed from the cytoplasmic face. The domains are numbered (1-10) in one quarter of the tetramer molecule (Figure adapted from[73]).

1.2.2 RyR modulators

1.2.2.1 Endogenous modulators

Ca^{2+} has major importance in the regulation of the RyR, because other ligands seem to require Ca^{2+} for maximum effect [78]. RyR1 is activated by Ca^{2+} at micromolar concentrations and inhibited at millimolar concentrations [79]. It has been suggested that the RyR contains a high-affinity Ca^{2+} binding site, which stimulates Ca^{2+} release [80] and a low-affinity Ca^{2+} binding site, which inhibits Ca^{2+} release [81].

Mg^{2+} is a potent inhibitor of RyRs. In skeletal muscle, Mg^{2+} exerts its inhibitory effect by two different mechanisms. Mg^{2+} competes with Ca^{2+} for binding at the high affinity binding site and can displace calcium preventing channel opening. It can also bind to a low affinity Ca^{2+} /Mg^{2+} inhibitory site [82, 83].

Adenine nucleotides have been reported to activate the RyRs. Several calcium release studies performed on skeletal muscle have reported increased Ca^{2+} release in the presence of adenine nucleotides, even at nanomolar Ca^{2+} concentration and/or in the presence of Mg^{2+} [84]. Ca^{2+} (μM) and adenine nuceotides (mM) have been shown to elicit persistent channel opening [84, 85] indicating that the presence of both ATP and Ca^{2+} are required for maximal opening of the channel.

Various studies have shown that palmitoyl carnitine and other long-chain acyl carnitines induce calcium release from the SR. Palmitoyl carnitine has been shown to stimulate ^{3}[H]ryanodine binding and activity of the SR calcium release channel in mammals [86] and in birds [87].

1.2.2.2 Modulation by associated proteins

Calmodulin is a cytosolic protein of about 16.7 kDa and is an important RyR modulatory protein [88]. Calmodulin exists in cells in its Ca2+-bound form (CaCaM) or Ca^{2+}-free form (apoCaM) and both forms have been reported to have a single binding site for each RyR subunit. The effect of CaM on RyRs depends upon the free Ca^{2+} concentrations. While it inhibits the channel at free [Ca^{2+}]>1 μM, it has a stimulatory effect at lower Ca^{2+} (nanomolar) concentrations [89].

Calsequestrin (CSQ) is the major Ca^{2+} binding glycoprotein present in the lumen of the SR with a molecular weight of about 42 kD [90, 91]. It is highly acidic and has high capacity for the divalent Ca^{2+} ion and is believed to be responsible for increased Ca^{2+} levels within the SR [92]. A number of studies using electron microscopy have reported that calsequestrin constitutes most of the contents of the terminal cisternae of the SR [93], [94]. CSQs regulate the RyR through the integral membrane proteins triadin and junctin. Two regions at the N-terminus of CSQ have been reported to form the binding site for triadin and junctin proteins [95]. Triadin and junctin are present on the SR membranes and can bind to both RyR and CSQ. CSQs also undergo conformational changes upon Ca^{2+} binding. It has been suggested that modulation of RyR activity by CSQ is regulated by luminal Ca^{2+} concentrations [96].

FK-506 binding proteins (FKBPs) are also associated with the RyRs. Two FKBPs, namely, FKBP12 and FKBP12.6, have been identified which are associated with RyR1 and RyR2, respectively. The FKBPs bind to RyRs stoichiometrically, a molecule binding to each monomer of the RyR [97]. FKBPs stabilize the RyR (calcium channel) in its closed state by stabilizing subunit interactions and decreasing the open pore probability of the channel [98].

Dihydropyridine receptors (DHPRs) are L-type voltage gated calcium channels located on the membrane of the T-tubule. They play a major role in the SR calcium release and interact closely with the RyR1 channel in the E-C coupling mechanism. DHPR is a heterotetramer encoded by four different genes. The α1-subunit is encoded by the CACNA1S (CACNL1A3) gene which maps to chromosome 1q31-32 [99]. The β-subunit is encoded by the CACNLB1 gene and the γ-subunit by the CACNLG gene and both map to chromosome 17q11.2-q24 [100, 101] and the α2/δ-subunit is encoded by the CACNL2A which maps to chromosome 7q21-22 [102]. Of the four subunits mutations have been reported and linked to MHS in the α1-subunit only [34, 103]. Genes encoding the other subunits of DHPR have not yet been linked to MHS.

The α1-subunit contains 4 homologous internal loops (DHPR I-IV) each consisting of 6 transmembrane segments and plays a major role in E-C coupling mechanism. Studies involving expression of chimeras of cardiac and skeletal muscle DHPR in dysgenic myotubes, which lack a functional gene for the skeletal muscle DHPR α1S subunit [104], have established the II-III loop of the skeletal and cardiac muscle DHPR α1 subunits plays a critical role in E-C coupling mechanism [105]. Lu et al. (1994) provided evidence for a direct functional interaction of the cytoplasmic II-III loop of the DHPR α1 subunit with the SR Ca^{2+} release channel [106]. El-Hayek (1995) identified different regions within the II-III loop which interact with the RyR [107]. Similar studies involving expression of chimeras of RyR1 (skeletal) and RyR2 (cardiac) using dyspedic (lacking functional RyR1) myotubes showed a region in the cytoplasmic domain of RyR1 that interacts with DHPR and plays a role in skeletal muscle EC-coupling [108].

1.3 Associated myopathies

1.3.1 CCD

CCD is a congenital human myopathy first described in 1956 [109] and like MH is usually inherited in an autosomal dominant fashion, although autosomal recessive cases have also been reported [110, 111]. CCD is characterized by the presence of amorphous areas, known as cores, in type 1 skeletal muscle fibres that run along the whole length of the muscle fibre (Figure 7). The amorphous areas are well-demarcated and mostly located centrally in the muscle fibres and typically lack mitochondria and oxidative enzyme activity.

The clinical features associated with CCD are quite variable and usually non-progressive [112]. Most patients show hypotonia and proximal muscle weakness during infancy and motor developmental delay in childhood. In addition, congenital hip dislocation, kyphoscoliosis and joint contractures are also commonly seen in CCD patients [113]. In more severe forms fetal akinesia syndrome has been reported [114].

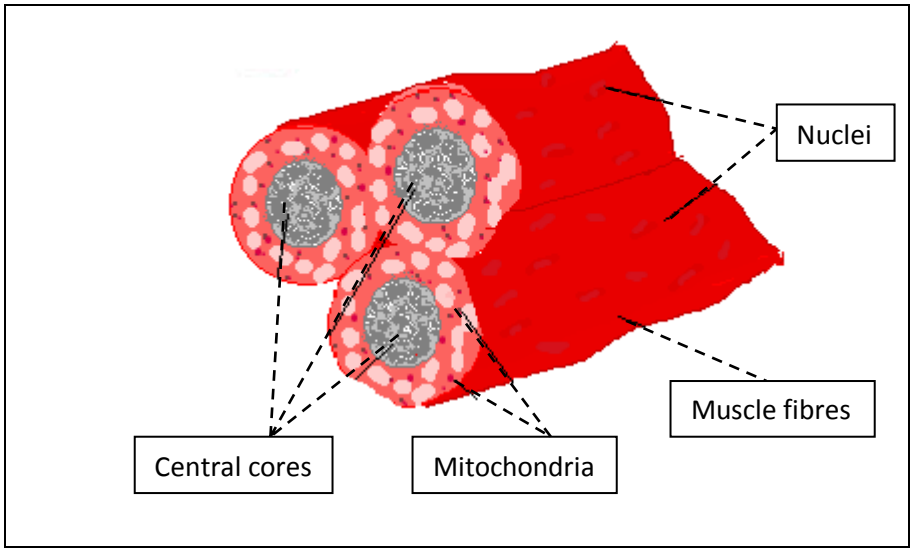

Figure 7. Central cores within the muscle fibre

A cross-section of the muscle fibres showing metabolically inactive cores (grey) at the centre. Normal Mitochondria (peach) are seen in remainder of the muscle fibre.

A number of studies have linked CCD to mutations in the *RYR1* gene which is also linked to MH and thus considered an allelic disease of MH [115]. A number of mutations causing MH are also responsible for the CCD phenotype, although there

are mutations that are linked to either MH-only or CCD-only phenotypes as well. Most of the CCD mutations are clustered in the 3' end of the *RYR1* gene encoding the C-terminal region of protein comprising the transmembrane pore forming domain [30, 116].

The functional effects of mutations on the *RYR1* gene linked to CCD have been explained by two hypotheses. The first is the "leaky channel hypothesis" according to which the mutations causing CCD result in a leaky calcium release channel, thus, leading to depleted SR Ca^{2+} stores which accounts for the muscle weakness observed. The second is the 'E-C uncoupling hypothesis' which suggests that the muscle weakness observed in CCD is a result of a defective E-C coupling mechanism [117].

1.3.2 Multi-mini core disease

Multi-mini core disease (MmD) is an early onset congenital myopathy first described by Engel et al. in 1971 [118]. MmD shows autosomal recessive inheritance and is characterized by the presence of multiple cores of short length, lacking mitochondria and oxidative enzyme activity, in both type 1 and 2 muscle fibres. It is divided into four subgroups based on the clinical features. MmD is a heterogeneous condition and linked to mutations in the *RYR1* gene as well as the selenoprotein N gene (*SEPN1*) located on chromosome 1_p36 [119].

1.4 RESEARCH QUESTION AND OBJECTIVE

1.4.1 Background

It was observed during the course of studies involving immortalized lymphocytes obtained from MHS patients carrying the mutation C14997T (causing the aminoacid substitution H4833Y), that when initially cultured the lymphocytes expressed both wild type and mutant alleles but after several weeks in culture they appeared to lose the mutant allele. Allele specific PCR using cDNA showed loss of expression and high resolution amplicon melting assays using gDNA showed that the loss occurred at the genomic level as well [120].

1.4.2 Research objective

The present work explored the reproducibility of the observed phenomenon as well as its cell-line and mutation specificity.

Different cell lines were used to study two mutations, C7354T and C14477T, leading to amino acid substitutions R2452W and T4826I, respectively, as well as the C14997T mutation leading to the H4833Y substitution.

In a separate and unrelated research objective an attempt was made to functionally analyse two uncharacterized *RYR1* mutations associated with CCD.

1.4.3 Significance

Immortalized B-lymphocytes are cultured worldwide and are used for various functional assays and biomarker studies. Immortalized lymphoblastoid-like lymphocytes (LCLs) are generally considered to be stable during culture and subsequent freeze-thaw involved in maintaining lymphocytes over long periods for repeated assays. The observation that changes occur in the genotype of the cell lines during culture (9-11 weeks) could have enormous implications on the use of immortalized lymphocytes for research worldwide.

2. MATERIALS AND METHODS

2.1 Materials

Only specialized reagents and kits used in this study are listed below. All general laboratory chemicals were of analytical grade.

- Oligonucleotides were purchased from Sigma-Aldrich, Castle Hill,NSW , Australia.

- Opti-MEM® I and penicillin/streptomycin were purchased from Gibco Carlsbad, CA, USA.

- LightCycler® high resolution melting master and LightCycler® fastStart DNA master^{PLUS}, HybProbe, FastStart *Taq* DNA polymerase were purchased from Roche Diagnostics GmbH, Mannheim, Germany.

- Phusion™ high-fidelity DNA polymerase (Finnzymes, Espoo, Finland).

- Pluronic F-126 and EGTA were purchased from Sigma-Aldrich, GmbH, Steinheim, Germany.

- Fura-2 was purchased from Invitrogen™, Molecular Probes®, Eugene, Oregon, USA.

- 4-CmC and Triton-X 100 were purchased from BDH Chemicals Ltd. Poole, England.

- Wizard™ Genomic DNA extraction kit and Wizard® SV Gel and PCR Clean-Up System were purchased from Promega Corporation, Madison, WI, USA.

All genomic DNA samples and lymphoblastoid cell lines used in this study were obtained with informed consent from participating subjects. All studies were carried out after obtaining ethical approval from the Whanganui-Manawatu human ethics committee.

2.2 METHODS

2.2.1 Mammalian Cell Culture

B-lymphocytes isolated from patients had previously been immortalized using Epstein-Barr virus and continuously dividing B-lymphoblastoid cell lines (BLCL) had been established [121]. These cell lines had been frozen and stored in liquid nitrogen for later use.

2.2.1.1 Reactivation of lymphoblastoid cell lines from liquid nitrogen stocks

The stock vials from the liquid nitrogen storage were thawed quickly and resuspended in 5 mL of medium (Opti-MEM® I Reduced Serum Media, containing 2% FCS and 1x penicillin/streptomycin). The cells were then centrifuged for 5 min at 200 *g*. The supernatant was discarded and the pelleted cells were resuspended in 2 mL of medium and dispensed into two T25 flasks each containing 9 mL of medium. The flasks were then placed upright in the incubator at 37°C and 5% CO_2 and checked daily. The cells clump together when growth starts and additional medium was added gradually depending upon the cell number. When cells began to form larger clumps the medium was replenished every 2 days. This was done by removing ~2 mL of the medium without disturbing the cells which tend to collect at the bottom of the flask and adding 3-5 mL of fresh medium. After the cells formed large clumps and the cell density reached about 1 X 10^5 cells/mL in the two T25 flasks, they were pooled together and passaged into T75 flasks. Cells were grown in T75 flasks to a maximum volume of 20 mL and to densities of 1-2 X10^7/mL.

2.2.1.2 Freezing down BLCL for storage

Cells were frozen for long-term storage in liquid nitrogen by centrifuging at 100 *g* for 10 min in 15 mL centrifuge tubes. The supernatant was removed and the pelleted cells were resuspended in freezing media containing FCS with 10% dimethylsulfoxide (DMSO). About 1 mL of the cell suspension was then aliquoted

into each of the two cryovials which were labelled with date, cell line, number of cells, media used as well as the passage number where appropriate. The cryovials were wrapped in tissue paper to slow the freezing rate and kept at -80°C overnight before being placed in liquid nitrogen for long-term storage.

2.2.2 Isolation of genomic DNA from lymphoblastoid cell lines

Genomic DNA was isolated from the cultured lymphoblastoid cell lines at various time points using the Wizard™ Genomic DNA extraction kit protocol (Promega Corporation, Madison, WI, USA). Extraction was done following the manufacturer's instructions. Nuclei lysis solution was used to lyse the cells and the nuclei thus releasing the nucleic acids. An RNAase digestion step was then carried out to remove the cellular RNAs. Cellular proteins were removed using a salt precipitation step which precipitates the proteins leaving the genomic DNA in solution. Isopropanol precipitation was used for desalting and isolation of the DNA from solution. The extracted DNA was resuspended in rehydrating solution (supplied with the kit) and stored at -20°C or -80°C for long-term storage.

2.2.3 Quantification of genomic DNA

The isolated genomic DNA was quantitated using the The NanoDrop® ND-1000 spectrophotometer (Thermo Scientific, Wilmington, DE, USA), by measuring the concentration of the samples based on its absorbance at 260 nm. The ratio of absorbance at 260 nm and 280 nm and at 260:230 nm was used to assess the purity of DNA. A 260:280 ratio of ~1.8 and 260:230 ratio of ~2 is considered as acceptable purity for DNA samples (Thermoscientific, ND-1000, spectrophotometer v3.7 user's manual).

2.2.4 High Resolution Melting Assays

High-resolution amplicon melting (HRM) is a closed-tube method of genotyping PCR products, which allows genotyping and gene scanning using saturating double stranded DNA binding dyes [122]. HRM analysis depends on the melting of the double-stranded DNA in the presence of DNA intercalating dyes which specifically bind to double stranded DNA and fluoresce brightly. As the temperature is increased to about 95°C at some point the melting temperature of the amplicon is reached and the two strands of DNA separate. This results in the intercalating

fluorescent dye being separated from the DNA and consequently a decrease in fluorescence occurs.

The melting behaviour of the amplicon varies depending upon the length and the GC content. Shorter amplicons result in better discrimination of small variations in the DNA sequence such as SNPs. Also, as the size of the amplicons decreases, the T_m differences among the different genotypes increases correspondingly resulting in better differentiation between the different genotypes[123].

2.2.4.1 Melting curve analysis

Different sequence variants can be identified based on differences in melting curves using the LightCycler® 480 Gene Scanning Software. The data were analyzed using normalized and temperature shifted melting curves, difference plots, and derivative melting curves (Figure 8a, b and c respectively) as described previously [124].

Heterozygous samples are best distinguished from homozygous samples by an altered shape in the melting curve and difference plots (Figure 8a and b). Homozygous samples are differentiated by the difference in T_m. Homozygous wildtype and mutant samples can be differentiated by clearly defined single melting peaks separated by about 0.3-1°C, whereas heterozygous samples show a lower melting temperature shoulder in addition to the main peak as a result of the heteroduplex formation which have a lower melting temperature (figure 8c).

HRM assays were carried out in the the LightCycler® 480 System (Roche Diagnostics GmbH, Mannheim, Germany). The LightCycler® 480 Gene Scanning Software was used to differentiate the different sequence variants based on differences in the melting curves. The reaction mixture used for the LightCycler® 480 HRM master is shown in Table 1. The HRM master mix contains FastStart *Taq* DNA polymerase for hot start PCR and LightCycler® 480 High resolution dye for monitoring of formation and denaturation of double stranded DNA. A stock solution of 25 mM $MgCl_2$ is supplied with the LightCycler® 480 HRM Master for optimization of Mg^{2+} concentrations if necessary. Optimization was achieved using 3 mM $MgCl_2$.

a. Normalized and temperature shifted melting curves temperature

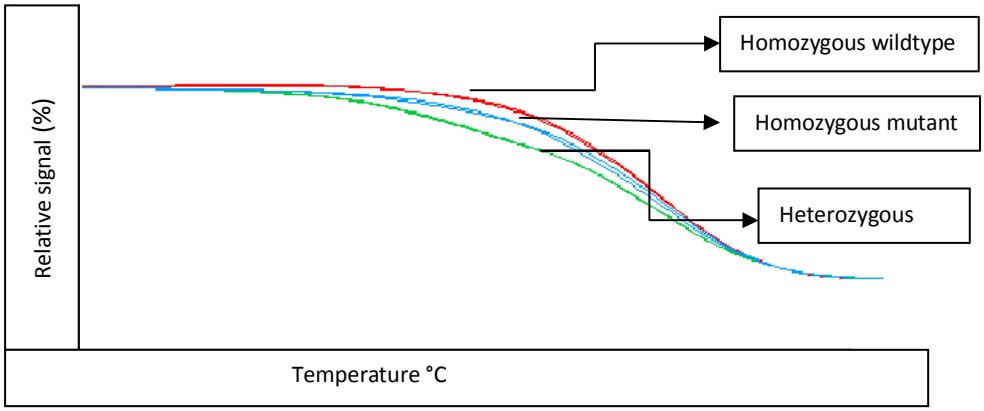

b. Normalized and temperature shifted Difference plots

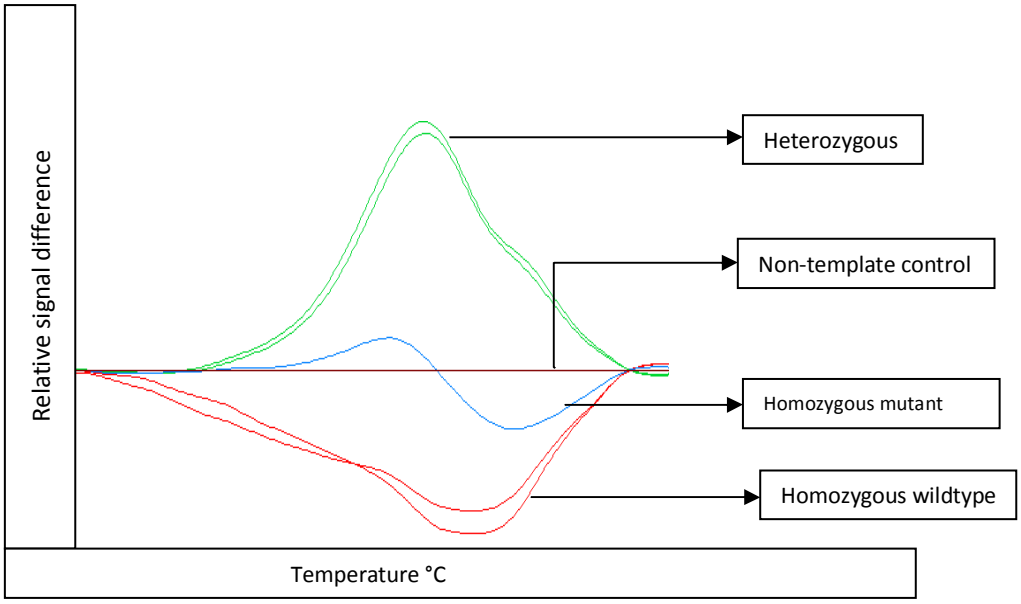

c. Melting curve

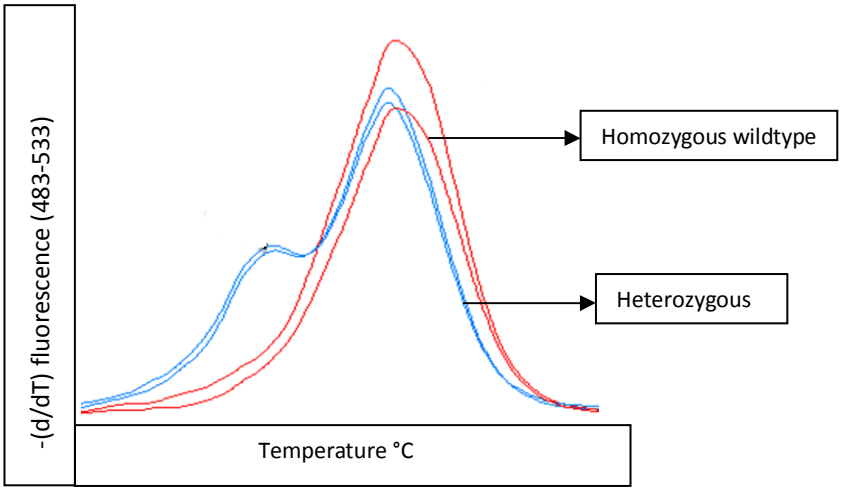

Figure 8. HRM assay using LightCycler® 480 gene scanning software

a. Normalized and temperature shifted melting curves
   The temperature is shifted to a point where the entire ds DNA is denatured.

b. Normalized and temperature shifted Difference plots
   These are obtained by subtracting the melting curves from the reference (base) curve.

c. Melting peaks
   x-axis is the first derivative of fluorescence and y-axis is temperature. Heterozygous samples show a 'shoulder' at a lower melting temperature, while the homozygous samples show a single peak.

For the assays genomic DNA with known genotypes were used as controls to validate the results. Primers were designed using the LightCycler Probe Design Software 2.0. Primer sequences used in PCR are listed in the appendix V. All assays were carried out using the touchdown PCR cycle program and the HRM program used for the analyses is listed in Table 2.

Component	**Final concentration**	**Volume (µL)**
Forward Primer	0.3 µM	1
Reverse Primer	0.3 µM	1
Template	100 ng/µL gDNA	1
LightCycler® 480 HRM master	1x	5
$MgCl_2$	3 mM	1.2
PCR grade H_2O	-	Up to 10 µL

Table 1. Reaction components for the HRM protocol using LightCycler® 480 HRM Master

Pre-incubation	95°C	10 min	1x
Amplification	95°C 58 72	1 sec 10 sec 12 sec	45x
Melting	95 45 72 92	1 sec 1 min 1 sec -	1x
Cool	40	10 sec	1x

Table 2. High resolution melting program

2.2.5 Hybridization Probe assay

Hybridization probe (HybProbe) assay is a homogeneous or “closed tube” assay which allows amplification and genotyping by melting curve analysis using fluorescence resonance energy transfer (FRET) probes. Primers and probes required for amplification and genotyping were added simultaneously.

The reaction mixture in the HybProbe assay uses two fluorescent labelled oligonucleotide probes for genotyping. One probe is complementary to the mutation site and is termed the mutant probe while the other probe, termed the anchor probe, is complementary to an adjacent site. The adjacent 3’ and 5’ ends of the two probes are fluorescently labelled (Figure 9). The fluorescence emitted by the donor dye on one probe excites the acceptor dye on the other probe by FRET. The excited donor dye emits red fluorescence which is measured at the end of annealing step in each cycle by the LightCycler 1.2 system.

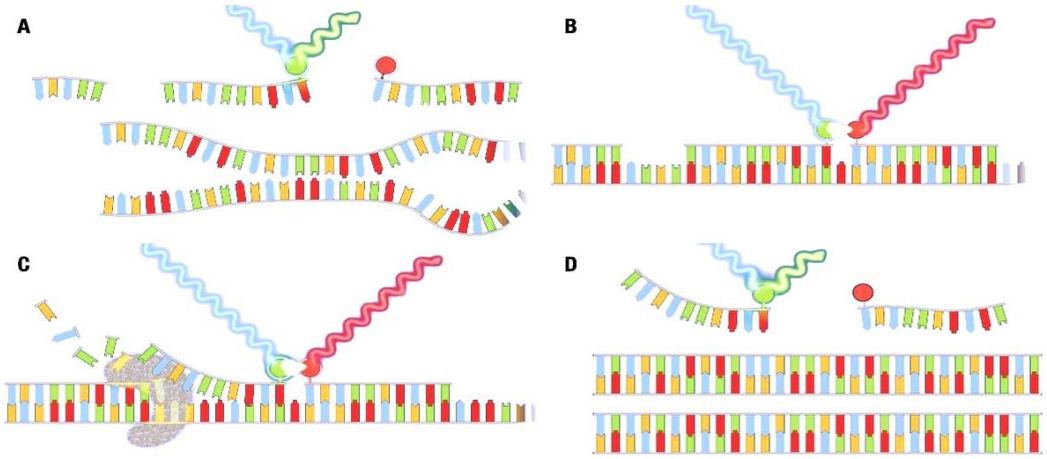

Figure 9. The principle of mutation detection using LightCycler 1.2 system

A. the anchor probe has a red acceptor dye at its 5' end and the mutant probe has fluorescein dye at its 3' end. B. Probes hybridize to the amplified DNA fragment bringing the two dyes into close proximity. Fluorescein emits green fluorescent light which excites the acceptor dye by FRET. The red thus emitted by the acceptor dye is measured at the end of each annealing step. C. Increase in temp after annealing leads to displacement of probes. D. At the end of each PCR cycle DNA is double stranded and the probes are displaced and the distance between the dyes prevents FRET [LightCycler® FastStart DNA MasterPLUS HybProbe instruction manual, version 2006].

Melting of the amplified DNA samples will cause the probe to separate from the DNA complex. This results in a decrease in the measured fluorescence. The resultant melting curves are used to analyze the genotype of the amplified DNA. The homozygous mutant DNA would show a melting peak (peak at a lower melting temperature (T_m) than the homozygous wildtype and the heterozygous sample exhibits two distinct peaks corresponding to the mutant and the wild-type locus.

HybProbe assays were carried out in the The LightCycler 1.2 System (Roche Diagnostics GmbH, Mannheim, Germany) which allows DNA samples to be quantified and analyzed simultaneously by monitoring the fluorescence during amplification. Melting curve analysis was done using the LightCycler 1.2 software version 4.0 by measuring the melting temperature (T_m) of each sample to be measured. Figure 10 is a representation of the melting curve chart (10a) and the melting peak chart (10b) from a T_m analysis. The T_m of each sample appears as a peak which makes it easier to discern differences between different genotypes.

The reaction mixture is pipetted into LightCycler capillaries which are placed into the sample carousal before being placed into the LightCycler 1.2 system. It uses the LightCycler Carousel Centrifuge 1.2, a specially designed table-top centrifuge. The capillaries were placed on the carousal which was centrifuged and the capillaries were transferred onto the LightCycler 1.2 system.

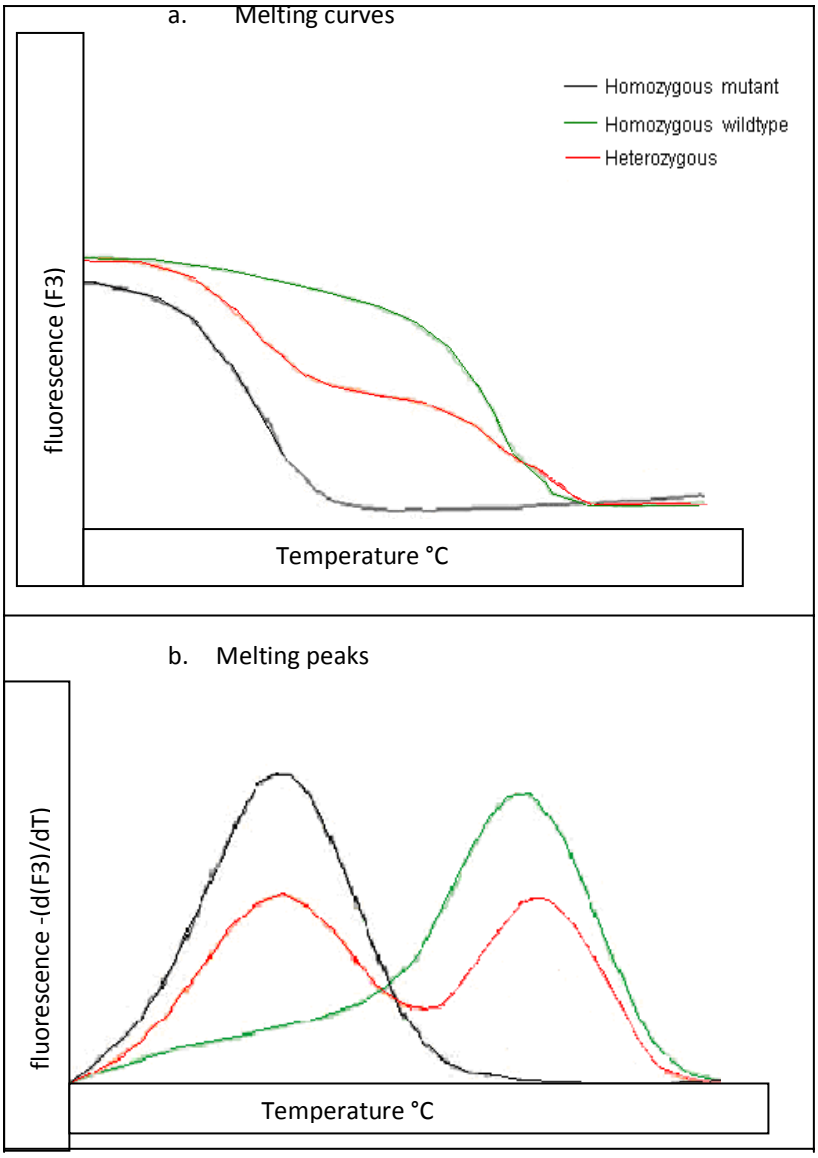

Figure 10. HybProbe assay

a. Melting curves. The fluorescence of the samples is plotted against the temperature. A downward curve is obtained as the temperature increases and the samples melt.

b. The melting peaks. The homozygous mutant sample (black) shows a peak at a lower melting temperature, where as the wildtype sample (green) shows a peak at a higher melting temperature. Heterozygous sample (red) shows two peaks due to the two different genotypes present.

The reaction mixture used for the LightCycler 1.2 DNA master HybProbe is shown in Table 3. The DNA master HybProbe mix contains *Taq* DNA polymerase, reaction buffer, dNTP mix (with dUTP instead of dTTP). Primers were designed using the LightCycler Probe Design Software 2.0. Primer sequences used in PCR are listed in the appendix V. The HybProbe program used for the assay is listed in Table 4.

Component	**Final concentration**	**Volume (µL)**
Forward Primer	0.5 µM	0.1
Reverse Primer	0.5 µM	0.1
Anchor probe	2 µM	0.08
Mutation probe	2 µM	0.08
Template	100 ng/µL gDNA	0.5
LC HybProbe master	1X	1.0
$MgCl_2$	2 mM	1.2
Uracil-DNA Glycosylase	0.5 units	0.5
PCR grade H_2O	-	Up to 10 µL

Table 3 HybProbe assay using the FastStart DNA MasterPLUS HybProbe

Pre-incubation	95°C	10 min	1x
Amplification	95°C 58 72	1 sec 10 sec 12 sec	45x
Melting	95 45 72 92	1 sec 1 min 1 sec -	1x
Cool	40	10 sec	1x

Table 4. HybProbe LightCycler program

2.2.6 SEQUENCING

2.2.6.1 Polymerase chain reaction

Sequencing of various regions across the *RyR1* gene was then carried out including exon 100 (The H4833Y mutation is on exon 100). Previously designed primer pairs for various exonic regions of the *RyR*1 gene were used and PCR reactions were carried out using FastStart Taq polymerase. The primer sequences are given in the appendix V. The PCR protocol and the PCR program used are listed in Table 5 and Table 6, respectively (labelled forward primer in table 5 is only for the microsatellite D19S47). Exons 26-27, 43-45, 46-47, 50-52, 55-58 and 100-103 were PCR amplified for sequencing.

2.2.6.2 Agarose gel electrophoresis

About 10% of the PCR product was analysed by agarose gel electrophoresis (1% agarose in 1x TAE buffer (980 mL MQ water + 20 mL 50x TAE buffer) to confirm the size and purity of the PCR product obtained.

2.2.6.2 Purification of PCR products

Purification of PCR products was carried out using the Wizard® SV Gel and PCR Clean-Up System (Promega Corporation, Madison, WI, USA) following the manufacturer's instructions.

Purification of the PCR products was carried out to remove excess nucleotides and primers. A membrane-based system (silica membrane) is used exploiting the ability of DNA to bind to silica membranes in the presence of chaotropic salts, allowing quick recovery/purification of the DNA.

2.2.6.3 DNA sequencing

The purified PCR products were sent for sequencing to the Allan Wilson Center, Massey University (http://awcmee.massey.ac.nz). The amount of template used varied with the size of the PCR product. As most of the PCR products were about 500 bp in size about ~10 ng of the template in a 15 µL reaction mixture was used. Primers were added to a final concentration of 3.2pmol/15µL and the samples were submitted for sequencing. Sequencing was performed on the AB13730 Genetic analyzer using the BigDye™ Terminator Version 3.1 Sequencing Kit. Sequences were analysed using the Chromas 2.13 software (Technelysium Pty Ltd, Helenvale, Queensland, Australia).

2.2.7 Genotyping

Genotyping using two (CA)n repeat microsatellite markers tightly linked to the *RYR1* gene and three intragenic restriction fragment length polymorphisms (RFLPs) was carried out. The relative position of the two microsatellite markers and the 3 RFLPs with respect to the two mutations is shown in Figure 11.

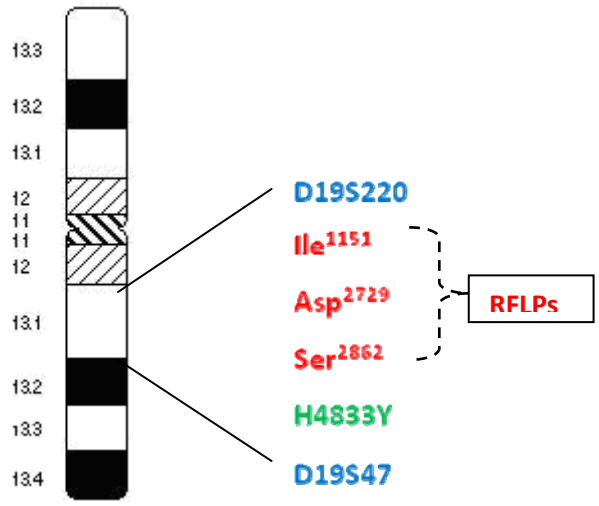

Figure 11. Relative positions of the markers on chromosome 19

Relative positions of the two microsatellite markers and three RFLPs with respect to the H4833Y mutation on the long arm of chromosome 19. Adapted from online GDB interacted chromosome 19 map [MAPVIEW].

2.2.7.1 *Microsatellite analysis*

Microsatellites, also known as simple sequence repeats (SSRs), are tandem nucleotide repeats in the DNA sequences about 1-6 bases in length. The number of repeats is variable within a population and within the alleles of an individual. They are highly polymorphic and genome wide in distribution and exhibit co-dominant inheritance [125].

In this study microsatellites were amplified by PCR wherein one of the PCR primers were fluorescently labelled using the dye 6-FAM.The resulting amplicons would differ in size according to the size of the microsatellite (Figure 12). Analysis of the fluorescent amplicons was carried out by capillary electrophoresis on the ABI3730 Genetic Analyzer (Allan Wilson Center, Massey University).

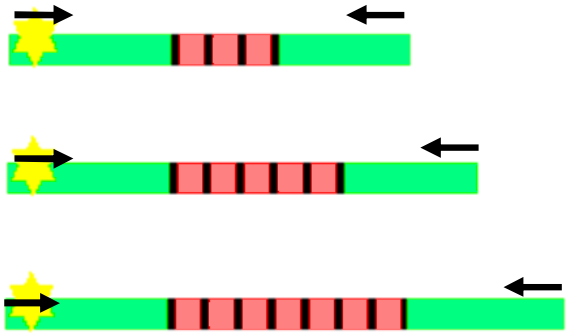

Figure 12. Microsatellite marker analysis

Two PCR primers (shown as arrows) flank the microsatellite region with the forward primer fluorescent-labelled with 6-FAM (shown as star). The size of the PCR product differs according to the number of tandem repeats.

Two microsatellite markers, D19S47 and D19S220, flanking the *RYR1* gene and tightly linked to the gene were used. While D19S220 lies at the 5' end D19S47 lies at the 3' end of the gene (Figure 11).

For the marker D19S47 PCR amplification was carried out using the Fast-Start DNA polymerase (Roche Diagnostics, GmbH, Mannheim, Germany). The reaction components used for the PCR using Fast-Start polymerase are described in table 5. The primer sequences used are listed in appendix V. The forward primer was labelled with the fluorescent dye 6-FAM. The PCR program used is described in Table 6.

Component	Volume/25µL reaction	Final Concentration
10x PCR buffer + 20 mM $MgCl_2$	2.5 µL	1x PCR buffer + 2 mM $MgCl_2$
FastStart *Taq* polymerase	0.4 µL	2 U/µL
Forward Primer (labelled with 6-FAM)	2.5 µL	0.5 µM
Reverse Primer	2.5 µL	0.5 µM
dNTPs	0.5 µL	200 µM
PCR-grade H_20	Up to 25 µL	-

Table 5. Reaction components for the microsatellite D19S47 using FastStart Taq polymerse

Initial denaturation	94°C	5 min	1x
Denaturation	94°C	1 sec	30x
Annealing	62°C	30 sec	
Extension	72°C	30sec	
Final extension	72°C	6 min	1x
Cool	4°C	hold	-

Table 6. FastStart PCR programme

For the marker D19S220 PCR amplification was carried out using the Phusion™ high-fidelity DNA polymerase (Finnzymes, Espoo, Finland). The reaction components are described in table 7. The forward primer was labelled with 6-FAM. The primer sequences used are listed in appendix V and the PCR program used is described in table 8.

Component	**Volume/20µL reaction**	**Final Concentration**
5x PCR buffer	4 µL	1X PCR buffer
Phusion DNA polymerase	0.2 µL	0.02 U/µL
Forward Primer (labelled with 6-FAM)	2 µL	0.5 µM
Reverse Primer	2 µL	0.5 µM
dNTPs	0.4 µL	200 µM
DMSO	0.6 µL	3%
PCR-grade H_20	Up to 20 µL	-

Table 7. Reaction components for PCR for the microsatellite D19S220 Phusion Polymerase

Initial denaturation	98°C	30 sec	1x
Denaturation Annealing Extension	98°C 57°C 72°C	10 sec 30 sec 30sec	30x
Final extension	72°C	8 min	1x
Cool	4°C	hold	-

Table 8. Phusion Polymerase PCR protocol

The reactions were analysed by agarose gel electrophoresis (1% agarose gel in 1x TAE buffer) by adding 3 µL of the PCR products to check for amplification. The amplicons were then sent to the Allan Wilson Center, Massey University, Palmerston North, capillary electrophoresis on the ABI3730 Genetic Analyzer. The size standard GS500 (-250) LIZ was used as a reference.

The chromatogram obtained was analysed using the Peak scanner v1.0 software (Applied Biosystems Inc, Foster city, CA, USA). The DNA samples were typed with respect to the microsatellites D19S220 and D19S47 according to the alleles described in Table 9 and Table 10, respectively (www.gdb.org).

Allele	Value	Frequency
1	106 bp	3%
2	104 bp	1%
3	102 bp	11%
4	100 bp	38%
5	98 bp	6%
6	96 bp	4%
7	94 bp	4%
8	92bp	31%
9	88 bp	1%

Table 9. D19S47 alleles

Allele	Value	Frequency
1	265 bp	3%
2	267 bp	9%
3	269 bp	1%
4	271 bp	9%
5	273 bp	27%
6	275 bp	16%
7	277 bp	16%
8	279 bp	11%
9	281 bp	1%
10	283 bp	1%

Table 10. D19S220 alleles

2.2.7.2 *Restriction fragment length polymorphisms*

Restriction fragment length polymorphisms are polymorphisms that result in the creation or elimination of a restriction endonuclease site. In this study, RFLPs were detected using an HRM-assay which allows rapid and accurate RFLP genotyping as opposed to the more time-consuming and laborious technique using conventional restriction digestion followed by gel electrophoresis to determine the presence and absence of restriction sites [126]. By convention PCR products containing the restriction site were classed as allele '2' and products without the restriction site were classed as allele '1'. Therefore, three different genotypes are possible for each RFLP: 1:1, 1:2, 2:2. Three samples with known genotypes as established with standard restriction endonuclease digestion (data not shown) [10] were used as melting standards. The DNA samples analysed were grouped into these genotypes according to their melting behaviour

DNA samples were amplified using real-time PCR and the amplicons were melted and monitored using the LightCycler® 480 system as described above (section 2.2.4). Primer sequences are given in appendix V. The two sets of DNA samples were typed with respect to three intragenic *RYR1* RFLPs [127] described in table Table 11 below.

Aminoacid	Substitution	RE change	Allele frequency 1	2	Heterozygote frequency
Ile^{1151}	ATC ⟶ ATT	*Taq* I loss	45%	55%	52%
Asp^{2729}	GAT ⟶ GAC	*Fok* I loss	25%	75%	20%
Ser^{2862}	AGT ⟶ AGC	*Cfo* I loss	74%	26%	37%

Table 11. Properties of RFLPs

2.2.8 Functional assays

2.2.8.1 Calcium release assay

Several studies have established that the mammalian B-lymphocytes express RyR1 (the skeletal muscle isoform of RyR) in considerable amounts and can be used in functional assays [54], [55],[128]. RyR1 can be activated pharmacologically by a number of compounds like 4-CmC, caffiene, halothane, E-218 and calcium [129].

Calcium assays work on the principle that the activating compound stimulates the RyR1 to release calcium from the ER/SR stores into the cytosol and the amount of calcium released is measured using a calcium-sensitive indicator molecule like fura-2. Fura-2 is a dual excitation Ca^{2+} indicator and allows ratiometric measurements of emission signals (at 510 nm) to monitor $[Ca^{2+}]_c$ [130]. Ratiometric dyes like fura-2 are useful as the ratio signal is not dependent on parameters like illumination intensity, path length and dye concentration, thus, leading to increased sensitivity of the assays. As fura-2 free acid is calcium-sensitive but membrane impermeable, before loading the dye cells are incubated with fura-2 pentaacetoxymethyl (AM) ester which is an ester form of fura-2 free acid and is

Ca^{2+} insensitive but membrane permeable. Once inside the cell endogenous esterase enzymes sequentially cleave the AM groups leaving the fura-2-free acid inside the cells which is Ca^{2+}-sensitive and can bind to calcium.

In low Ca^{2+} concentration fura-2 shows an excitation peak at 380 nm. When bound to calcium the excitation peak shows an increase in intensity and also shifts further into the UV region of the spectrum as shown in Figure 13.

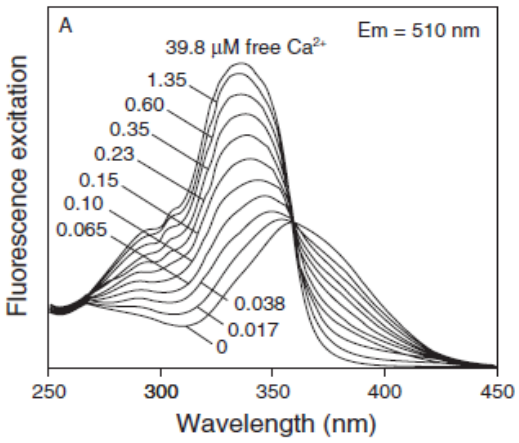

Figure 13. Fluorescence excitation spectra of Fura-2AM

Fluorescence excitation spectra of Fura-2AM in solutions containing 0 to 39.8 µM free Ca^{2+}. (http://probes.invitrogen,com/media/pis/mp02100.pdf)

If the dye is excited at 340 nm an increase in fluorescence would be observed upon Ca^{2+} binding, whereas when excited at 380 nm a decrease in fluorescence signal is observed. In Ca+ free conditions on the other hand maximum fluorescence is observed at 380 nm.

Thus, when the dye is excited at 340 nm and 380 nm in quick succession, a ratio of the fluorescence at 340/380 at a emission wavelength of 510 nm can be used to monitor $[Ca^{2+}]_c$ as it would be proportional to the free intracellular Ca^{2+}. This can be calculated using the equation:

$$[Ca^{2+}] = K_d * Q * (F_{340} - F_{min})/F_{max} - F_{380}$$

where, Kd is the Ca^{2+} dissociation constant of fura-2AM. Q is the ratio of F_{min} to F_{max} (F_{min}/ F_{max}) at 380 nm. F_{max} is the 340/380 ratio when the indicator is saturated with calcium. F_{max} was determined in this study using 0.1% triton X-100 to disrupt the cell membrane and measure the released intracellular Ca^{2+}. F_{min} is the 340/380 ratio when no calcium is bound to the indicator Fura-2AM. Figure 14 shows a typical response of a Fura-AM loaded cell in a Ca^{2+} release assay after it is treated with different compounds and excited at 340 and 380 nm.

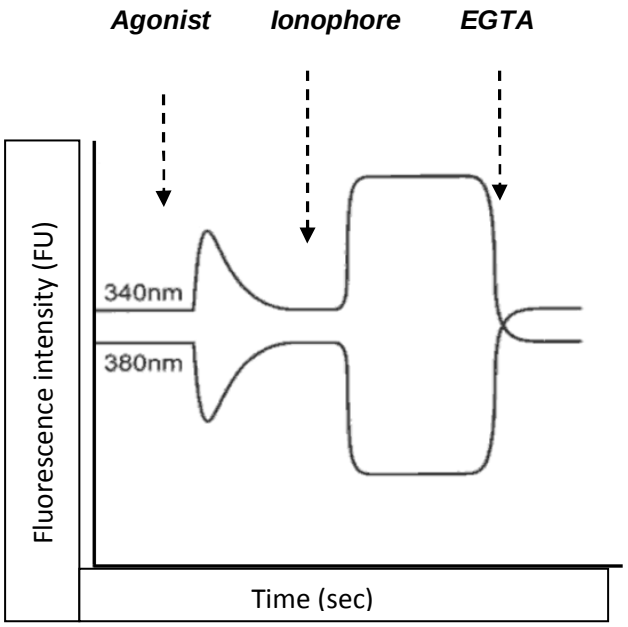

Figure 14. Typical signals obtained when a cell loaded with Fura-2AM is excited at 340 and 380 nm (Modified from [131]

The assay

About 10 mL of the cell culture (of the 3 cell lines used, 1360, 1431 and 1537) was centrifuged at 100 *g* for 10 min. The supernatant was removed and about 10 mL of the balanced salt solution (BSS) buffer (composition in appendix VI) containing 0.2% calcium was added and centrifuged again as above. The supernatant was removed and the pellet was resuspended in 1 mL of BSS containing calcium. Two microliters of 2 mM fura-2AM and 2 µL of pluronic F-127 (a non-ionic detergent) were premixed and added to the cell suspension. Pluronic helps to improve the

physiological stability of fura as esterified indicators like fura-2AM show poor stability in physiological media. The cells were then incubated in the dark (tubes were wrapped in aluminium foil) at room temperature for about 25-30 min. Care was taken that after the addition of Fura-2AM the cells were kept in the dark as much as possible throughout the rest of the assay as fura-2AM is degraded when exposed to light. After about 30 min the tubes were centrifuged for 3 min at 100 *g.* The supernatant was removed and pellet resuspended in 1mL fresh BSS buffer containing calcium. The tubes were then incubated in the dark at room temperature for about 15 min. The cell suspension was centrifuged again for 3 min at 100 *g*. The supernatant was removed and 1 mL of fresh BSS buffer containing Ca^{2+} was added and centrifuged for 3 min at 100 *g*. The cells were washed twice in this manner with BSS containing 0.2 % calcium and twice with BSS buffer without calcium [131].

The cells were then assayed in the LS50B spectrophotometer. About 100-200 µL of the cell suspension was diluted to about 2 mL in Ca^{2+}-free BSS in plastic cuvettes and placed in the spectrophotometer. The assay was carried out at 37°C maintained by the water bath which is connected to the cuvette holder. The cells loaded with fura-2AM were excited at 340 and 380 nm and the resultant fluorescent intensity was measured at an emission wavelength of 510 nm.

3. RESULTS

3.1 Mutation detection using high resolution melting assay

High resolution amlicon melting, which is a PCR-based technique for SNP genotyping, was used to analyse the different mutations in this study. As the three mutations studied are SNPs and known to occur in the heterozygous state in patients, an HRM assay (which differentiates between heterozygous and homozygous samples) could be used to study the different cell lines to detect any change in the SNP genotype during cell culture.

The two cell lines carrying the H4833Y mutation were cultured for about 9-10 weeks and DNA was isolated at various time points during the culture period. SNP genotyping of the isolated DNA was carried out using an HRM assay specific for the H4833 mutation in the LightCycler® 480 system as described in section 2.2.4.

The LightCycler® 480 genotyping software groups the DNA samples using the difference plots or the melting peaks as described in section 2.2.4.

Genomic DNA samples with known genotypes (heterozygous and wildtype) were used as the standards for the assay. Figure 15 and Figure 16 show representative HRM assays for the 1051 cell line at 3 and 9 weeks culture, respectively. In figure 15a, the temperature shifted difference plots were used to differentiate between the heterozygous and homozygous samples. Figure 15b shows the melting peaks. The DNA sample without the mutation (wildtype control) shows a melting peak at 86.5 °C. The heterozygous control DNA (blue peak) shows a slightly lower melting peak at 85.5 °C and the characteristic shoulder at a lower melting lower temperature. The melting peak of 1051 DNA isolated after 4 weeks is concordant with the heterozygous control DNA with the characteristic ‘shoulder’.

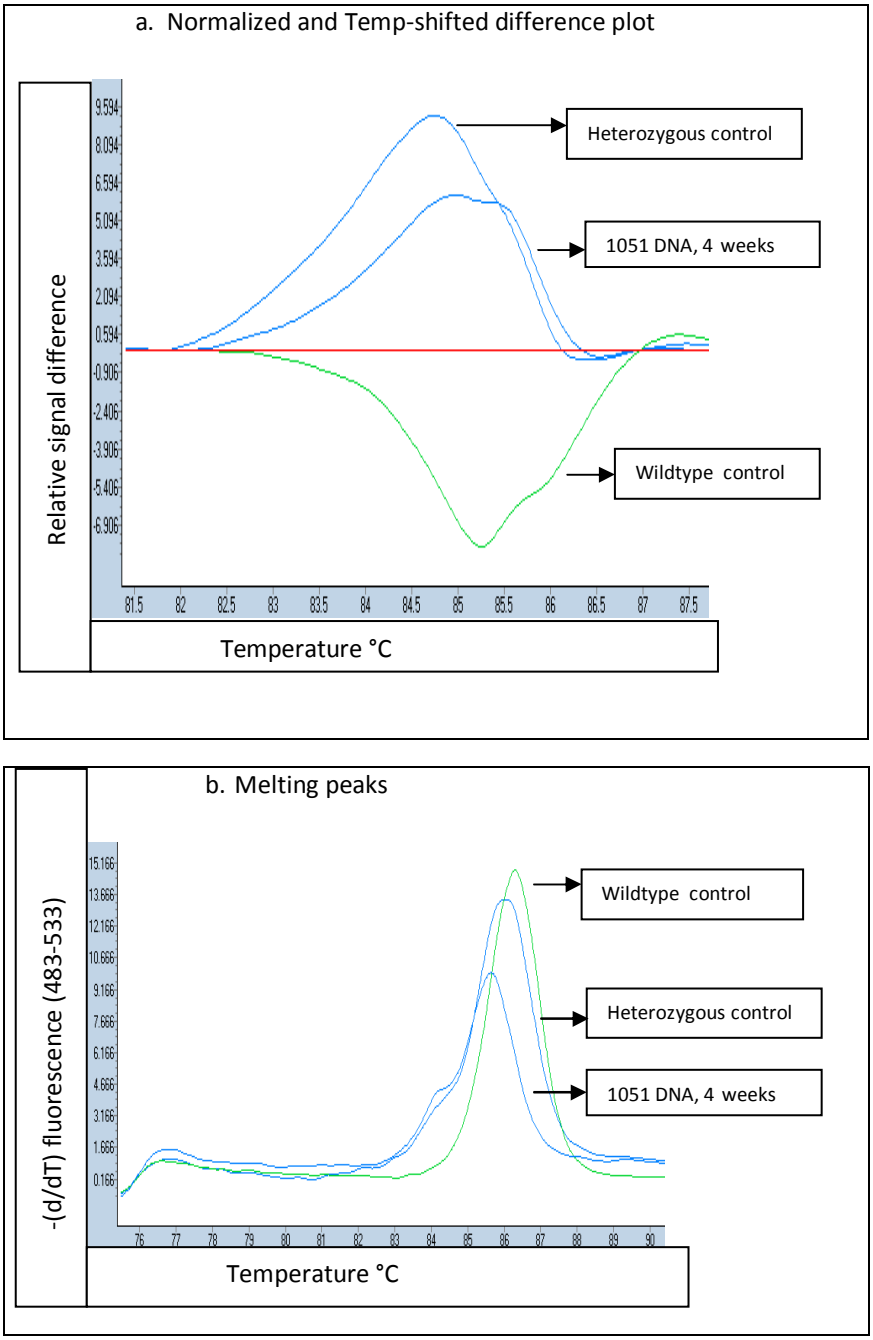

Figure 15. HRM assay at 4 weeks culture

a. Normalized and temperature shifted difference plot

b. Melting peaks

The x-axis in both a and b is the temperature and the y-axis is relative signal difference and first derivative of the fluorescence in a and b, respectively. Wildtype (green peak) indicates homozygous without the mutation (MHN) and heterozygous (blue peak) indicates heterozygous for the mutation (MHS) . NTC (red, in figure 15 a) indicates the non-template control.

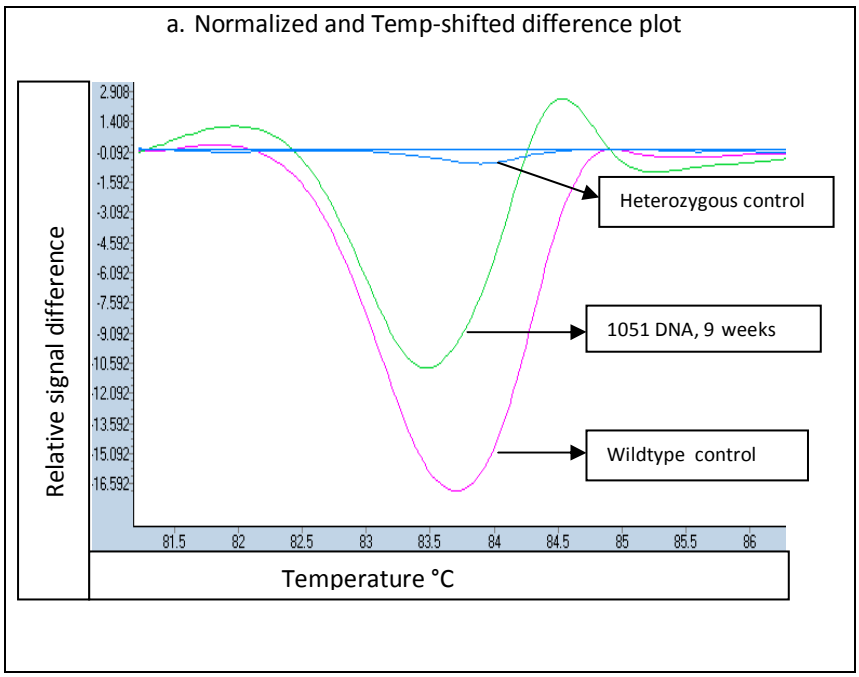

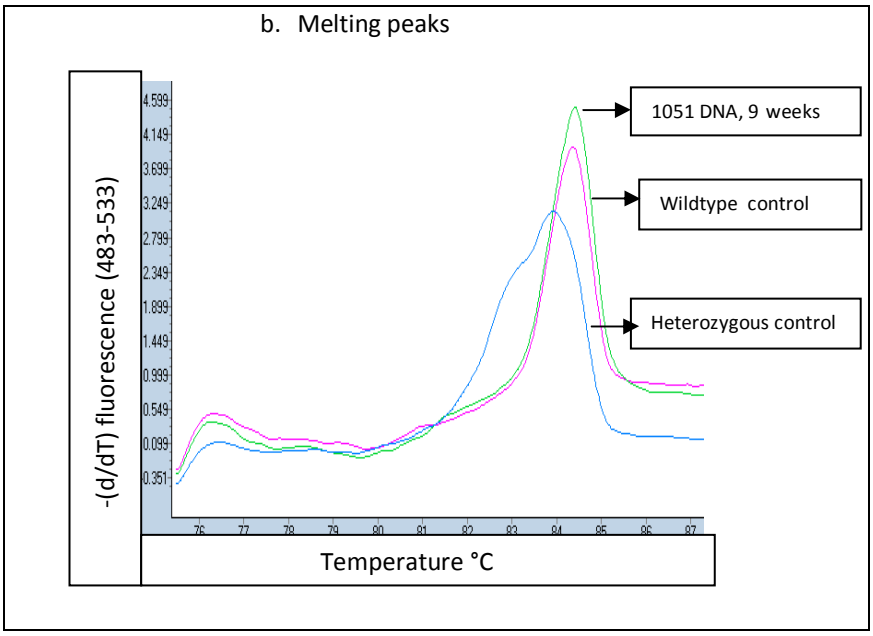

Figure 16. HRM assay at 9 weeks culture

a. Normalized and temperature shifted difference plot

b. Melting peaks

The x-axis in both a and b is the temperature and the y-axis is relative signal difference and first derivative of the fluorescence in a and b, respectively. Wildtype (pink peak) indicates homozygous without the mutation (MHN) and Heterozygous (blue) indicates heterozygous for the mutation (MHS). NTC (red, in figure 16 a) indicates the non-template control.

Figure 16a and b above shows the difference plots and melting peaks obtained from HRM assay of the 1051 cell line after 9 weeks of culture. In the difference plots the DNA after 9 weeks culture (green peak) shows a peak that is concordant with the wildtype control (pink peak). The melting peaks show that the 1051 DNA no longer shows the characteristic ‘shoulder’ and is now concordant with the wildtype control. The result suggests that after 9 weeks in culture the mutant has reverted to wildtype.

The cell line 1042 also carrying the H4833Y mutation was cultured similarly and DNA was isolated at various time-points during culture and HRM assays carried out. Figure 17 shows a representative HRM assay for the 1042 cell line at 4 and 9 weeks culture.

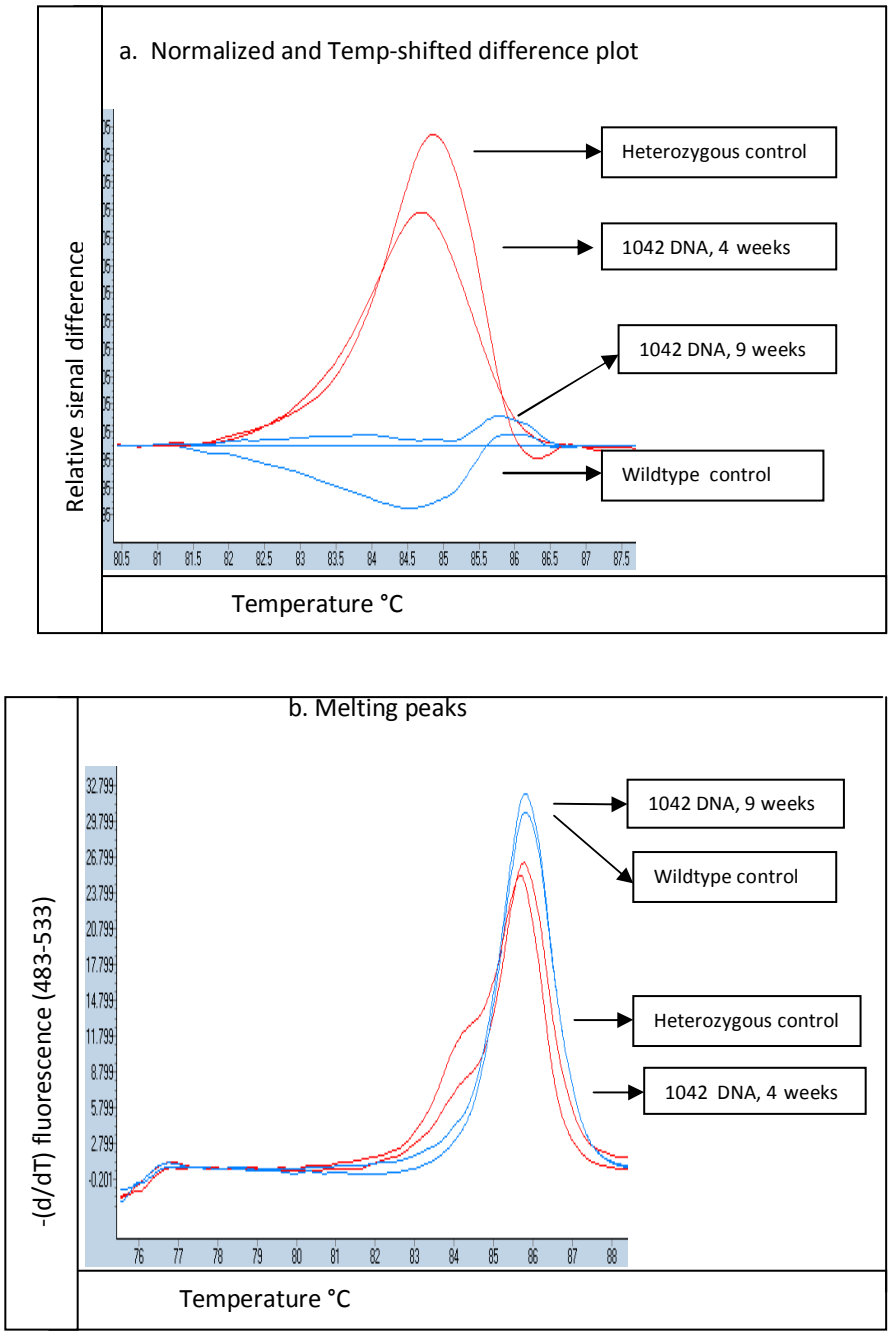

Figure 17. HRM assay for 1042 at 4 and 9 weeks culture

a. Normalized and temperature shifted difference plot

b. Melting peaks

The x-axis in both a and b is the temperature and the y-axis is relative signal difference and first derivative of the fluorescence in a and b, respectively. Wildtype (green peak) indicates homozygous without the mutation (MHN) and Heterozygous (blue peak) indicates heterozygous for the mutation (MHS) . NTC (red, in figure 17a) indicates the non-template control.

Two other cell lines studied, with T4826I and R2452W mutations, did not show any change in genotype after 9-12 weeks of culture.

Figure 18 and Figure 19 show the melting peaks for the HRM assays for 1261 and 1052 cell lines carrying the T4826I and R2452W mutations, respectively.

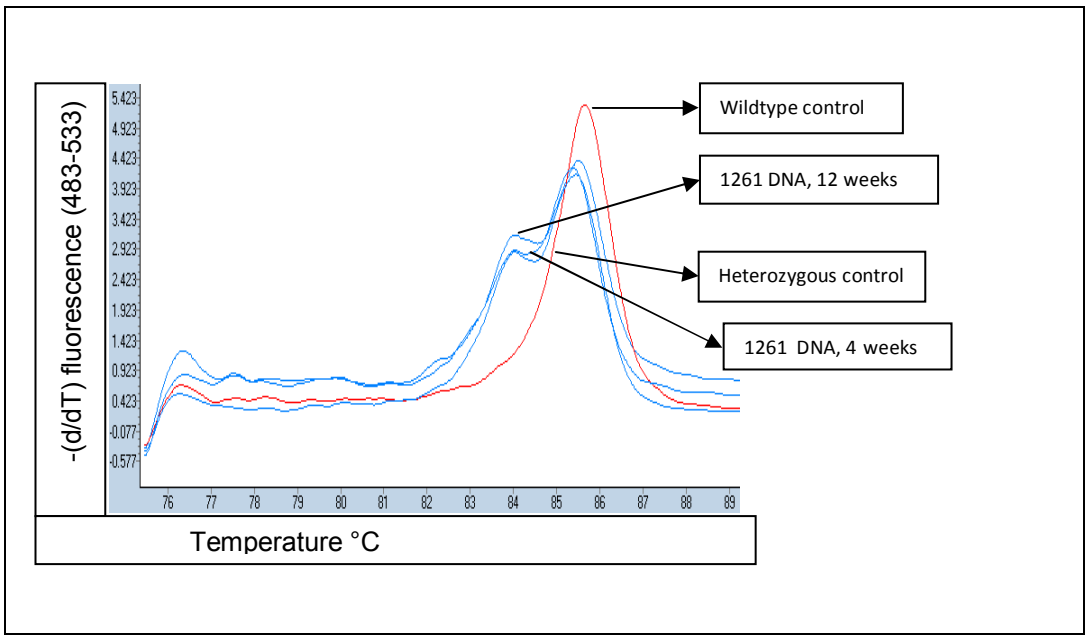

Figure 18. Melting peaks for 1261 DNA at 4 and 12 weeks culture

The x-axis is the temperature and the y-axis is first derivative of the fluorescence. Wildtype (red peak) indicates homozygous without the mutation (MHN) and heterozygous control (blue peak) indicates heterozygous for the mutation (MHS). 1261 DNA at 4 and 12 weeks culture are shown (blue peaks).

Figure 18 shows the melting peaks obtained from the HRM assay for the 1261 cell line at 4 and 12 weeks of culture. DNA sample without the mutation (wildtype control) shows a melting peak at 86 °C. The heterozygous control DNA (blue peak) shows a slightly lower melting peak and the characteristic shoulder at a lower melting temperature. The melting peak of 1261 DNA isolated after 4 and 12 weeks is concordant with the heterozygous control DNA with the characteristic 'shoulder' indicating that the DNA remained heterozygous for the mutation (T4826I) through the 12 weeks of culture.

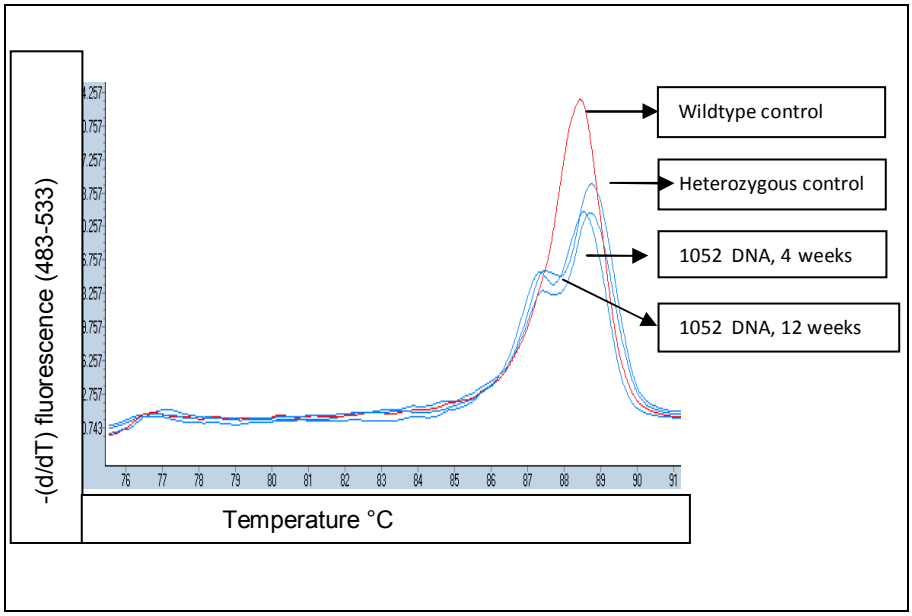

Figure 19. Melting peaks for 1052 DNA at 4 and 12 weeks culture

The x-axis is the temperature and the y-axis is first derivative of the fluorescence in a and b, respectively. Wildtype (red peak) indicates homozygous without the mutation (MHN) and heterozygous control (blue peak) indicates heterozygous for the mutation (MHS). 1052 DNA at 4 and 12 weeks culture are shown (blue peaks).

Figure 19 shows the melting peaks obtained from the HRM assay for the 1052 cell line at 4 and 12 weeks of culture. DNA sample without the mutation (wildtype control) shows a melting peak at 88.5 °C. The heterozygous control DNA (blue peak) shows the characteristic shoulder at a lower melting temperature. The results indicate that the 1052 DNA also remained heterozygous for the mutation (R2452W) after 12 weeks of culture (the melting peaks being concordant with the heterozygous control).

3.2 Mutation detection using hybridization probe assay

Hybridization probe assay is also a PCR-based SNP genotyping assay that uses fluorescent-labelled probes to differentiate between heterozygous and homozygous cultures. DNA samples from the two cell lines with the mutation were assayed using the 4833-specific assay developed previously as a means for double checking the HRM results. SNP genotyping using HybProbe assay using the LightCycler 1.2 system was carried out as described in section 2.2.5. Genomic DNA samples with known genotypes (heterozygous and wildtype) were used as the standards for the assay. Figure 20 shows a representative HybProbe assay for the 1051 cell line at 4 and 9 weeks culture.

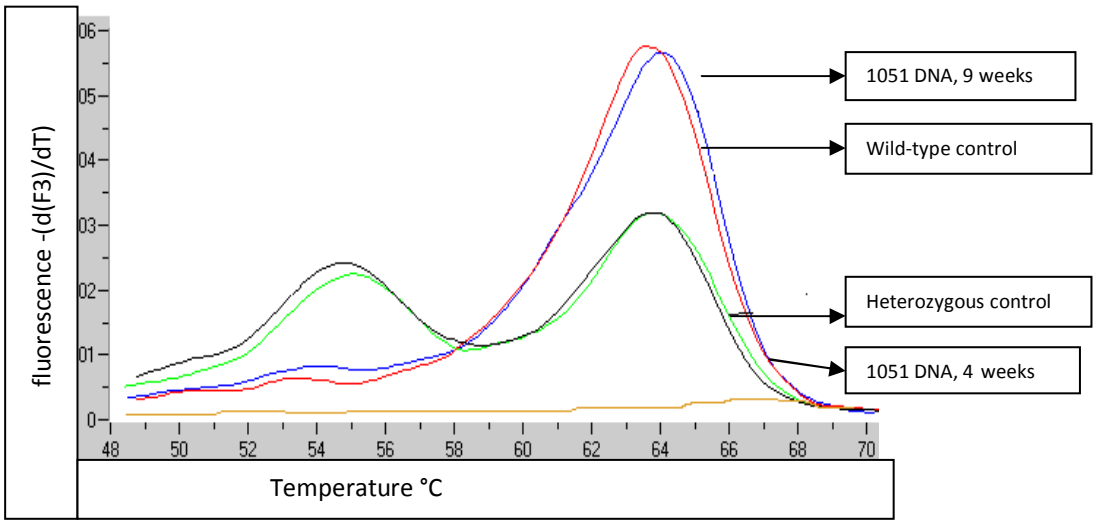

Figure 20. HybProbe assay for 1051 DNA

x-axis is the temperature and the y-axis is the third derivative of the fluorescence. Two melting standards used are the Heterozygous control which is heterozygous for the H4833Y mutation (Black peaks) and wildtype control (blue peak; negative for the mutation) . Wildtype control and the 1051 DNA at 9 weeks culture (red peak) shows a single peak . Heterozygous control DNA and 1051 DNA at 4 weeks culture (green peaks) show two peaks, one of which is at the same temperature as the wildtype control (negative standard).

In the assay shown above, two DNA samples with known genotypes were used as melting standards or assay controls. The wild-type control (red peak) is negative for the H4833Y mutation. The heterozygous control (black peak) was a DNA sample heterozygous for mutation and shows two melting peaks. As seen in the figure, the

DNA from the 1051 cell line isolated after 4 weeks of culture (green peaks) shows two melting peaks, at 55°C and 64°C, respectively, indicative of the wildtype allele and the mutant allele as described in section 2.2.5.

On the other hand, DNA isolated after 9 weeks of culture shows a single melting peak (blue peak) at 64°C concordant with the single peak of the wildtype control / negative melting standard.

The assay was repeated for the 1042 cell line and similar results were obtained for the DNA isolated after 4 and 9 weeks (data in appendix I). The HybProbe assays thus confirmed the loss of the H4833Y mutation in both the cell lines.

3.3 Mutation screening using DNA sequencing

Once the DNA was screened for the mutation by HRM and found to have lost the mutation, sequencing was carried out to confirm the loss of the mutation in the DNA isolated after 9 weeks. A ~500 bp region covering exons 100-103 (H4833Y mutation is on exon 100) was PCR amplified using FastStart DNA polymerase as described in section 2.2.6.1. The gel image obtained after electrophoresis of the PCR products is shown in Figure 21.

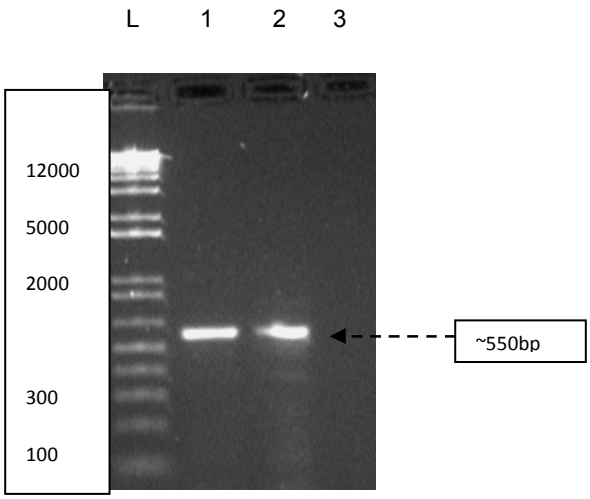

Figure 21. PCR of exon 100-103

L-1 Kb plus DNA ladder™

1- 1051 DNA at 4 weeks culture

2- 1051 DNA at 9 weeks culture

3- Blank (MQ water)

10% of the PCR products were loaded onto a 1% agarose gel in 1X TAE buffer. The gel was stained with 0.3 µg/mL ethidium bromide. Electrophoresis was carried out for 50 min at 90 V.

PCR products were purified using the Wizard® SV Gel and PCR Clean-Up System as described in section 2.2.3.2 and submitted for sequencing to the Allan Wilson Center, Massey University (http://awcmee.massey.ac.nz) after the appropriate primers were added at the required concentrations. Sequencing was performed on the ABI3730 Genetic analyzer as described in section. 2.2.6.3. The chromatograms obtained were analysed using the Chromas 2.13 software (Technelysium Pty Ltd, Helenvale, Queensland, Australia).

Chromatograms obtained from the two sets of 1051 DNA are shown in Figure 22 (a and b). The sequencing showed reversion to C (b) from the original C-T transition which is the cause of the H4833Y mutation (a). The sequencing did not show any other differences between the two DNA samples in the ~500 bp region sequenced.

Sequencing of various regions across the *RyR1* gene was then carried out to compare any differences between the two sets of DNA samples within other regions in the gene. Previously designed primer pairs for various exonic regions of the RyR1 gene were used for PCR amplification of regions between exons 26-27, 43-45, 46-47, 50-52, 55-58 and 100-103. Primer sequences are included in appendix V. The amplified PCR products were then submitted for sequencing (AWC, Massey University).

No differences in the sequencing results were found for the two sets of DNA samples when various other regions within the RYR1 gene were sequenced apart from the transitions leading to the known intragenic RFLPs. (Data in appendix). This combined with the fact that no other changes in the sequencing of the region containing the 4833 mutation indicated recombination repair as a possible mechanism.

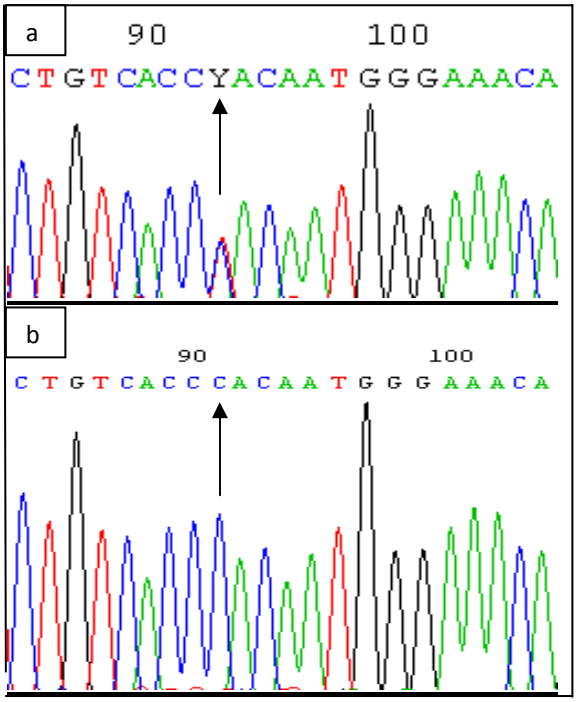

Figure 22. Chromatogram of the sequencing of 1051 DNA at 4 and 9 weeks of culture.

The sequence shows the region on exon 100 of the RYR1 gene where the Cytosine to thymine transition (arrow) occurs causing the H4833Y mutation. 'a' shows sequence after 4 weeks of culture containing the changed base (Y) in place of Cytosine. 'b' shows the sequence after 9 weeks of culture containing the reversion to wildtype (i.e., cytosine (C).

3.4 Genotyping by haplotype analysis

Although two different PCR-based SNP genotyping assays showed the loss of the point mutation which was confirmed by sequencing, further genotyping at the *RYR1* locus was carried out using intragenic RFLPs and two flanking microsatellite markers. Genotyping had the potential to indicate any other changes apart from the few single base changes showed in the sequencing results of various exons on the *RYR1*. Also, as both the SNP genotyping assays were PCR based the possibility of allele fallout during PCR could not be ruled out and microsatellite marker analysis along with the RFLPs were likely to provide further information about the genotypes of the two cell lines.

3.4.1 Genotyping with intragenic restriction fragment length polymorphisms

Genotyping was carried out using the intragenic RFLPs [127]. Each RFLP was examined for the two cell lines with the H4833Y mutation using HRM assay. Analysis was carried out using the LightCycler® 480 genotyping software as described in section 2.2.7.2.

By convention PCR products containing the restriction site were classed as allele '2' and products without the restriction site were classed as allele '1'. Therefore, three different genotypes are possible for each RFLP: 1:1, 1:2 and 2:2.

3.5.1.1 RFLP Ile^{1151}

The two sets of DNA samples isolated from cell line 1051 at 4 and 9 weeks, respectively, were examined for RFLP Ile^{1151}, which results in loss of restriction site for *Taq* I. HRM assays were used as described in section 2.2.7.2. DNA isolated directly from patient's leucocytes was used as a control for the assays. DNA samples with known genotypes as established by standard restriction endonuclease digestion were used as melting standards.

Figure 23a shows the difference plots for a typical HRM assay for RFLP Ile^{1151}. Three different types of samples are shown concordant with the three possible genotypes; homozygous with restriction site (2:2), homozygous without restriction site (1:1) and heterozygous (2:1). The three melting standards were used to group the DNA samples into different genotypes according to their melting behaviour. 1051 DNA at 4 weeks of culture and the DNA isolated from fresh leucocytes were concordant with the standard 2:2. DNA isolated after 9 weeks of culture showed a changed genotype and was concordant with the melting standard 1:1. Therefore, both alleles were altered at this SNP.

3.5.1.2 RFLP Asp^{2729}

The two sets of DNA samples were also examined for RFLP Asp^{2729}, which results in loss of restriction site for *Fok I*. HRM assays were used as described in section 2.2.7.2. Assay control and melting standards were same as that for RFLP Ile^{1151}. Figure 23b shows difference plots for a typical result of HRM assay for RFLP Asp^{2729} using cell line 1051.

1051 DNA at 4 weeks of culture and the DNA isolated from fresh leucocytes were concordant with the standard 2:2. DNA isolated after 9 weeks of culture showed a change in genotype and was concordant with the melting standard 2:1. This result suggests an alteration in only one allele.

3.5.1.3 RFLP Ser^{2862}

The two sets of DNA samples were examined for third RFLP at Ser^{2862}, which results in loss of restriction site for *Cfo* I. HRM assays were used a described in section 2.2.7.2. Assay control and melting standard were used as described above. Figure 23c shows difference plots for a typical result of HRM assay for RFLP Ser^{2862} using cell line 1051 indicating the presence of three different types of samples. While, 1051 DNA at 4 weeks of culture and the DNA isolated from fresh leucocytes were concordant with the standard 1:1, DNA isolated after 9 weeks of culture was concordant with the melting standard 2:1. This result also suggests an alteration in one allele.

a. Ile^{1151}

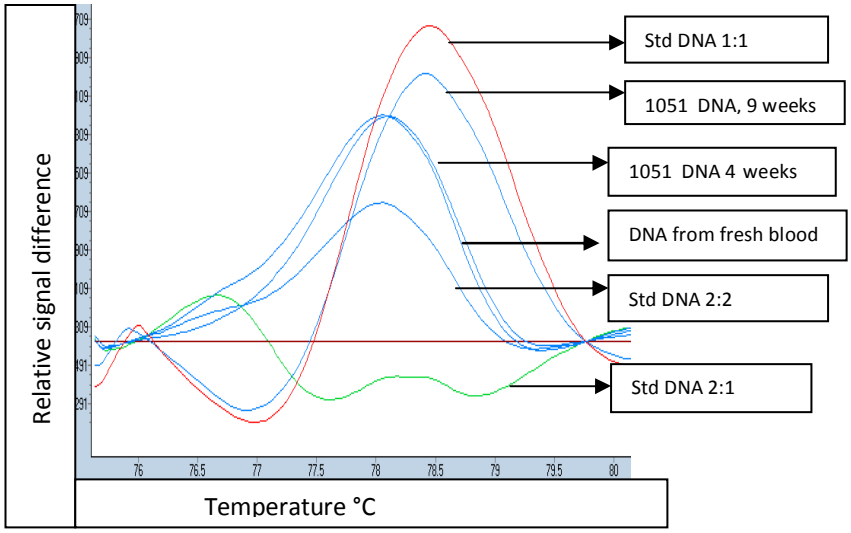

b. Asp^{2729}

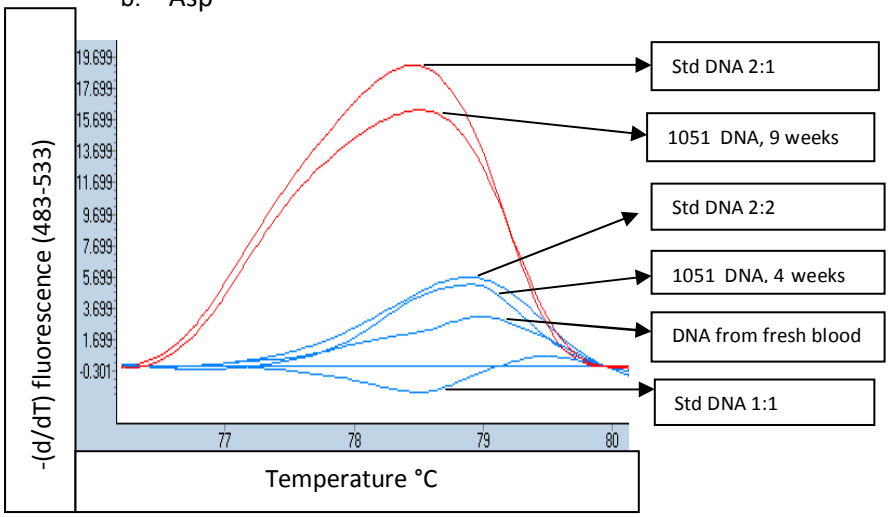

c. Ser^{2862}

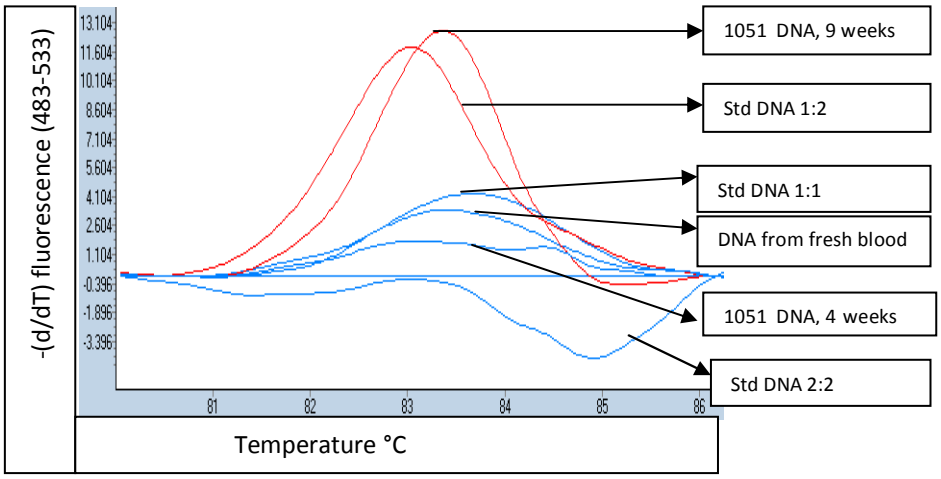

Figure 23. HRM assay for the three RFLPs using the cell line 1051

Normalized and temperature shifted difference plot are shown for

a. Ile^{1151}
b. Asp^{2729}
c. Ser^{2862}

x-axis is the temperature and y-axis is the relative signal difference and first derivative of the fluorescence. Three standards 1:1, 2:1, and 2:2 are shown along with the 1051 DNA at 4 and 9 weeks of culture. DNA from patient's leucocytes (fresh blood) was used as assay control.

The RFLP analysis was also carried out for the 1042 cell line (data in appendix II) and the results are summarized below in table 12.

As both the HRM assays and microsatellite marker analysis failed to show any change in genotype for the two other mutation studied, T4826I and R2452W, RFLP analysis was not carried out for these two mutations.

3.4.2 Microsatellite analysis

Haplotype analysis also involved the use of two highly polymorphic microsatellite markers, D19S220 [132] and D19S47 [133] which are tightly linked to the *RYR1* gene. The two sets of DNA samples were genotyped for the two markers.

3.4.2.1 D19S220

For the microsatellite D19S220, PCR reactions were carried out using Phusion™ high-fidelity DNA polymerase (Finnzymes, Espoo, Finland) as described in section 2.2.7.1. The gel image obtained after electrophoresis of the PCR products is shown in Figure 24.

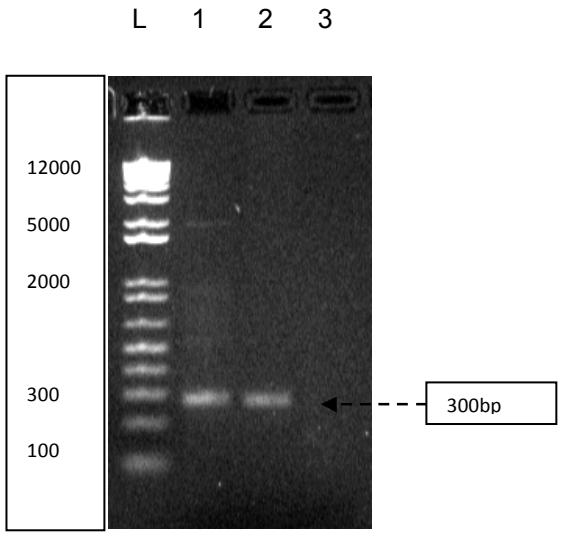

Figure 24. HRM assay for the three RFLPs using the cell line 1051

L-1 Kb plus DNA ladder™

1- 1051 DNA at 4 weeks culture

2- 1051 DNA at 9 weeks culture

3- Blank (MQ water)

10% of the PCR products were loaded onto a 1% agarose gel in 1X TAE buffer. The gel was stained with 0.3 µg/mL ethidium bromide. Electrophoresis was carried out for 50 min at 90 V.

The PCR products show a single strong band at about 300 bp, which is the expected size of the amplicon for D19S220 microsatellite. PCR products were separated by capillary electrophoresis on the ABI3730 Genetic Analyzer as described in section 2.2.7.1 and the resultant chromatogram was analysed using the peak scanner v1.0 software.

3.4.2.2 D19S47

The microsatellite D19S47 was PCR amplified using the FastStart *Taq* polymerase (Roche Diagnostics GmbH, Mannheim, Germany), described in section 2.2.7.1. Figure 25 shows the gel image obtained after electrophoresis of the PCR products.

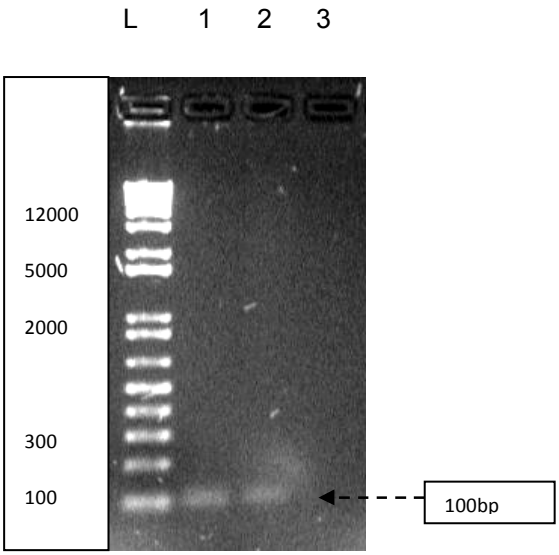

Figure 25 PCR of D19S47 with FastStart Taq polymerase

L-1 Kb plus DNA ladder™

1- 1051 DNA at 4 weeks culture

2- 1051 DNA at 9 weeks culture

3- Blank (MQ water)

10% of the PCR products were loaded onto a 1% agarose gel in 1X TAE buffer. The gel was stained with 0.3µg/mL ethidium bromide. Electrophoresis was carried out for 50 min at 90 V.

The PCR products show a single strong band at about 100 bp, which is the expected amplicon size for D19S47 microsatellite. PCR products were separated by capillary electrophoresis on the ABI3730 Genetic Analyzer as described in section 2.2.7.1 and the resultant chromatogram was analysed using the peak scanner v1.0 software. Figure 26, Figure 27 and Figure 28 show the chromatograms obtained from the DNA at 4 weeks culture, the leucocyte DNA and DNA at 9 weeks culture, respectively.

a. Chromatogram for 1051 DNA at 4 weeks culture

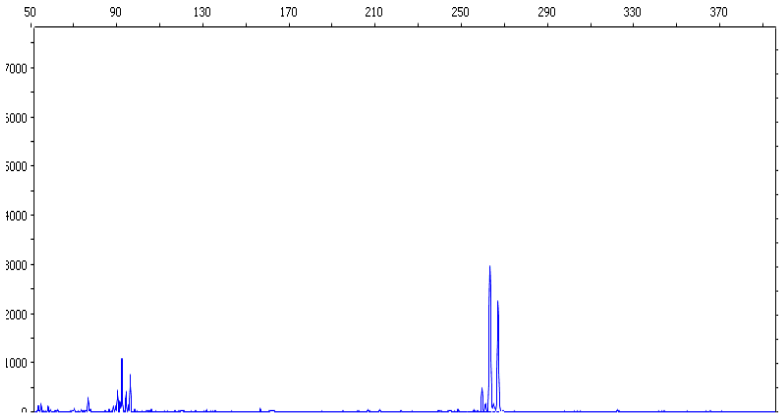

b. Data table for 'a'.

B,30	B12_dianab.7.1051	76.66	224	2008	1750
B,31	B12_dianab.7.1051	88.5	88	623	1878
B,32	B12_dianab.7.1051	90.35	331	3088	1898
B,33	B12_dianab.7.1051	92.39	805	7212	1920
B,34	B12_dianab.7.1051	94.34	278	1995	1941
B,35	B12_dianab.7.1051	96.28	562	4779	1962
B,36	B12_dianab.7.1051	262.06	65	440	3883
B,37	B12_dianab.7.1051	263.96	861	6251	3906
B,38	B12_dianab.7.1051	264.79	253	1502	3916
B,39	B12_dianab.7.1051	265.87	5403	42227	3929
B,40	B12_dianab.7.1051	267.78	4021	30133	3952
O,1	B12_dianab.7.1051	12.5	62	550	988
O,2	B12_dianab.7.1051	13.4	127	1243	999

Figure 26. Chromatogram for D19S47 and D19S220 with 4 week cultured 1051 cell line

a. x-axis in the chromatogram represents size of the products in basepairs and y-axis is the height of the peaks.

b. Data table for genotyping with the two markers for 4 week cultured 1051 DNA.

The chromatogram in Figure 26a shows two main peaks for both the microsatellite markers. For D19S47 two main peaks are observed at 92 bp and 96 bp (data table in figure 25b). For D19S220 two main peaks are observed at 265 bp and 267 bp. These represent the sizes of the microsatellite on the two alleles at that locus and indicate that the patient from whom the DNA was isolated was heterozygous for both the markers. The size of the PCR products obtained after genotyping was compared to the allele size in Tables 9 and 10 (section 2.2.7.1) and the allele combination found for the patient 1051 was 8,6 and 1,2 for D19S47 and D19S220, respectively. DNA isolated from fresh leucocytes from the patient was used as an assay control and the chromatogram obtained from the leucocyte DNA (figure 27a

and b) suggests two main peaks for the two microsatellites of the same size as that obtained from the lymphocytes after 4 weeks culture.

a. Chromatogram for 1051 DNA from fresh blood

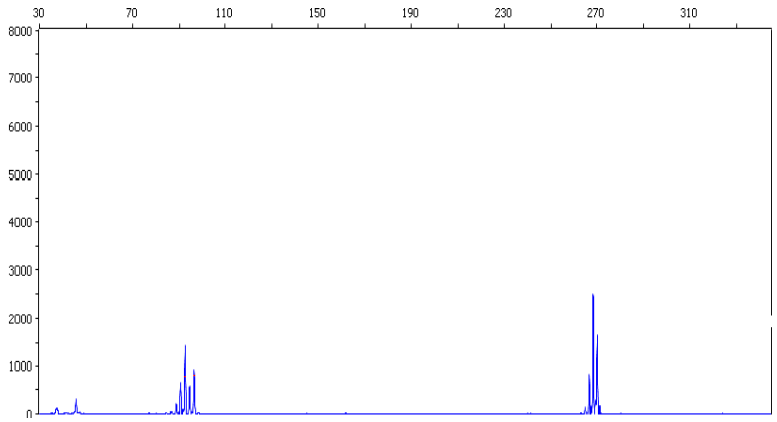

b. Data table for 'a'.

B,19	C12_dianab.7.1051Blood_	84.49	78	533	1826
B,20	C12_dianab.7.1051Blood_	86.45	236	1616	1847
B,21	C12_dianab.7.1051Blood_	88.41	797	5747	1868
B,22	C12_dianab.7.1051Blood_	90.37	2595	20285	1889
B,23	C12_dianab.7.1051Blood_	92.33	6054	50413	1910
B,24	C12_dianab.7.1051Blood_	94.29	2325	17885	1931
B,25	C12_dianab.7.1051Blood_	96.35	3888	31066	1953
B,26	C12_dianab.7.1051Blood_	98.31	121	805	1974
B,27	C12_dianab.7.1051Blood_	263.98	206	1402	3889
B,28	C12_dianab.7.1051Blood_	265.89	1431	11256	3912
B,29	C12_dianab.7.1051Blood_	267.73	1130	11523	3934
B,30	C12_dianab.7.1051Blood_	269.06	225	1691	3950
O,1	C12_dianab.7.1051Blood_	12.7	101	1024	981
O,2	C12_dianab.7.1051Blood_	13.59	191	1835	992
O,3	C12_dianab.7.1051Blood_	17.81	580	5131	1044
O,4	C12_dianab.7.1051Blood_	19.59	1301	12141	1066

Figure 27. Chromatogram for D19S47 and D19S220 with 1051 DNA from fresh leucocytes

a. *Chromatogram for D19S47 and D19S220 obtained from leucocyte DNA from the patient*

x-axis represents size of the products in basepairs and y-axis is the height of the peaks.

b. Data table for genotyping with the two markers for leucocyte DNA

The chromatogram obtained from DNA isolated from lymphocytes after 9 weeks culture showed different results (figure 28). Two peaks were observed for both the microsatellites indicating that the DNA was heterozygous for both markers (figure 28a). For D19S47 the two main peaks are observed at 88 bp and 96 bp and for D19S220 two main peaks are observed at 271 bp and 277 bp (Data table in figure 28b).

When the sizes were compared with the allele size in Tables 9 and 10 (section 2.2.7.1), the allele combination was found to change to 9,6 and 4,7 for D19S47 and D19S220, respectively, as compared to 8,6 and 1,2 genotype obtained for the DNA at 4 weeks culture and the control leucocyte DNA.

a. Chromatogram for 1051 DNA at 9 weeks culture

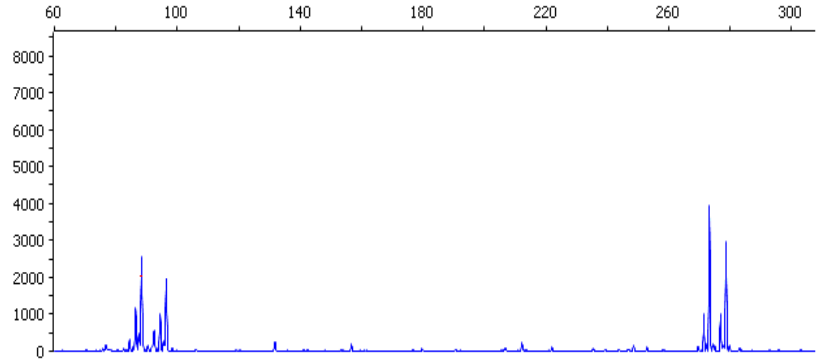

b. Data table for 'a'.

B,30	A12_dianab.7.1051	82.54	57	364	1808
B,31	A12_dianab.7.1051	84.49	233	1698	1829
B,32	A12_dianab.7.1051	86.45	892	7827	1850
B,33	A12_dianab.7.1051	88.41	1940	17947	1871
B,34	A12_dianab.7.1051	90.37	113	823	1892
B,35	A12_dianab.7.1051	92.42	428	4221	1914
B,36	A12_dianab.7.1051	94.38	726	5620	1935
B,37	A12_dianab.7.1051	96.35	1494	13071	1956
B,38	A12_dianab.7.1051	131.75	180	1354	2356
B,39	A12_dianab.7.1051	156.73	148	1070	2621
B,48	A12_dianab.7.1051	270.62	125	722	3972
B,49	A12_dianab.7.1051	271.62	2882	21611	3984
B,50	A12_dianab.7.1051	272.87	151	1643	3999
B,51	A12_dianab.7.1051	275.45	754	6645	4030
B,52	A12_dianab.7.1051	277.36	2211	17548	4053
B,53	A12_dianab.7.1051	278.61	122	937	4068
B,54	A12_dianab.7.1051	281.94	60	567	4108
B,55	A12_dianab.7.1051	415.56	58	542	5722

Figure 28. Chromatogram for D19S47 and D19S220 with 9 week cultured 1051 cell lines

a. x-axis represents size of the products in basepairs and y-axis is the height of the peaks.

b. b. Data table for genotyping with the two markers for 4 week cultured 1051 DNA.

The experiments were repeated at least twice for all the DNA samples to confirm the accuracy of the results. The same experiment was repeated for the 1042 cell line (shown in appendix) and the results are summarized in table 12. The Microsatellite analysis was also carried out for the T4826I and the R2452W cell lines. (Data not shown). No changes in the microsatellites were found between the DNA isolated at different times in culture for either of the cell lines.

DNA sample	D19S220	Intragenic RFLPs			D19S47
		Ile^{1151}	Asp^{2729}	Ser^{2862}	
1051 DNA					
4 weeks culture	1,2	2:2	2:2	1:1	8,6
DNA from leucocytes	1,2	2:2	2:2	1:1	8,6
9 weeks culture	4,7	1:1	2:1	1:2	6,9
1042 DNA					
4 weeks culture	2,6	2:2	2:2	1:1	6,7
DNA from leucocytes	2,6	2:2	2:2	1:1	6,7
9 weeks culture	4,7	1:1	2:1	1:2	6,9

Table 12. Summary of the genotyping results for 1051 and 1042 cell lines

As shown in the table above the genotyping of the two cell lines, 1051 and 1042, the markers D19S220, Ile^{1151}, Asp^{2729}, Ser^{2862} and D19S47 indicated a change in genotype for both the cell lines. As both 1051 and 1042 are obtained from MHS patients belonging to the same family (1051 being the maternal aunt of 1042), similar haplotypes were obtained from the DNA isolated from fresh leucocytes and EBV-immotalized lymphocytes after 4 weeks of culture. The haplotype 2-2-2-1-6 for the markers D19S220, Ile^{1151}, Asp^{2729}, Ser^{2862} and D19S47, respectively, coincides with the inheritance of MHS phenotype in this family. But a change in the haplotype was observed for both the cell lines after 9 weeks of culture, especially on the 5' end of the gene (Table 13).

1051	**1042**
1 2 2, 2 2, 2 1, *1* *8, 6*	2, 6 2, 2 2, 2 1, 1 6, 7
After 9 weeks	
4, 7 1, 1	4, 7 1, 1
2, 1 1, 2 6, 9	2, 1 1, 2 6, 9

Table 13. Haplotypes for 1051 and 1042 cell lines

Haplotypes as obtained by the genotyping of the two cell lines for the markers D19S220, Ile^{1151}, Asp^{2729}, Ser^{2862} and D19S47.

3.6 Calcium release assays

Another objective of this study focussed on functional analysis of two uncharacterized CCD mutations (cell lines from patients confirmed with CCD) which might potentially exist on the *RYR1* gene.

Demonstration of an altered calcium release in the cell lines using RyR1 agonists would be the first step in determining if the mutations exist in the *RYR1* so that further studies into identification of a potential mutation and further functional

analysis could be carried out. Although the majority of CCD mutations have been identified on the *RYR1* gene [115] there are potential mutations in the genes encoding the adjacent DHPR channel as well as over 30 other proteins involved in the cellular calcium homeostasis, which were not studied in this work.

In this study EBV-immortalized B-lymphocytes from two patients diagnosed with CCD were treated with, 4-CmC, a potent and specific activator of the RyR1 which has been used pharmacologically to discriminate between MHN and MHS as well as to functionally characterize different CCD mutations [134, 135]. Two cell lines obtained from patients studied along with a wildtype cell line (from a patient with no known MH or CCD mutation) which was used as a control to validate the assays.

Increasing concentrations of 4-CmC were added and sensitivities of lymphoblastoid cells were tested for each of the 3 cell lines in Ca^{2+}-free BSS medium. Changes in $[Ca^{2+}]_i$ were calculated using mean amount of Ca^{2+} released from each cell line from the patients harbouring suspected CCD mutations and the control cell line with no *RYR1* mutation.

The results were expressed as percentage release of Ca^{2+} in response to different concentrations of 4-CmC with respect to the maximal release of calcium by 0.1% triton X-100 (Figure 29).

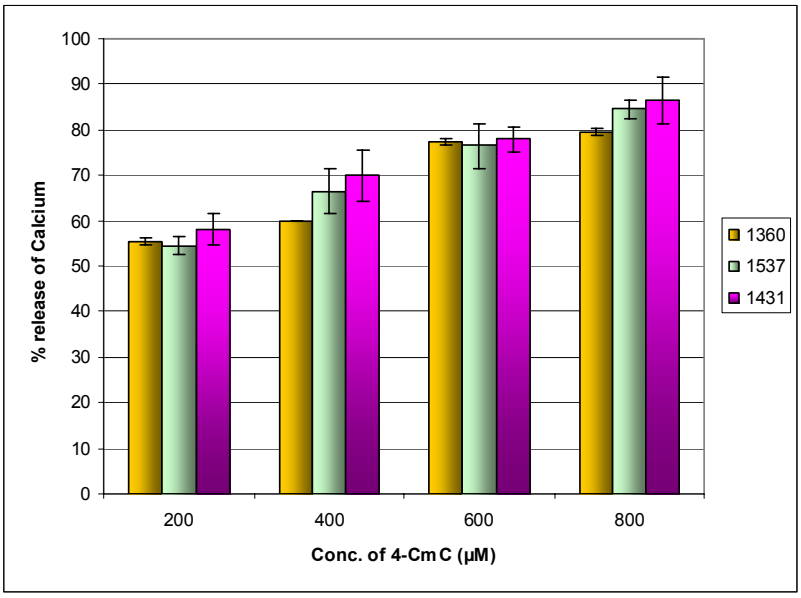

Figure 29 . Calcium release stimulated by 4-CmC in human B-lymphoblastoid cell lines

EBV immortalized B-lymphocytes from 3 cell lines, 1360,1431 (both harbouring suspected CCD mutations) and 1537 (control, with no known MH or CCD mutation) were treated with increasing concentrations of 4-CmC in Ca^{2+}-free BSS buffer. The increases in $[Ca^{2+}]_i$ indicated were calculated as percentage of the maximal amount released by 0.1% triton X-100. (± S.E)

Each cell line showed maximal response at 800 µM 4-CmC. No significant difference in Ca^{2+} release was observed between the three cell lines, and all the three cell lines, including the MHN cell line (1537), showed about 50% release of of the total releasable calcium at 200 µM, which is regarded as a low agonist concentration in some studies using lymphoblastoid cell lines. MHN cell lines are expected to show 50% releasable Ca^{2+} at about 400 µM 4-CmC [128]. The results presented are an average of 3 experiments and as more experiments could not be performed for want of time the data was not sufficient to establish if a significant difference exists between the between the 3 cell lines. Also, resting Ca^{2+} concentrations and sensitivity to thapsigargin-sensitive stores using 400 nM were not calculated for the three cell lines which could suggest a difference between the three cell lines in intracellular Ca^{2+} homeostasis.

4. DISCUSSION

The present study is based on an observation during the course of studies with EBV-immortalized human lymphoblastoid cell lines derived from peripheral blood lymphocytes of MH patients carrying the H4833Y mutation. The H4833Y mutation, which results from a C14997T transition has been established as a causative mutation for MH [136]. It was observed that cell lines, when initially cultured, were heterozygous for the mutation H4833Y, but seemed to lose the mutation after several weeks in culture [120].

Two cell lines with the H4833Y mutation were grown in culture for a period of 9-10 weeks. SNP genotyping carried out at various points during the culture showed loss of the mutation after about 9 weeks. This was confirmed using sequencing and further analysis was carried out on the DNA isolated initially and after 9 weeks of culture.

It has been reported previously that EBV-immortalized human lymphoblastoid cell lines from peripheral blood lymphocytes from healthy donors as well as from tissues derived from Burkitt lymphoma and chronic myeloid leukemia acquire chromosomal aberrations after prolonged culture (up to 1 year or more). Steel et al. (1977) studied 80 lymphoblastoid cell lines (including healthy adults, those with constitutional chromosomal aberrations, Burkitt lymphoma and lympho-reticular malignancies) and observed a non-random gain in the form of trisomy or partial trisomy for 5 autosomes (3, 7, 8, 9, 12) and the sex chromosomes. The genotype changes observed in the EBV-immortalized lymphocytes in this study occurred after about 9 weeks in culture and appeared to be mutation specific [137].

Loss of heterozygosity and microsatellite instability *in vivo* has been extensively studied and implicated in a number of tumours and inherited cancers. Loss of heterozygosity is essentially the loss of a functional allele at any heterozygous locus. The loss of heterozygosity can be due to multi locus chromosomal events like deletions and mitotic recombinations, point mutations or gene conversions at a particular locus or epigenetic inactivation of the alleles [138, 139].

4.1 SNP genotyping

High resolution amplicon melting was used to carry out SNP genotyping of the DNA isolated from the different EBV-immortalized cell lines at different time points.

Gundry et al. (2003) introduced HRM analysis for genotyping and mutation scanning using fluorescent labelled primers [140]. A closed-tube system for mutation scanning was then developed using generic saturating double stranded DNA-binding dyes, thus avoiding the use of expensive fluorescent-labelled primers [141].

In this study LightCycler® 480 genotyping software which uses the LightCycler® 480 HRM master dye was used to identify different sequence variants. Normalized and temperature shifted difference plots and different melting curves were used to differentiate the homozygous samples from the heterozygous ones. Although PCR products as large as 544 bp have been genotyped [140], it has been suggested that shorter amplicons are more reliable for HRM assays [142-144]. In the present study reasonably short PCR amplicons were used which varied in size between 77 and 102 base pairs for the 3 mutations studied.

All assays showed unambiguous results differentiating heterozygous samples from homozygous ones. The results obtained showed the loss of heterozygosity (reversion to wildtype) for the H4833Y mutation. This was later double-checked using a hybridization probe assay specific for the mutation (section 3.2).

The results of the SNP genotyping were then confirmed by sequencing of the region of the gene containing the mutation for both sets of DNA samples. Sequencing results showed that the transition C14997T had reverted back to wildtype ‘C’. Interestingly, the sequencing did not show any other difference between the two sets of DNA samples in the ~500 bp region sequenced. Recombination repair was thus thought of as a potential mechanism for the observed reversion to ‘wildtype’ genotype.

4.2 Haplotype analysis

An attempt was made to study the *RYR1* gene beyond the region of the mutation to try and detect any other changes in the genotype between the two sets of DNA samples and also to check whether recombination repair was a possible mechanism for the observed reversion of the point mutation. Further genotyping studies were carried out using microsatellite markers and intragenic RFLPs.

4.2.1 Restriction fragment length polymorphisms

Three intragenic RFLPs were used for genotyping. Although RFLPs are not as polymorphic as the microsatellite markers with only two alleles possible, they were studied in order to establish any other detectable change within the *RYR1* gene between the two samples. HRM assay was used for RFLP genotyping. The three control DNA samples, genotypes of which were established by conventional RFLP analysis were used as melting standards [10]

As described in section 2.2.4, HRM assays clearly differentiate between heterozygous and homozygous samples but also between two different types of homozygous DNA samples (in this case samples classed as 1:1 and 2:2).

For the RFLP Ile^{1151}, DNA isolated after 4-weeks of culture of the EBV-immortalized cell lines (1051 and 1042) showed that they were homozygous with the restriction site present on both the alleles (2:2). But after about 9 weeks of culture both the cell lines had acquired a different genotype. The DNA showed a completely changed genotype (1:1), indicating that it had lost the restriction site for *Taq* I on both the alleles (figure 23a). For RFLP Asp^{2729}, the results indicated that the cell lines after about 9 weeks in culture had lost the restriction site for *Cfo I* on one of the alleles (figure 23b). A similar change was also found for the RFLP Ser^{2862} after 9-10 weeks in culture wherein the genotype changed from an initial 1:1 to 1:2, thus gaining the restriction site for *Fok* I at one of the alleles (figure 23c).

The patients from whom the two cells lines were obtained belong to the same family, one generation apart, which explains the RFLP haplotypes being the same initially. Although it is interesting to note that the cell lines exhibit similar RFLP changes after about 9 weeks in culture.

All the three RFLPs studied occur as a result of transition mutations (C-T or T-C). Transitions can occur spontaneously due to tautomerization, oxidative deamination and insertion of natural or artificial base-analogues. Tautomerization occurs when the DNA bases undergo tautomeric shifts thus changing the base pairing. For example tautomerization of the the amino ($-NH_2$) group on adenine forms an imino (NH) form in which adenine basepairs with cytosine rather than the normal thymine. As the base pairing is unstable, in the next replication cycle adenine returns to the normal state and basepairs with thymine and the cytosine basebairs with guanine. Thus, changing an A-T pair to a G-C. Similar tautomeric shifts can occur when the keto forms of thymine and guanine are converted into enol tautomers. Chemicals like nitrous acid can cause oxidative deamination of the bases. Adenine for example can undergo oxidative deamination to give hypoxanthine which in its keto form can basepair with cytocine. Thus, a normal A-T pair changes to H-C (where H is hypoxanthine), which in the next replication cycle changes back to a G-C pair. Base analogues can easily be incorporated into the DNA strand instead of the normal bases during replicatin leading to transitions. For example 5-bromo uracil (5'-BU) in its keto form is a structural analogue of thymine and can basepair with adenine, but in its rare enol form it basepairs with guanine. The unstable basepairing is usually reversed in the next replication cycle when guanine pairs with the normal cytosine leading to the AT-GC transition.

Although there are twice as many possible transversions, transitions are more commonly observed within the genome. This is because they result due to substitution of chemically similar bases (purine:purine or pyrimidine:pyrimidine) and thus are less likely to result in amino acid substitutions (and if they do they usually result in chemically similar amino acids). Therefore, they are more likely to persist and hence are more frequently observed in populations as single nucleotide polymorphisms (SNPs) than are transversions.

Changes in the RFLP genotype indicate point mutations being introduced at different regions within the *RYR1* gene and do not indicate recombination repair as being a potential mechanism.

4.2.2 Microsatellite markers

Genotyping was also carried out using microsatellites. Microsatellite markers are considered more informative than RFLPs as they exhibit greater polymorphism and a large number of possible alleles for the same locus. For example, one of the microsatellites studied (D19S220) had a total of 10 different alleles.

Two highly polymorphic chromosome 19 microsatellite markers, both $(CA)_n$ dinucleotide repeats, were used for genotyping. Two different cell lines (1051 and 1042) established from patients with the H4833Y mutation were studied. Both the patients were heterozygous for the two microsatellite markers which flank the *RYR1* gene (figure 11; section 2.2.7). After 9 weeks of culture the LCLs showed expansion of the microsatellite on both the alleles (Table 12) indicating insertion/duplication of the dinucleotide repeats. The observed expansion of the microsatellites indicating insertion mutations, are in agreement with a number of studies carried out on microsatellite mutations.

Previous studies on microsatellite mutations, most of which involve $(CA)_n$-dinucleotide repeats, have suggested that rates of insertion of repeats leading to microsatellite expansion are higher than deletions [145, 146]. Xu et al (2000) reported the role of allele length in microsatellite expansion and contraction, with shorter allele lengths showing a bias towards expansion [147]. Weber et al (1993) studied 28 microsatellite markers for chromosome 19 (using both transformed and untransformed lymphocytes*)* including 15 CA-dinucleotide repeats and 12 $(GATA)_n$-tetranucleotide repeats and observed a heavy bias towards insertions [148].

DNA polymerase slippage during replication is understood to be the major mechanism resulting in microsatellite mutations [149]. Amos et al. (1996, 1998) reported increased rates of mutations in microsatellites that are heterozygous especially with large difference in the microsatellite length between the two alleles (heterozygote instability) [145, 150]. In the present study although both the cell lines were heterozygous for both the microsatellites, the difference between the length of the two alleles was not large. For the 1051 cell lines the haplotype was 1,2 and 8,6 for D19S220 and D19S47, respectively. Microsatellite analysis rules out

recombination repair as expansion of both the alleles cannot be explained by this mechanism.

Also, it is interesting to note that although D19S220 marker is at a greater genetic distance (~0.8cM) to *RYR1* than D19S47 (~0.5cM), greater expansion for the marker was observed for both the cell lines compared to D19S47. This indicates changes in genotype are not likely to be linked to the mutation under study or the *RYR1* gene itself. Haplotype analysis also suggest that the cell lines seem to retain the same haplotype after 9 weeks in culture at the 3' end of the gene in spite of losing the mutation, but greater changes in the haplotype are seen at the 5' end of the gene (Table 13, section 3.4.2).

Also, the fact that both the microsatellite markers and the RFLPs showed two alleles for both sets of DNA samples, the possibility of allele fallout during PCR could also be ruled out.

It must also be mentioned that the observed loss of heterozygosity could also be due to contamination of the cell lines in culture.

4.3 Functional assays

Mutations causing MH and CCD are known to disrupt normal calcium homeostasis. This can be studied using pharmacologic RyR1 activators like caffeine, halothane, 4-Chloro-*m*-cresol and ryanodine. The "gold standard" for MH diagnosis, the *IVCT*, measures the sensitivity of RyR1 to caffeine and halothane. Functional assays for diagnosis of MH have long been suggested as an alternative to the IVCT but have not yet been established as an accepted diagnostic tool for MH susceptibility.

Several studies have established the use of RyR agonists including 4-CmC and ryanodine to study change in Ca^{2+} homeostasis. Increased sensitivity of the RyR1 to lower agonist concentrations combined with an the increase in resting $[Ca^{2+}]_i$ levels is considered to be indication of increased channel activity. 4-CmC is a chlorocresol and is a specific and a potent activator of RyR1. It was first used as an activator for RyR1-mediated calcium release in 1993 [151] and has been used to differentiate between MHS and MHN in muscle samples and immortalized lymphocytes in recent years as well as in the functional analysis of CCD mutations

[54, 55, 134, 152-154]. In this study cell lines from two CCD patients were used to test the response to the RyR1 agonist 4-CmC using fura-2 as the indicator of Ca^{2+} release (section 3.6). In addition, the release of Ca^{2+} at 200 µM was considered higher than that which would normally be expected for CCD.

The results were preliminary and largely inconclusive as it was not possible to make a distinction between the Ca^{2+} release by the two mutants and the wild-type cell line, with no known MH/CCD mutation, in response to 4-CmC.

Also to be considered is that although B-lymphocytes have been used for Ca^{2+} release assays it is accepted that sensitivity of lymphocytes to RyR1 agonists is lower than the muscles. Apart from the reduced expression of the *RYR1* in the ER of lymphocytes compared to the SR, another reason could be the difference in the RyR1 conformation between the ER and the SR membranes. While the RyR1s are present diffusely in the ER in the SR they are tightly packed and coupled to the DHPRs in a precise manner [51].

Expression studies using dysgenic myotubes have shown that most of the CCD mutations, especially those in the NH_2-terminal of RyR1 lead to varying degrees of SR Ca^{2+} leak [53, 128, 154]. This results in store depletion and low resting $[Ca^{2+}]_i$ levels thus reducing calcium release in response to agonists. Studies on some of the mutations in the pore region (COOH-terminus) have suggested that these lead to EC-uncoupling, which results in reduced voltage-gated Ca^{2+} release with no detectable store depletion. A study involving 7 CCD mutations in exon 102 of the *RYR1* gene using dyspedic (RyR1-knockout) myotubes showed reduced (almost 90% reduced) voltage-gated Ca^{2+} release with no SR Ca^{2+} store depletion or change in resting Ca^{2+} suggesting EC-uncoupling mechanism [155].

As a number of studies have linked CCD mutations to EC-uncoupling mechanism mentioned above it would be important to study the voltage-gated SR Ca^{2+} release, i.e., the voltage dependence of the calcium release from the SR. Avila and Dirksen (2001) used whole-cell patch clamp technique to measure voltage-gated L-currents in myotubes expressing the mutations studied [156]. CCD mutations have also been shown to lead to a reduced sensitivity to Ca^{2+} induced Ca^{2+} release [157]. Also, functional assays using B-lymphocytes cannot be used to assess mutations

on the *CACNA1S* gene encoding the α1-subunit of DHPR as the gene is not known to be expressed in lymphocytes.

In summary, the present study could establish a loss of heterozygosity for the point mutation H4833Y on the *RYR1* gene in EBV-immortalized cell lines after several weeks in culture. Further changes in the genotype of the cell lines was also observed in the study by haplotype analysis using two microsatellite markers flanking the *RYR1* gene and three intragenic RFLPs. As the genotype changes were limited to one specific mutation and not observed in other mutations studied during the same period, the phenomenon seems to be mutation-specific.

The DNA isolated from the two cell lines carrying the H4833Y mutation were sent to the Cyto-Molecular Genetic Services Laboratory, Wellington Hospital, for array comparative genomic hybridization (aCGH) and results are awaited. aCGH is a microarray based genomic hybridization technique which can detect DNA copy number variations and submicroscopic deletions and duplications within chromosomes and generate high resolution karyotypes *in silico* (virtual karyotyping) from the DNA. It could be interesting to compare the results with the results from Steel et al (1977) which suggested that 5 autosomes (3, 7, 8, 9, 12) and the sex chromosomes seemed to gain chromosomal aberrations more often than the other chromosomes in the karyotype.

For the functional assays on the two cell lines with potential causative mutations for CCD, as several reports on CCD mutations identified suggest defects in the voltage-gated Ca^{2+} release as a possible mechanism it would be useful to study the voltage dependence of SR Ca^{2+} release in myoblasts obtained from the two patients. Further studies could also be carried out to study the Ca^{2+}-induced Ca^{2+} release which has also been shown to be altered in some CCD mutations.

Also, the assays using lymphocytes could include studies on the thapsigargin-sensitive stores and resting Ca^{2+} concentrations along with dose-response relationship with the agonists as these would also give an indication regarding any difference in Ca^{2+} homeostasis that exists between the three cell lines.

5. REFERENCES

1. Stowell, K.M., *Malignant hyperthermia: a pharmacogenetic disorder.* Pharmacogenomics, 2008. **9**(11): p. 1657-1672.
2. Rosenberg, H., et al., *Malignant hyperthermia.* Orphanet Journal of Rare Diseases, 2007. **2**: p. 21.
3. Robinson, R., et al., *Mutations in RYR1 in malignant hyperthermia and central core disease.* Human Mutation, 2006. **27**(10): p. 977-989.
4. Davis, M., et al., *Malignant hyperthermia associated with exercise-induced rhabdomyolysis or congenital abnormalities and a novel RYR1 mutation in New Zealand and Australian pedigrees.* British Journal of Anaesthesia, 2002. **88**(4): p. 508-515.
5. Nishio, H., et al., *Identification of malignant hyperthermia-susceptible ryanodine receptor type 1 gene (RYR1) mutations in a child who died in a car after exposure to a high environmental temperature.* Legal Medicine, 2009. **11**(3): p. 142-143.
6. Robinson, R.L., et al., *A genome wide search for susceptibility loci in three European malignant hyperthermia pedigrees.* Human Molecular Genetics, 1997. **6**(6): p. 953-961.
7. Maclennan, D.H., et al., *Ryanodine receptor gene is a candidate for predisposition to malignant hyperthermia.* Nature, 1990. **343**(6258): p. 559-561.
8. Ibarra, C.A., et al., *Malignant hypethermia in Japan - Mutation screening of the entire ryanodine receptor type 1 gene coding region by direct sequencing.* Anesthesiology, 2006. **104**(6): p. 1146-1154.
9. Monnier, N., et al., *Presence of two different genetic traits in malignant hyperthermia families - Implication for genetic analysis, diagnosis, and incidence of malignant hyperthermia susceptibility.* Anesthesiology, 2002. **97**(5): p. 1067-1074.
10. Brown, R.L., et al., *A novel ryanodine receptor mutation and genotype-phenotype correlation in a large malignant hyperthermia New Zealand Maori pedigree.* Human Molecular Genetics, 2000. **9**(10): p. 1515-1524.
11. Britt, B.A., *Malignant hyperthermia.* Canadian Anaesthetists Society Journal, 1985. **32**(3): p. S40-S41.
12. Maclennan, D.H. and M.S. Phillips, *Malignant hyperthermia.* Science, 1992. **256**(5058): p. 789-794.
13. Denborough, M., *Malignant hyperthermia.* Lancet, 1998. **352**(9134): p. 1131-1136.
14. Denborough, M.A., *Malignant hyperthermia.* Anesthesiology, 2008. **108**(1): p. 156-157.
15. Denborough, M.A. and R.R.H. Lovell, *Anaesthetic deaths in a family.* Lancet, 1960. **2**(JUL2): p. 45-45.
16. Denborough, M.A., et al., *Anaesthetic deaths in a family.* British Journal of Anaesthesia, 1962. **34**(6): p. 395-&.
17. MacLennan, D.H., *Ca^{2+} signalling and muscle disease.* European Journal of Biochemistry, 2000. **267**(17): p. 5291-5297.
18. Nelson, T.E., *Porcine malignant hyperthermia - critical-temperatures for in vivo and in vitro responses.* Anesthesiology, 1990. **73**(3): p. 449-454.
19. Fletcher, J.E., H. Rosenberg, and M. Aggarwal, *Comparison of European and North American malignant hyperthermia diagnostic protocol outcomes for use in genetic studies.* Anesthesiology, 1999. **90**(3): p. 654-661.
20. Krause, T., et al., *Dantrolene - A review of its pharmacology, therapeutic use and new developments.* Anaesthesia, 2004. **59**(4): p. 364-373.

21. Wappler, F., *Malignant hyperthermia.* European Journal of Anaesthesiology, 2001. **18**(10): p. 632-652.
22. Nelson, T.E., et al., *Dantrolene sodium can increase or attenuate activity of skeletal muscle ryanodine receptor calcium release channel - Clinical implications.* Anesthesiology, 1996. **84**(6): p. 1368-1379.
23. Parness, J. and S.S. Palnitkar, *Identification of dantrolene binding-sites in porcine skeletal-muscle sarcoplasmic-reticulum.* Journal of Biological Chemistry, 1995. **270**(31): p. 18465-18472.
24. Sengupta, C., U.A. Meyer, and E. Carafoli, *Binding of dantrolene sodium to muscle intracellular membranes.* Febs Letters, 1980. **117**(1): p. 37-38.
25. Paul-Pletzer, K., et al., *The dantrolene binding site on the skeletal muscle ryanodine receptor comprises amino acids 590-609.* Biophysical Journal, 2002. **82**(1): p. 394.
26. El-Hayek, R., et al., *A postulated role of the near amino-terminal domain of the ryanodine receptor in the regulation of the sarcoplasmic reticulum Ca^{2+} channel.* Journal of Biological Chemistry, 1999. **274**(47): p. 33341-33347.
27. Phillips, M.S., et al., *The structural organization of the human skeletal muscle ryanodine receptor (RYR1) gene.* Genomics, 1996. **34**(1): p. 24-41.
28. McCarthy, T.V., et al., *Localization of the malignant hyperthermia susceptibility locus to human-chromosome 19q12-13.2.* Nature, 1990. **343**(6258): p. 562-564.
29. Lynch, P.J., et al., *Identification of heterozygous and homozygous individuals with the novel RYR1 mutation Cys35Arg in a large kindred.* Anesthesiology, 1997. **86**(3): p. 620-626.
30. McCarthy, T.V., K.A. Quane, and P.J. Lynch, *Ryanodine receptor mutations in malignant hyperthermia and central core disease.* Human Mutation, 2000. **15**(5): p. 410-417.
31. Sambuughin, N., et al., *Screening of the entire ryanodine receptor type 1 coding region for sequence variants associated with malignant hyperthermia susceptibility in the North American population.* Anesthesiology, 2005. **102**(3): p. 515-521.
32. Broman, M., et al., *Mutation screening of the RYR1-cDNA from peripheral B-lymphocytes in 15 Swedish malignant hyperthermia index cases.* British Journal of Anaesthesia, 2009. **102**(5): p. 642-649.
33. Galli, L., et al., *Mutations in the RYR1 gene in Italian patients at risk for Malignant Hyperthermia: evidence for a cluster of novel mutations in the C-terminal region.* Cell Calcium, 2002. **32**(3): p. 143-151.
34. Monnier, N., et al., *Malignant-hyperthermia susceptibility is associated with a mutation of the alpha(1)-subunit of the human dihydropyridine-sensitive L-type voltage-dependent calcium-channel receptor in skeletal muscle.* American Journal of Human Genetics, 1997. **60**(6): p. 1316-1325.
35. Carpenter, D., et al., *The role of CACNA1S in predisposition to malignant hyperthermia.* Bmc Medical Genetics, 2009. **10**.
36. Carafoli, E., *Intracellular Calcium Homeostasis.* Annual Review of Biochemistry, 1987. **56**: p. 395-433.
37. Kraev, A., I. Chumakov, and E. Carafoli, *The organization of the human gene NCX1 encoding the sodium-calcium exchanger.* Genomics, 1996. **37**(1): p. 105-112.
38. Jorgensen, A.O., et al., *Ultrastructural-localization of calsequestrin in rat skeletal-muscle by immunoferritin labeling of ultrathin frozen-sections.* Journal of Cell Biology, 1983. **97**(5): p. 1573-1581.
39. Pozzan, T., et al., *Molecular and cellular physiology of intracellular calcium stores.* Physiological Reviews, 1994. **74**(3): p. 595-636.
40. Brini, M., et al., *Effects of PMCA and SERCA pump overexpression on the kinetics of cell Ca2+ signalling.* Embo Journal, 2000. **19**(18): p. 4926-4935.

41. Flucher, B.E., et al., *Triad formation - organization and function of the sarcoplasmic-reticulum calcium-release channel and triadin in normal and dysgenic muscle in-vitro.* Journal of Cell Biology, 1993. **123**(5): p. 1161-1174.
42. Sandow, A., *Excitation-contraction coupling in muscular response.* Yale Journal of Biology and Medicine, 1952. **25**(3): p. 176-&.
43. Protasi, F., et al., *Multiple Regions of RyR1 Mediate Functional and Structural Interactions with [alpha]1S-Dihydropyridine Receptors in Skeletal Muscle.* Biophysical Journal, 2002. **83**(6): p. 3230-3244.
44. Jurkat-Rott, K., T. McCarthy, and F. Lehmann-Horn, *Genetics and pathogenesis of malignant hyperthermia.* Muscle & Nerve, 2000. **23**(1): p. 4-17.
45. Nakai, J., et al., *Enhanced dihydropyridine receptor channel activity in the presence of ryanodine receptor.* Nature, 1996. **380**(6569): p. 72-75.
46. Galinska-Rakoczy, A., et al., *Structural Basis for the Regulation of Muscle Contraction by Troponin and Tropomyosin.* Journal of Molecular Biology, 2008. **379**(5): p. 929-935.
47. Catterall, W.A., *Excitation contraction coupling in vertebrate skeletal-muscle - a tale of 2 calcium channels.* Cell, 1991. **64**(5): p. 871-874.
48. Larach, M.G., *Standardization of the caffeine halothane muscle contracture test.* Anesthesia and Analgesia, 1989. **69**(4): p. 511-515.
49. Ording, H., et al., *In vitro contracture test for diagnosis of malignant hyperthermia following the protocol of the European MH Group: Results of testing patients surviving fulminant MH and unrelated low-risk subjects.* Acta Anaesthesiologica Scandinavica, 1997. **41**(8): p. 955-966.
50. EMHG, E.M.H.G., *A protocol for the investigation of malignant hyperthermia susceptibility.* British Journal of Anaesthesia, 1984. **56**: p. 1267-1269.
51. McKinney, L.C., et al., *Characterization of ryanodine receptor-mediated calcium release in human B cells.* Anesthesiology, 2006. **104**(6): p. 1191-1201.
52. Querfurth, H.W., et al., *Expression of ryanodine receptors in human embryonic kidney (HEK293) cells.* Biochemical Journal, 1998. **334**: p. 79-86.
53. Treves, S., et al., *Alteration of intracellular Ca2+ transients in COS-7 cells transfected with the cdna-encoding skeletal-muscle ryanodine receptor carrying a mutation associated with malignant hyperthermia.* Biochemical Journal, 1994. **301**: p. 661-665.
54. Girard, T., et al., *B-lymphocytes from Malignant Hyperthermia-susceptible Patients Have an Increased Sensitivity to Skeletal Muscle Ryanodine Receptor Activators.* Journal of Biological Chemistry, 2001. **276**(51): p. 48077-48082.
55. Sei, Y., K.L. Gallagher, and A.S. Basile, *Skeletal muscle type ryanodine receptor is involved in calcium signaling in human B lymphocytes.* Journal of Biological Chemistry, 1999. **274**(9): p. 5995-6002.
56. Wehner, M., et al., *Increased sensitivity to 4-chloro-m-cresol and caffeine in primary myotubes from malignant hyperthermia susceptible individuals carrying the ryanodine receptor 1 Thr2206Met (C6617T) mutation.* Clinical Genetics, 2002. **62**(2): p. 135-146.
57. Yang, T.Z., et al., *Functional defects in six ryanodine receptor isoform-1 (RyR1) mutations associated with malignant hyperthermia and their impact on skeletal excitation-contraction coupling.* Journal of Biological Chemistry, 2003. **278**(28): p. 25722-25730.
58. Klingler, W., et al., *Detection of proton release from cultured human myotubes to identify malignant hyperthermia susceptibility.* Anesthesiology, 2002. **97**(5): p. 1059-1066.
59. Ellis, F.R., *A protocol for the investigation of malignant hyperpyrexia (mh) susceptibility.* British Journal of Anaesthesia, 1984. **56**(11): p. 1267-1269.

60. Deufel, T., *Discordance, in a malignant hyperthermia pedigree, between in-vitro contracture-test phenotypes and haplotypes for the mhs1 region on chromosome comprising the c1840t transition in the ryr1 gene.* American Journal of Human Genetics, 1995. **57**(2): p. 520-520.
61. Fortunato, G., et al., *A case of discordance between genotype and phenotype in a malignant hyperthermia family.* European Journal of Human Genetics, 1999. **7**(4): p. 415-420.
62. Fill, M. and J.A. Copello, *Ryanodine receptor calcium release channels.* Physiological Reviews, 2002. **82**(4): p. 893-922.
63. Airey, J.A., et al., *3 Ryanodine receptor isoforms exist in avian striated muscles.* Biochemistry, 1993. **32**(22): p. 5739-5745.
64. Murayama, T. and Y. Ogawa, *Roles of Two Ryanodine Receptor Isoforms Coexisting in Skeletal Muscle.* Trends in Cardiovascular Medicine, 2002. **12**(7): p. 305-311.
65. Ogawa, Y., *Role of ryanodine receptors.* Critical Reviews in Biochemistry and Molecular Biology, 1994. **29**(4): p. 229-274.
66. Sorrentino, V. and P. Volpe, *Ryanodine receptors - how many, where and why.* Trends in Pharmacological Sciences, 1993. **14**(3): p. 98-103.
67. Hamilton, S.L., *Ryanodine receptors.* Cell Calcium, 2005. **38**(3-4): p. 253-260.
68. Otsu, K., et al., *Molecular-cloning of cDNA-encoding the Ca2+ release channel (ryanodine receptor) of rabbit cardiac-muscle sarcoplasmic-reticulum.* Journal of Biological Chemistry, 1990. **265**(23): p. 13472-13483.
69. Jeyakumar, L.H., et al., *Purification and characterization of ryanodine receptor 3 from mammalian tissue.* Journal of Biological Chemistry, 1998. **273**(26): p. 16011-16020.
70. Hakamata, Y., et al., *Primary structure and distribution of a novel ryanodine receptor calcium release channel from rabbit brain.* Febs Letters, 1992. **312**(2-3): p. 229-235.
71. Takeshima, H., et al., *Primary structure and expression from complementary-DNA of skeletal-muscle ryanodine receptor.* Nature, 1989. **339**(6224): p. 439-445.
72. Meissner, G., *Ryanodine receptor Ca^{2+} release channels and their regulation by endogenous effectors.* Annual Review of Physiology, 1994. **56**: p. 485-508.
73. Sharma, M.R., Wagenknecht, T, *Cryo-electron microscopy and 3D reconstruction of ryanodine receptors and their interactions with E-C coupling proteins.* Basic and Applied Myology, 2004. **14**(5): p. 299-306.
74. Radermacher, M., et al., *Cryo-electron microscopy and three-dimensional reconstruction of the calcium release channel/ryanodine receptor from skeletal muscle.* J. Cell Biol., 1994. **127**(2): p. 411-423.
75. Sharma, M.R., et al., *Three-dimensional structure of ryanodine receptor isoform three in two conformational states as visualized by cryo-electron microscopy.* Journal of Biological Chemistry, 2000. **275**(13): p. 9485-9491.
76. Sharma, M.R., et al., *Cryoelectron microscopy and image analysis of the cardiac ryanodine receptor.* Journal of Biological Chemistry, 1998. **273**(29): p. 18429-18434.
77. Ludtke, S.J., et al., *The pore structure of the closed RyR1 channel.* Structure, 2005. **13**(8): p. 1203-1211.
78. Zucchi, R. and S. RoncaTestoni, *The sarcoplasmic reticulum Ca^{2+} channel/ryanodine receptor: Modulation by endogenous effectors, drugs and disease states.* Pharmacological Reviews, 1997. **49**(1): p. 1-51.
79. Copello, J.A., et al., *Heterogeneity of Ca^{2+} gating of skeletal muscle and cardiac ryanodine receptors.* Biophysical Journal, 1997. **73**(1): p. 141-156.
80. Chen, S.R.W., L. Zhang, and D.H. Maclennan, *Characterization of a ca^{2+} binding and regulatory site in the ca^{2+} release channel (ryanodine receptor) of rabbit skeletal-muscle sarcoplasmic-reticulum*

Journal of Biological Chemistry, 1992. **267**(32): p. 23318-23326.
81. Zorzato, F., et al., *Molecular cloning of cDNA-encoding human and rabbit forms of the Ca^{2+} release channel (ryanodine rceptor) of skeletal muscle sarcoplasmic reticulum.* Journal of Biological Chemistry, 1990. **265**(4): p. 2244-2256.
82. Laver, D.R., T.M. Baynes, and A.F. Dulhunty, *Magnesium inhibition of ryanodine-receptor calcium channels: Evidence for two independent mechanisms.* Journal of Membrane Biology, 1997. **156**(3): p. 213-229.
83. Steele, D.S. and A.M. Duke, *Defective Mg^{2+} regulation of RyR1 as a causal factor in malignant hyperthermia.* Archives of Biochemistry and Biophysics, 2007. **458**(1): p. 57-64.
84. Meissner, G., *Adenine-nucleotide stimulation of Ca2+-induced Ca2+ release in sarcoplasmic-reticulum.* Journal of Biological Chemistry, 1984. **259**(4): p. 2365-2374.
85. Smith, J.S., R. Coronado, and G. Meissner, *A nucleotide stimulated calcium conducting channel from sarcoplasmic-reticulum incorporated into planar lipid bilayers.* Biophysical Journal, 1985. **47**(2): p. A451-A451.
86. el-Hayek, R., et al., *Activation of the Ca^{2+} release channel of skeletal muscle sarcoplasmic reticulum by palmitoyl carnitine.* Biophysical Journal, 1993. **65**(2): p. 779-789.
87. Dumonteil, E., H. Herre, and G. Meissner, *Effects of palmitoyl carnitine and related metabolites on the avian Ca2+-atpase and Ca2+ release channel.* Journal of Physiology-London, 1994. **479**(1): p. 29-39.
88. Meissner, G., *Regulation of mammalian ryanodine receptors.* Frontiers in Bioscience, 2002. **7**: p. D2072-D2080.
89. Tripathy, A., et al., *Calmodulin activation and inhibition of skeletal-muscle Ca2+ release channel (ryanodine receptor).* Biophysical Journal, 1995. **69**(1): p. 106-119.
90. Beard, N.A., et al., *Calsequestrin is an inhibitor of skeletal muscle ryanodine receptor calcium release channels.* Biophysical Journal, 2002. **82**(1): p. 310-320.
91. Cozens, B. and R.A.F. Reithmeier, *Size and shape of rabbit skeletal-muscle calsequestrin.* Journal of Biological Chemistry, 1984. **259**(10): p. 6248-6252.
92. Maclenna.Dh and P.T.S. Wong, *Isolation of a calcium-sequestering protein from sarcoplasmic reticulum (rabbit/deoxycholate/column chromatography/transport).* Proceedings of the National Academy of Sciences of the United States of America, 1971. **68**(6): p. 1231-&.
93. Lau, Y.H., A.H. Caswell, and J.P. Brunschwig, *Isolation of transverse tubules by fractionation of triad junctions of skeletal-muscle.* Journal of Biological Chemistry, 1977. **252**(15): p. 5565-5574.
94. Campbell, K.P., C. Franziniarmstrong, and A.E. Shamoo, *Further characterization of light and heavy sarcoplasmic-reticulum vesicles - identification of the sarcoplasmic-reticulum feet associated with heavy sarcoplasmic-reticulum vesicles.* Biochimica Et Biophysica Acta, 1980. **602**(1): p. 97-116.
95. Zhang, L., et al., *Complex formation between junction, triadin, calsequestrin, and the ryanodine receptor - Proteins of the cardiac junctional sarcoplasmic reticulum membrane.* Journal of Biological Chemistry, 1997. **272**(37): p. 23389-23397.
96. Donoso, P., H. Prieto, and C. Hidalgo, *Luminal calcium regulates calcium-release in triads isolated from frog and rabbit skeletal-muscle.* Biophysical Journal, 1995. **68**(2): p. 507-515.
97. Timerman, A.P., et al., *The Calcium-Release Channel Of Sarcoplasmic-Reticulum Is Modulated By Fk-506-Binding Protein - Dissociation And Reconstitution Of Fkbp-12 To*

The Calcium-Release Channel Of Skeletal-Muscle Sarcoplasmic-Reticulum. Journal of Biological Chemistry, 1993. **268**(31): p. 22992-22999.
98. Brillantes, A.M.B., et al., *Stabilization of calcium-release channel (ryanodine receptor) function by Fk506-binding protein.* Cell, 1994. **77**(4): p. 513-523.
99. Gregg, R.G., et al., *Assignment of the human gene for the alpha-1 subunit of the skeletal-muscle dhp-sensitive ca2+ channel (CACNLA3) to chromosome-1q31-q32.* Genomics, 1993. **15**(1): p. 107-112.
100. Gregg, R.G., P.A. Powers, and K. Hogan, *Assignment of the human gene for the beta-subunit of the voltage-dependent calcium-channel (CACNLB1) to chromosome-17 using somatic-cell hybrids and linkage mapping.* Genomics, 1993. **15**(1): p. 185-187.
101. Powers, P.A., et al., *Molecular characterization of the gene encoding the gamma-subunit of the human skeletal-muscle 1,4-dihydropyridine-sensitive ca2+ channel (CACNLG), cDNA sequence, gene structure, and chromosomal location.* Journal of Biological Chemistry, 1993. **268**(13): p. 9275-9279.
102. Powers, P.A., et al., *Localization of the gene encoding the alpha(2)/delta subunit (CACNL2A) of the human skeletal-muscle voltage-dependent ca2+ channel to chromosome 7q21-q22 by somatic-cell hybrid analysis.* Genomics, 1994. **19**(1): p. 192-193.
103. Hogan, K., *To Fire the Train: A Second Malignant-Hyperthermia Gene.* The American Journal of Human Genetics, 1997. **60**(6): p. 1303-1308.
104. Chaudhari, N., *A single nucleotide deletion in the skeletal muscle-specific calcium-channel transcript of muscular dysgenesis (mdg) mice.* Journal of Biological Chemistry, 1992. **267**(36): p. 25636-25639.
105. Tanabe, T., et al., *Regions of the skeletal-muscle dihydropyridine receptor critical for excitation contraction coupling.* Nature, 1990. **346**(6284): p. 567-569.
106. Lu, X.Y., L. Xu, and G. Meissner, *Activation of the skeletal-muscle calcium-release channel by a cytoplasmic loop of the dihydropyridine receptor.* Journal of Biological Chemistry, 1994. **269**(9): p. 6511-6516.
107. El-Hayek, R., et al., *Identification of Calcium Release-triggering and Blocking Regions of the II-III Loop of the Skeletal Muscle Dihydropyridine Receptor.* Journal of Biological Chemistry, 1995. **270**(38): p. 22116-22118.
108. Nakai, J., et al., *Two regions of the ryanodine receptor involved in coupling with L-type Ca2+ channels.* Journal of Biological Chemistry, 1998. **273**(22): p. 13403-13406.
109. Shy, G.M. and K.R. Magee, *A new congenital non-progressive myopathy.* Brain, 1956. **79**(4): p. 610-&.
110. Jungbluth, H., et al., *Autosomal recessive inheritance of RYR1 mutations in a congenital myopathy with cores.* Neurology, 2002. **59**(2): p. 284-287.
111. Manzur, A.Y., et al., *A severe clinical and pathological variant of central core disease with possible autosomal recessive inheritance.* Neuromuscular Disorders, 1998. **8**(7): p. 467-473.
112. Quinlivan, R.M., et al., *Central core disease: clinical, pathological, and genetic features.* Archives of Disease in Childhood, 2003. **88**(12): p. 1051-1055.
113. Lorenzon, N.M. and K.G. Beam, *Calcium channelopathies.* Kidney International, 2000. **57**(3): p. 794-802.
114. Romero, N.B., et al., *Dominant and recessive central core disease associated with RYR1 mutations and fetal akinesia.* Brain, 2003. **126**: p. 2341-2349.
115. Wu, S., et al., *Central core disease is due to RYR1 mutations in more than 90% of patients.* Brain, 2006. **129**(6): p. 1470-1480.

116. Monnier, N., et al., *Familial and sporadic forms of central core disease are associated with mutations in the C-terminal domain of the skeletal muscle ryanodine receptor.* Human Molecular Genetics, 2001. **10**(22): p. 2581-2592.
117. Treves, S., et al., *Congenital muscle disorders with cores: the ryanodine receptor calcium channel paradigm.* Current Opinion in Pharmacology, 2008. **8**(3): p. 319-326.
118. Engel, A.G., M.R. Gomez, and R.V. Groover, *Multicore disease - recently recognized congenital myopathy associated with multifocal degeneration of muscle fibers.* Mayo Clinic Proceedings, 1971. **46**(10): p. 666-&.
119. Moghadaszadeh, B., et al., *Mutations in SEPN1 cause congenital muscular dystrophy with spinal rigidity and restrictive respiratory syndrome.* Nature Genetics, 2001. **29**(1): p. 17-18.
120. Grievink, H., *Malignant hyperthermia: allele specific expression and mutation screening of the ryanodine receptor 1 : a dissertation presented to massey university in partial fulfilment of the requirements for the degree of doctor of philosophy in biochemistry*. 2009, Massey University: Palmerston North.
121. Neitzel, H., *A routine method for the establishment of permanent growing lymphoblastoid cell-lines.* Human Genetics, 1986. **73**(4): p. 320-326.
122. Grievink, H. and K.M. Stowell, *Identification of ryanodine receptor 1 single-nucleotide polymorphisms by high-resolution melting using the LightCycler 480 System.* Analytical Biochemistry, 2008. **374**(2): p. 396-404.
123. Erali, M., K.V. Voelkerding, and C.T. Wittwer, *High resolution melting applications for clinical laboratory medicine.* Experimental and Molecular Pathology, 2008. **85**(1): p. 50-58.
124. Wittwer, C.T., et al., *High-resolution genotyping by amplicon melting analysis using LCGreen.* Clinical Chemistry, 2003. **49**(6): p. 853-860.
125. Ellegren, H., *Microsatellites: Simple sequences with complex evolution.* Nature Reviews Genetics, 2004. **5**(6): p. 435-445.
126. Schultz, A.J., *Genetic characterization of malignant hyperthermia in New Zealand families.* 2009, Masssey University: Palmerston North.
127. Gillard, E.F., et al., *Polymorphisms and deduced amino-acid substitutions in the coding sequence of the ryanodine receptor (ryr1) gene in individuals with malignant hyperthermia.* Genomics, 1992. **13**(4): p. 1247-1254.
128. Ducreux, S., et al., *Functional properties of ryanodine receptors carrying three amino acid substitutions identified in patients affected by multi-minicore disease and central core disease, expressed in immortalized lymphocytes.* Biochemical Journal, 2006. **395**: p. 259-266.
129. Cavagna, D., et al., *Methyl p-hydroxybenzoate (E-218) a preservative for drugs and food is an activator of the ryanodine receptor Ca2+ release channel.* British Journal of Pharmacology, 2000. **131**(2): p. 335-341.
130. Grynkiewicz, G., M. Poenie, and R.Y. Tsien, *A new generation of Ca^{2+} indicators with greatly improved fluorescence properties.* Journal of Biological Chemistry, 1985. **260**(6): p. 3440-3450.
131. Lambert D, G., *Calcium Signalling Protocols*. 2nd edition ed. Methods in Molecular biology™, ed. G. Lambert D. 2006, NJ, Totowa: Humana Press.
132. Weissenbach, J., et al., *A second-generation linkage map of the human genome.* Nature, 1992. **359**(6398): p. 794-801.
133. Weber, J.L. and P.E. May, *Abundant class of human DNA polymorphisms which can be typed using the polymerase chain reaction.* American Journal of Human Genetics, 1989. **44**(3): p. 388-396.

134. Hermann-Frank, A., M. Richter, and F. Lehmann-Horn, *4-Chloro-m-cresol: A specific tool to distinguish between malignant hyperthermia-susceptible and normal muscle.* Biochemical Pharmacology, 1996. **52**(1): p. 149-155.
135. Lynch, P.J., et al., *A mutation in the transmembrane/luminal domain of the ryanodine receptor is associated with abnormal Ca^{2+} release channel function and severe central core disease.* Proceedings of the National Academy of Sciences of the United States of America, 1999. **96**(7): p. 4164-4169.
136. Anderson, A.A., et al., *Identification and Biochemical Characterization of a Novel Ryanodine Receptor Gene Mutation Associated with Malignant Hyperthermia.* Anesthesiology, 2008. **108**(2): p. 208-215 10.1097/01.anes.0000299431.81267.3e.
137. Steel, C.M., et al., *Non-random chromosome gains in human lymphoblastoid cell lines.* Nature, 1977. **270**(5635): p. 349-351.
138. Cappione, A.J., B.L. French, and G.R. Skuse, *A potential role for NF1 mRNA editing in the pathogenesis of NF1 tumors.* American Journal of Human Genetics, 1997. **60**(2): p. 305-312.
139. Metheny, L.J., A.J. Cappione, and G.R. Skuse, *Genetic and epigenetic mechanisms in the pathogenesis of neurofibromatosis type-I.* Journal of Neuropathology and Experimental Neurology, 1995. **54**(6): p. 753-760.
140. Gundry, C.N., et al., *Amplicon melting analysis with labeled primers: A closed-tube method for differentiating homozygotes and heterozygotes.* Clinical Chemistry, 2003. **49**(3): p. 396-406.
141. Wittwer, C.T., et al., *High-resolution genotyping by amplicon melting analysis using LC Green.* Clinical Chemistry, 2003. **49**(6): p. 853-860.
142. Liew, M., et al., *Genotyping of single-nucleotide polymorphisms by high-resolution melting of small amplicons.* Clinical Chemistry, 2004. **50**(7): p. 1156-1164.
143. Reed, G.H. and C.T. Wittwer, *Sensitivity and specificity of single-nucleotide polymorphism scanning by high-resolution melting analysis.* Clinical Chemistry, 2004. **50**(10): p. 1748-1754.
144. Zhou, L.M., et al., *High-resolution DNA melting analysis for simultaneous mutation scanning and genotyping in solution.* Clinical Chemistry, 2005. **51**(10): p. 1770-1777.
145. Amos, W., et al., *Microsatellites show mutational bias and heterozygote instability.* Nature Genetics, 1996. **13**(4): p. 390-391.
146. Twerdi, C.D., J.C. Boyer, and R.A. Farber, *Relative rates of insertion and deletion mutations in a microsatellite sequence in cultured cells.* Proceedings of the National Academy of Sciences of the United States of America, 1999. **96**(6): p. 2875-2879.
147. Xu, X., et al., *The direction of microsatellite mutations is dependent upon allele length.* Nature Genetics, 2000. **24**(4): p. 396-399.
148. Weber, J.L. and C. Wong, *Mutation of human short tandem repeats.* Human Molecular Genetics, 1993. **2**(8): p. 1123-1128.
149. Levinson, G. and G.A. Gutman, *Slipped-strand mispairing - a major mechanism for dna-sequence evolution.* Molecular Biology and Evolution, 1987. **4**(3): p. 203-221.
150. Amos, W. and J. Harwood, *Factors affecting levels of genetic diversity in natural populations.* Philosophical Transactions of the Royal Society of London Series B-Biological Sciences, 1998. **353**(1366): p. 177-186.
151. Zorzato, F., et al., *Chlorocresol: an activator of ryanodine receptor-mediated Ca^{2+} release.* Molecular Pharmacology, 1993. **44**(6): p. 1192-1201.
152. Ghassemi, F., et al., *A recessive ryanodine receptor 1 mutation in a CCD patient increases channel activity.* Cell Calcium, 2009. **45**(2): p. 192-197.

153. Richter, M., et al., *Functional characterization of a distinct ryanodine receptor mutation in human malignant hyperthermia-susceptible muscle.* Journal of Biological Chemistry, 1997. **272**(8): p. 5256-5260.
154. Tong, J.F., T.V. McCarthy, and D.H. MacLennan, *Measurement of resting cytosolic Ca^{2+} concentrations and Ca^{2+} store size in HEK-293 cells transfected with malignant hyperthermia or central core disease mutant Ca^{2+} release channels.* Journal of Biological Chemistry, 1999. **274**(2): p. 693-702.
155. Avila, G., K.M.S. O'Connell, and R.T. Dirksen, *The pore region of the skeletal muscle ryanodine receptor is a primary locus for excitation-contraction uncoupling in central core disease.* Journal of General Physiology, 2003. **121**(4): p. 277-286.
156. Avila, G. and R.T. Dirksen, *Functional effects of central core disease mutations in the cytoplasmic region of the skeletal muscle ryanodine receptor.* Journal of General Physiology, 2001. **118**(3): p. 277-290.
157. Du, G.G., et al., *Central core disease mutations R4892W, I4897T and G4898E in the ryanodine receptor isoform 1 reduce the Ca^{2+} sensitivity and amplitude of Ca^{2+}-dependent Ca^{2+} release.* Biochemical Journal, 2004. **382**: p. 557-564.

6. APPENDICES

APPENDIX- I

HybProbe assay for 1042 cell line

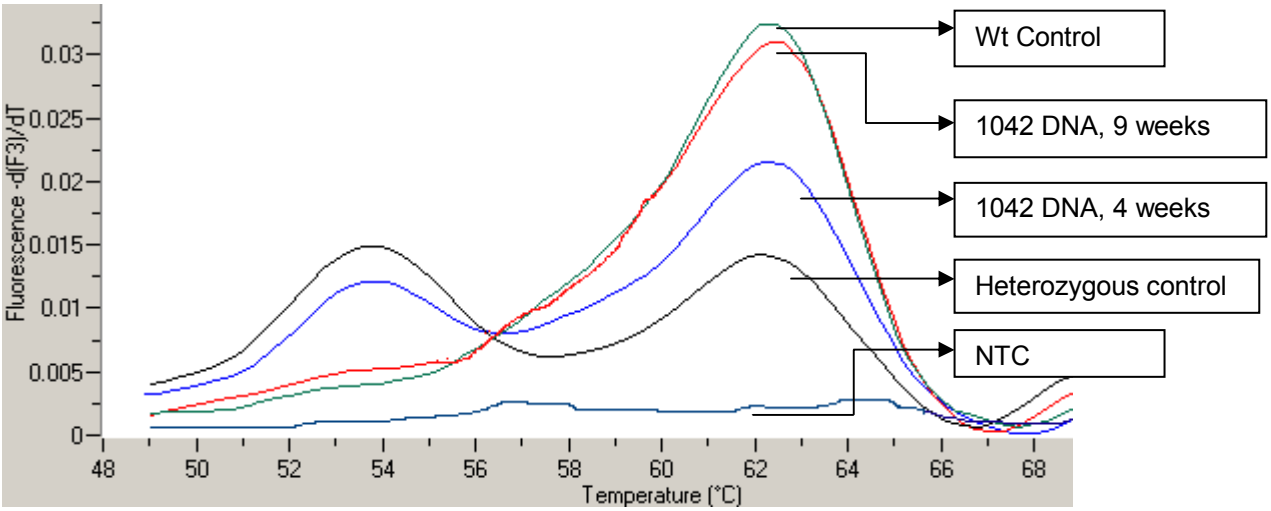

HybProbe assay for 1042 DNA

x-axis is the temperature and the y-axis is the third derivative of the fluorescence. Two melting standards used are the heterozygous control which is heterozygous for the H4833Y mutation (Black peaks) and wildtype control (green peak; negative for the mutation) . Wildtype control and the 1042 DNA at 9 weeks culture (red peak) show a single peak. Heterozygous control DNA and 1042 DNA at 4 weeks culture (blue peaks) show two peaks, one of which is at the same temperature as the wildtype control (negative standard).

APPENDIX- II

HRM assay for the three RFLPs using the 1042 cell line

a. Melting peaks for RFLP Ile^{1151}

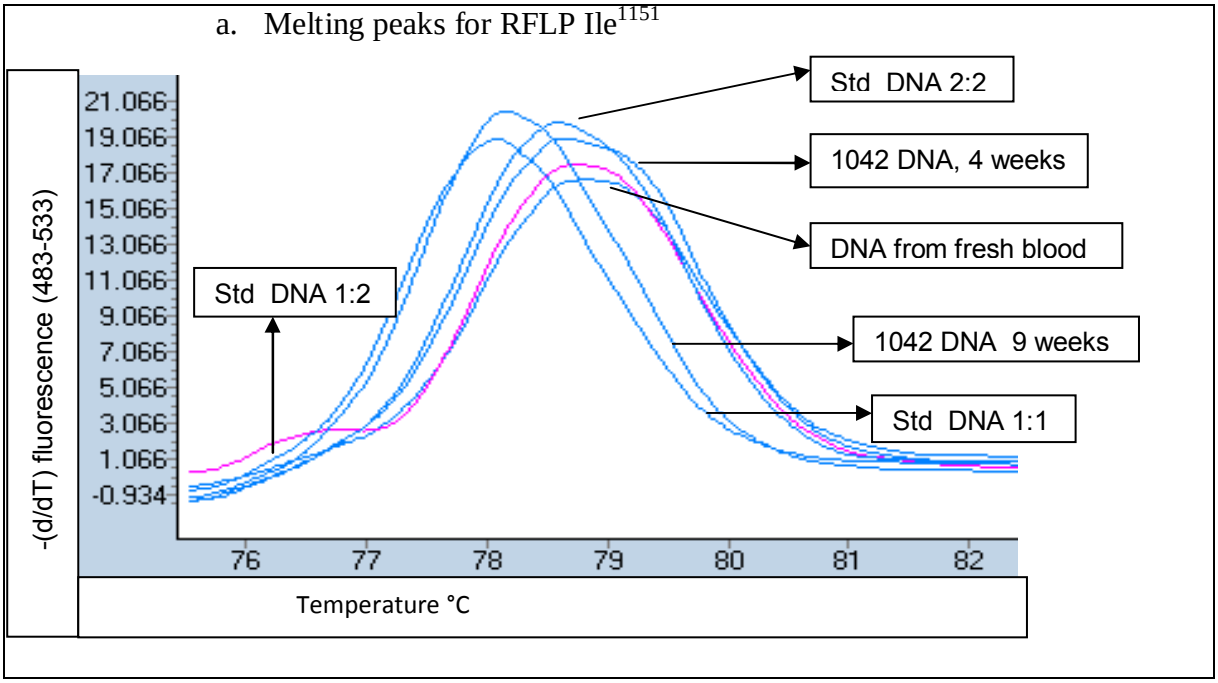

b. Melting peaks for RFLP Asp^{2729}

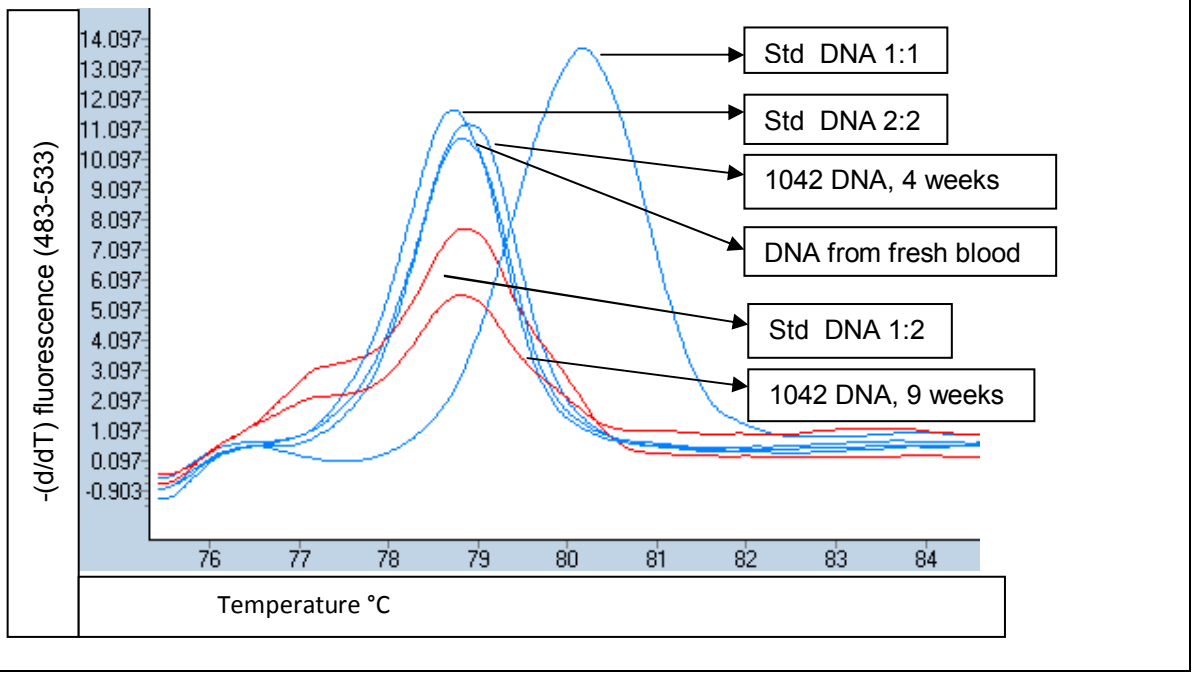

c. Melting peaks for RFLP Ser^{2862}

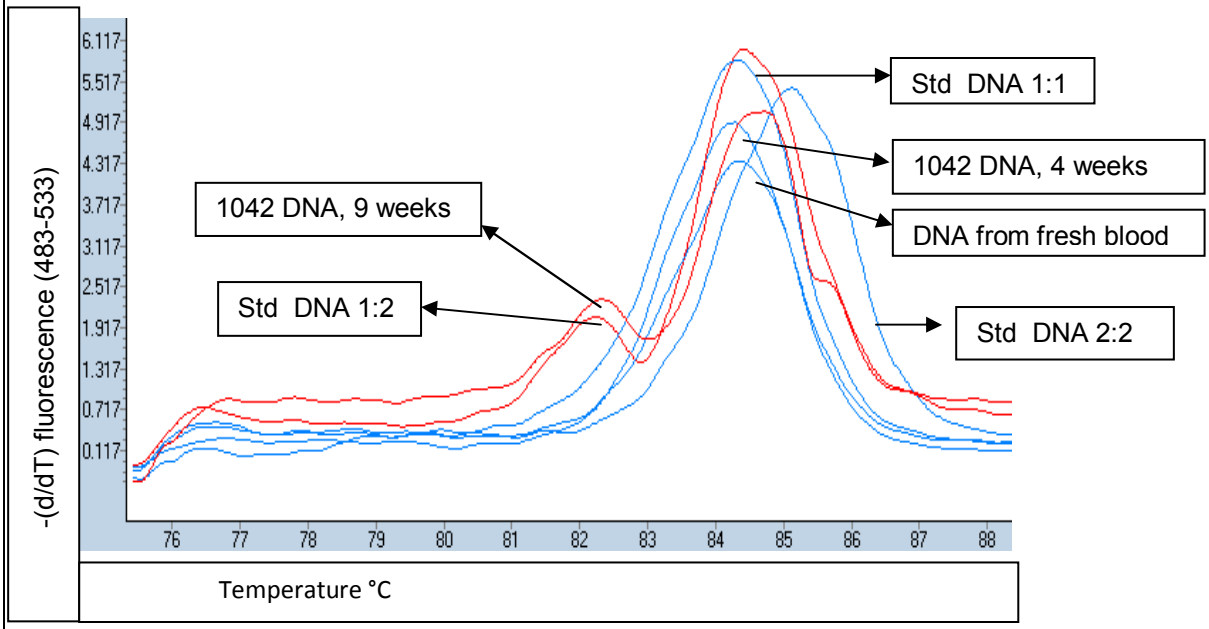

HRM assay for the three RFLPs using the cell line 1042

Melting peaks are shown for:

d. Ile^{1151}
e. Asp^{2729}
f. Ser^{2862}

The x-axis in is the temperature and the y-axis is relative signal difference and first derivative of the fluorescence. Three standards 1:1, 2:1, and 2:2 are shown along with the 1042 DNA at 4 and 9 weeks of culture. DNA from patient's leucocytes (fresh blood) was used as assay control.

APPENDIX-III

Sequencing results of exon 100

Sequencing of exon 100 using DNA isolated from 1051 cell line after 4 weeks culture with forwad and reverse primers. The SNP that causes the H4833Y aminoacid change (CAC-TAC) (seen here as 'Y' with forward and 'R' with reverse primer) is underlined. The codon encoding the H4833 (aminoacid) is highlighted in grey.

Forward primer

GGGTSATCTCTACAMACTTCTTCTTTGCTGCCCATCTCCTGGACATCGCCAT
GGGGGTCAAGACGCTGCGCACCATCCTGTCCTCTGTCACCYACAATGGGAA
ACAGGTGTGGGGAGGACCTGGCTGTGGGGCGTGGGCCAGCAGGGACCAG
CGTGGCAGTGGGTGGTGAAGGGATAAGGGCCGGGCAGCTGGGCTGAGGA
GGGGCAAGGCCAGGTGCGCTGAGCCGGGGGTGTGTGGGGCAGCAAGGTA
GAGCCACAGGGACTGAACCGGGGCCAGGACCCAGCATGGGCAGGGTGGG
GGGAGGGCAAGCCCAGGGCGGAGCTGACCTGGCCCCATCCTGCCCCCAG
CTGGTGATGACCGTGGGCCTTCTGGCGGTGGTCGTCTA

Reverse primer

GRRRRGRMYMYMMWMRWCTGGGGGCAGGATGGGGCCAGGTCAGCTCCG
CCCTGGGCTTGCCCTCCCCCCACCCTGCCCATGCTGGGTCCTGGCCCCGG
TTCAGTCCCTGTGGCTCTACCTTGCTGCCCCACACACCCCCGGCTCAGCGC
ACCTGGCCTTGCCCCTCCTCAGCCCAGCTGCCCGGCCCTTATCCCTTCACC
ACCCACTGCCACGCTGGTCCCTGCTGGCCCACGCCCCACAGCCAGGTCCT
CCCCACACCTGTTTCCCATTGTRGGTGACAGAGGACAGGATGGTGCGCAGC
GTCTTGACCCCCATGGCGATGTCCAGGAGATGGGCAGCAAAGAAGAAGTTG
TTGTAGTGTCCCAAGAGGGACATCACCATATACCAGCCCAGGTAW

Sequencing of exon 100 using DNA isolated from 1051 cell line after 9 weeks culture with forwad and reverse primers. The codon encoding the H4833 (aminoacid) is highlighted in grey.

Forward primer

AGGTATKGATCACACTTCTTCTTTGCTGCCCATCTCCTGGACATCGCCATGG
GGGTCAAGACGCTGCGCACCATCCTGTCCTCTGTCACCCACAATGGGAAAC
AGGTGTGGGGAGGACCTGGCTGTGGGGCGTGGGCCAGCAGGGACCAGCG
TGGCAGTGGGTGGTGAAGGGATAAGGGCCGGGCAGCTGGGCTGAGGAGG
GGCAAGGCCAGGTGCGCTGAGCCGGGGGTGTGTGGGGCAGCAAGGTAGA
GCCACAGGGACTGAACCGGGGCCAGGACCCAGCATGGGCAGGGTGGGGG
GAGGGCAAGCCCAGGGCGGAGCTGACCTGGCCCCATCCTGCCCCCAGCTG
GTGATGACCGTGGGCCTTCTGGCGGTGGTCGTCTACY

Reverse primer

GSGRRATWTMCRGCTGGGGGCAGGATGGGGCCAGGTCAGCTCCGCCCTG
GGCTTGCCCTCCCCCCACCCTGCCCATGCTGGGTCCTGGCCCCGGTTCAG
TCCCTGTGGCTCTACCTTGCTGCCCCACACACCCCCGGCTCAGCGCACCTG
GCCTTGCCCCTCCTCAGCCCAGCTGCCCGGCCCTTATCCCTTCACCACCCA
CTGCCACGCTGGTCCCTGCTGGCCCACGCCCCACAGCCAGGTCCTCCCCA
CACCTGTTTCCCATTGTGGGTGACAGAGGACAGGATGGTGCGCAGCGTCTT
GACCCCCATGGCGATGTCCAGGAGATGGGCAGCAAAGAAGAAGTTGTTGTA
GTGTCCCAAGAGGGACATCACCATATACCAGCCCAGGTAWAKGGTGACGTC
CCTCTYGGGACAYTACAAMAACYTCTTCTTTGCTGWCATCSKKGRATWTKRC
WGGGGGTSMAWKMTCTGCGCYMATCSGTCRSTKAACWWGWYSSAGYRGK
GKGGAARGGATC

Sequencing of exon 26-27, using DNA isolated from 1051 cell line after 4 weeks culture. RFLPIle^{1151} which results from an ATC-ATT change is in exon 26. The codon is highlighted in grey.

AMCGAMRAGGAMAGCRCTGGCACTTGGGCAGTGACCATTTGGGCGCCCCT
GGCAGCCGGGCGATGTCGTTGGCTGTATGATCGACCTCACAGAGAACACCA
TTATCTTCACCCTCAATGGCGAGGTCCTCATGTCTGACTCAGGCTCCGAAAC
AGCCTTCCGGGAGATTGAGATTGGGGACGGTGAGGGCTGAGACCCCTTCA
CATGCCCTTTCTTGTTTTCCTCTGTCTCTCCCAACCCTGCACTGCCCTTCTG
CCTCCAACTCTCCCATCCCTACCTCCTCCCCTCGGCTCCCTCTGCCCTGCC
CACCTGCCCTCACCCCTGCCCATCCATCCCCTCCCACCAGGCTTCCTGCCC
GTCTGCAGCTTGGGACCTGGCCAGGTGGGTCATCTGAACCTGGGCCAGGA
CGTGAGCTCTCTGAGGTTCTTTGCCATCTGTGGCCTCCAGGAAGGCTTCGA
GCCATTTGCCATCAACATGCAGCGCCCAGTCACCACCTGGTTCAGCAAAGG
CCTGCCCCAGTTTGAGCCAGTGCCCCTTGAACACCCTCACTATGAGGTAAG
GACTGAGCCCCTCAATGCCTTCTCATCTGCCTCCAAAGCTCCTTCCTTCCAC
AGTGCTCTTCTTTGAGTTTCTCTTTTCCCTCCATGTTAGGACACAAACCMAW
KKGRAAGCAAA

Sequencing of exon 26-27, using DNA isolated from 1051 cell line after 9 weeks culture. RFLPIle^{1151} which results from an ATC-ATT change is in exon 26. The codon is highlighted in grey.

CGGMSMAWWWGSMMMMSSSCTKGGCMTTGGGCAGTGAACCATTTGGGC
GCCCCTGGCAGCCGGGCGATGTCGTTGGCTGTATGATTGACCTCACAGAGA
ACACCATTATCTTCACCCTCAATGGCGAGGTCCTCATGTCTGACTCAGGCTC
CGAAACAGCCTTCCGGGAGATTGAGATTGGGGACGGTGAGGGCTGAGACC
CCTTCACATGCCCTTTCTTGTTTTCCTCTGTCTCTCCCAACCCTGCACTGCC
CTTCTGCCTCCAACTCTCCCATCCCTACCTCCTCCCCTCGGCTCCCTCTGCC
CTGCCCACCTGCCCTCACCCCTGCCCATCCATCCCCTCCCACCAGGCTTCC
TGCCCGTCTGCAGCTTGGGACCTGGCCAGGTGGGTCATCTGAACCTGGGC
CAGGACGTGAGCTCTCTGAGGTTCTTTGCCATCTGTGGCCTCCAGGAAGGC
TTCGAGCCATTTGCCATCAACATGCAGCGCCCAGTCACCACCTGGTTCAGC
AAAGGCCTGCCCCAGTTTGAGCCAGTGCCCCTTGAACACCCTCACTATGAG
GTAAGGACTGAGCCCCTCAATGCCTTCTCATCTGCCTCCAAAGCTCCTTCCT
TCCACAGTGCTCTTCTTTGAGTTTCTCTTTTCCCTCCATGTTAGGACACAAAC
CACATGGAAGCAAA

Sequencing of exon 44-47, using DNA isolated from 1051 cell line after 4 and 9 weeks of culture. Exon 46-47 is a region of the *RYR1* gene with a number of known polymorphisms. The sequencing results show no change in the sequence obtained from the two sets of DNA samples.

Sequencing after 4 weeks culture

CAAASGGWACCYASACMTTGKYTGGAACCCCTGTGGTGSMRAGCGCTACCT
GGACTTCCTGCGCTTTGCTGTCTTCKTCAACGGTGAGGAGGGGGTGGCAGT
GGCAKAGCGGGAAGTATGGAGTCACTGGTCACWCACCTCCCTCGAGATGA
CTGCTCGCACCCTGAGCCACAGATGGGGTCCAGGCAGGAATCCCTTCCAG
CAGGCCTGGGGCTGGCAGGGGCCTGTGTTACCCCTGGAGGTGTTGGGTCC
TGTGGCTGGCARTGTTGGATCCTGGGGCTGGCRGGASCCTGGTGWTACCC
CTAKAGGTGTTGGGTCCTGGGGCTGGCMKGGGCCTGGTGTTACCTCTGGA
GGTGTTGGGTCCTGGAGCTGGATGGGACCTGTGTTACCCCTGGASGTGTTG
GGTCCTGGGGMTGCATRGGSAGGTCTCTGATGGTGGCTCATGAGACCCCC
TTTCCCCATGCGGGTGGCCAGGCGAGAGCGTGSAGGAKAACGCCAMTGTG
GTGGTGCGGCTGCTCATCCGGAAGCCT

Sequencing after 9 weeks culture

CAAASGGTACCCASACATTGGCTGGAACCCCTGTGGTGGARAGCGCTACCT
GGACTTCCTGCGCTTTGCTGTCTTCGTCAACGGTGAGGAGGGGGTGGCAGT
GGCAGAGCGGGAAGTATGGAGTCACTGGTCACACACCTCCCTCGAGATGA
CTGCTCGCACCCTGAGCCACAGATGGGGTCCAGGCAGGAATCCCTTCCAG
CAGGCCTGGGGCTGGCAGGGGCCTGTGTTACCCCTGGAGGTGTTGGGTCC
TGTGGCTGGCAGTGTTGGATCCTGGGGCTGGCRGGRGCCTGGTGTTACYY

CTRGAGGTGTTGGGTCCTGGRGCTGGMWGGGRCCTGKKKTWMCCYYKGG
AGKKGTKGGKYCYKGGRSCTSRWKGGGASSTGTSTKAYSCCKGSWSRTGW
SRGSYCCTGKSGCMRYRTGGGKAGGTCTCYGATGGYGKMTMRTGARACSC
CMWTKYSCYRTGSSGGYKGCYMRTCSAGARCSYGGAGKRSAWCGSAMMYG
YSSTGSTGCGKSTGCTCRTCYSGAAGCYK

APPENDIX- IV

Microsatellite analysis with D19S47 and D19S220 using 1042 cell line

Chromatogram for D19S47 with DNA from fresh blood

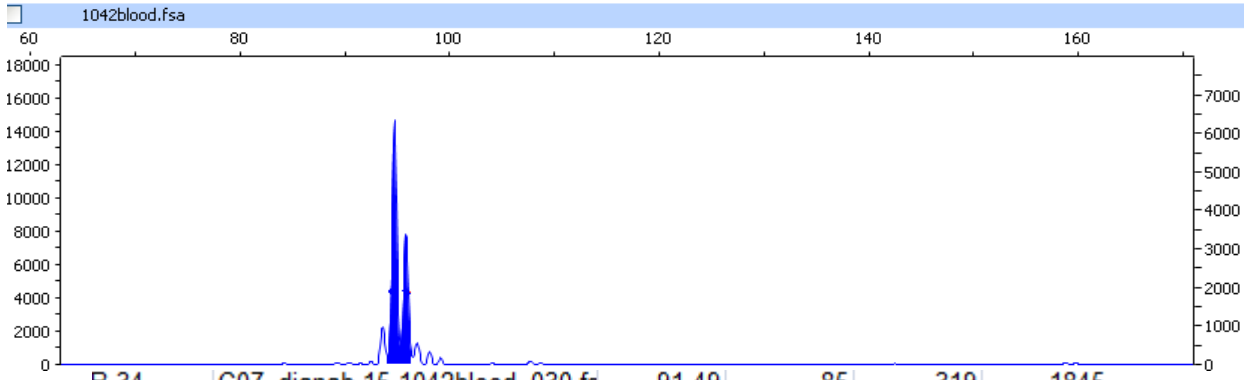

B,34	C07_dianab.15.1042blood_030.fs	91.49	85	319	1845
B,35	C07_dianab.15.1042blood_030.fs	92.52	206	806	1856
B,36	C07_dianab.15.1042blood_030.fs	93.64	2217	12595	1868
B,37	C07_dianab.15.1042blood_030.fs	94.76	14673	83107	1880
B,38	C07_dianab.15.1042blood_030.fs	95.79	7771	46227	1891
B,39	C07_dianab.15.1042blood_030.fs	96.91	1333	8062	1903
B,40	C07_dianab.15.1042blood_030.fs	98.13	794	3529	1916

Chromatogram for D19S220 with DNA from fresh blood

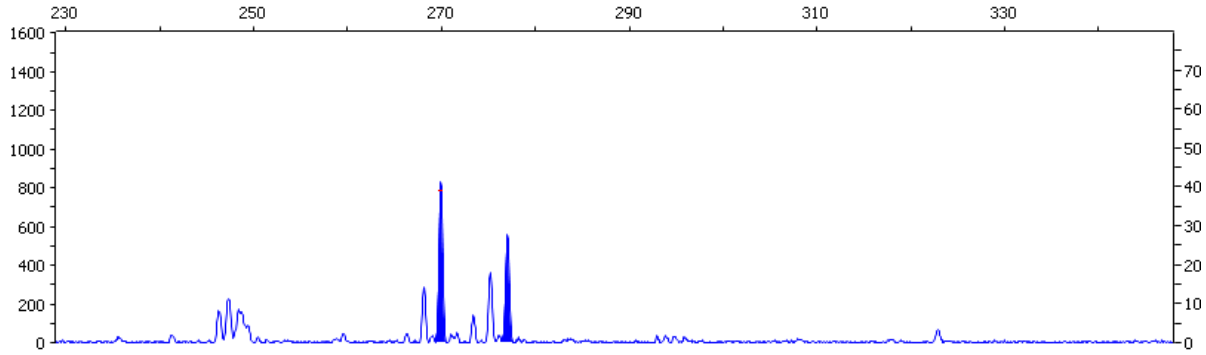

B,71	C07_dianab.15.1042blood_030.fs	265.89	366	2080	3848
B,72	C07_dianab.15.1042blood_030.fs	266.81	141	795	3859
B,73	C07_dianab.15.1042blood_030.fs	267.89	975	5601	3872
B,74	C07_dianab.15.1042blood_030.fs	269.72	67	296	3894
B,75	C07_dianab.15.1042blood_030.fs	271.55	161	866	3916
B,76	C07_dianab.15.1042blood_030.fs	272.47	53	247	3927
B,77	C07_dianab.15.1042blood_030.fs	273.47	463	2527	3939
B,78	C07_dianab.15.1042blood_030.fs	274.3	95	522	3949
B,79	C07_dianab.15.1042blood_030.fs	275.38	675	3757	3962
B,80	C07_dianab.15.1042blood_030.fs	293.43	50	257	4179
B,81	C07_dianab.15.1042blood_030.fs	294.43	57	306	4191

Chromatogram and data table for D19S47 with DNA isolated after 4 weeks culture

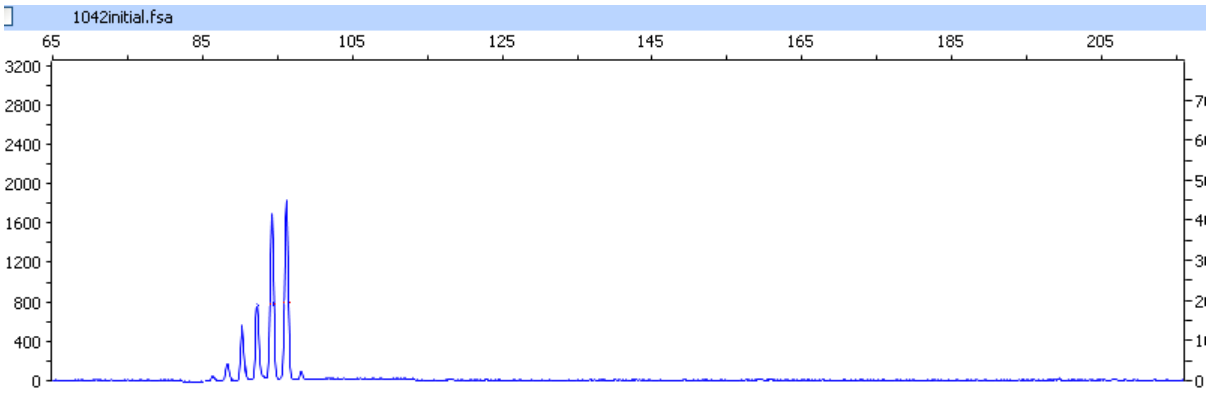

B,38	B01_dianab.14.1042initial_007.fs	90.37	6753	39498	1943
B,39	B01_dianab.14.1042initial_007.fs	92.35	9019	53163	1965
B,40	B01_dianab.14.1042initial_007.fs	94.33	14856	91299	1987
B,41	B01_dianab.14.1042initial_007.fs	96.31	15707	95419	2009
B,42	B01_dianab.14.1042initial_007.fs	98.29	58	1471	2788
B,43	B01_dianab.14.1042initial_007.fs	163.83	105	600	3312
B,44	B01_dianab.14.1042initial_007.fs	206.23	50	314	3378

Chromatogram and data table for D19S220 with DNA isolated after 4 weeks culture

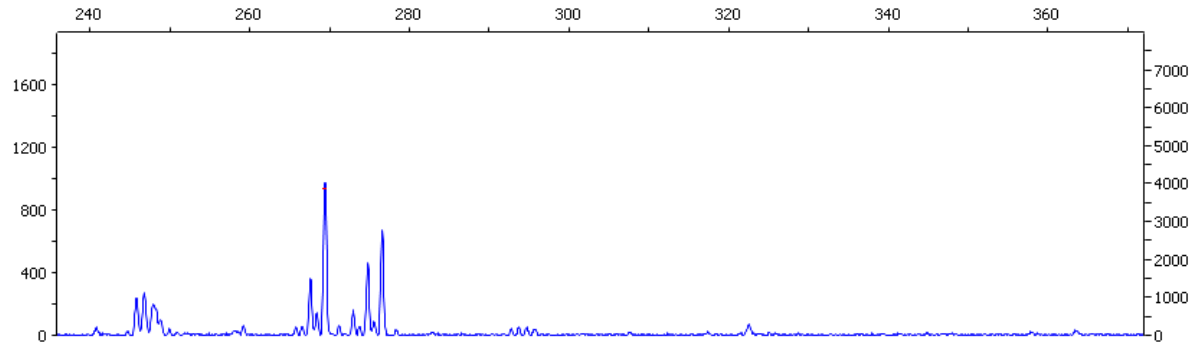

B,30	A07_dianab.15.1042initial_032.fs	266.83	107	524	3883
B,31	A07_dianab.15.1042initial_032.fs	267.83	898	4929	3895
B,32	A07_dianab.15.1042initial_032.fs	269.81	212	1150	3919
B,33	A07_dianab.15.1042initial_032.fs	270.64	53	192	3929
B,34	A07_dianab.15.1042initial_032.fs	271.72	173	635	983
B,35	A07_dianab.15.1042initial_032.fs	273.54	64	287	3964
B,36	A07_dianab.15.1042initial_032.fs	275.44	198	1176	3987
B,37	A07_dianab.15.1042initial_032.fs	276.27	53	291	3997

Chromatogram and the data table for D19S47 with DNA isolated after 9 weeks culture

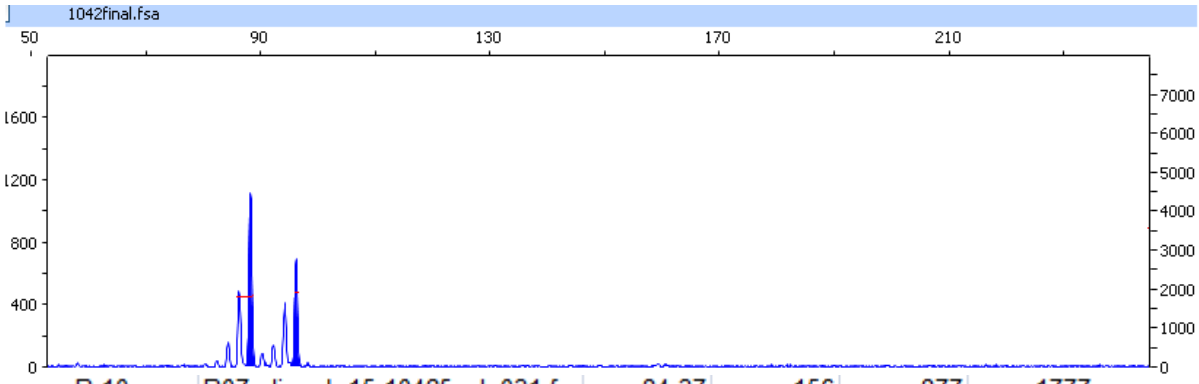

B,10	B07_dianab.15.1042final_031.fsa	84.37	156	877	1777
B,11	B07_dianab.15.1042final_031.fsa	86.23	486	3011	1797
B,12	B07_dianab.15.1042final_031.fsa	88.18	1110	6854	1818
B,13	B07_dianab.15.1042final_031.fsa	90.23	86	640	1840
B,14	B07_dianab.15.1042final_031.fsa	92.18	145	839	1861
B,15	B07_dianab.15.1042final_031.fsa	94.23	409	2604	1883
B,16	B07_dianab.15.1042final_031.fsa	96.18	693	4122	1904
B,17	B07_dianab.15.1042final_031.fsa	267.83	79	393	3888
B,18	B07_dianab.15.1042final_031.fsa	269.82	432	2460	3912

Chromatogram and the data table for D19S220 with DNA isolated after 9 weeks culture

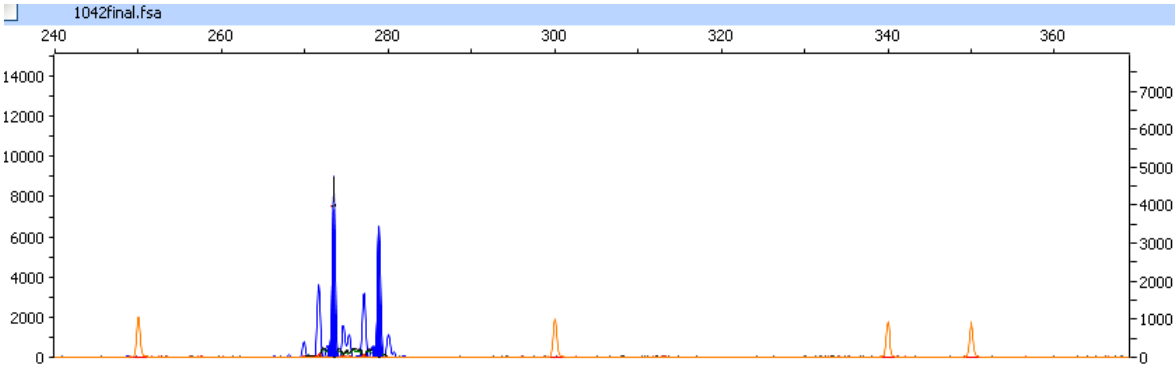

B,18	B07_dianab.15.1042final_031.fsa	269.82	432	2460	3912
B,19	B07_dianab.15.1042final_031.fsa	270.65	119	639	3922
B,20	B07_dianab.15.1042final_031.fsa	271.73	1042	5900	3935
B,21	B07_dianab.15.1042final_031.fsa	273.63	169	747	3958
B,22	B07_dianab.15.1042final_031.fsa	275.53	388	2131	3981
B,23	B07_dianab.15.1042final_031.fsa	276.28	81	464	3990
B,24	B07_dianab.15.1042final_031.fsa	277.44	763	4183	4004
B,25	B07_dianab.15.1042final_031.fsa	279.34	52	253	4027
O,1	B07_dianab.15.1042final_031.fsa	9.19	282	1665	889

APPENDIX-V

Primer sequences

Primer	Sequence (5'-3')
H4833Y Fwd	TCTCCTGGACATCGCC
H4833Y Rev	CACACCTGTTTCCCATTG
T4826I Fwd	ACTTCTTCTTTGCTGCC
T4826I Rev	GGTGACAGAGGACAGGAT
R2452W Fwd	CCTTCCCTCCCTCTACTC
R2452W Rev	CCACAAGGTCCTCCAAG
D19S47 Fwd	6-FAM-GATGTCTCCTTGGTAAGTTA
D19S47 Rev	AATACCTAGGAAGGGGAGGG
D19S220 Fwd	6-FAM-ATGTTCAGAAAGGCATGTCATTG
D19S220 Rev	TCCCTAACGGATACACAGCAACAC
Ile^{1151} Fwd	TCCATTTCTCTGTGTGTCTCC
Ile^{1151} Rev	AGGGTGAAGATAATGGTGTT
Asp^{2729} Fwd	ACTATGTGGATGCCTCATAC
Asp^{2729} Rev	GGGTCAGCAGATGTTGG
Ser^{2862} Fwd	GGGGTAGAATGGACTAGTGG
Ser^{2862} Rev	AGGATCAGGGCTCTCAC
26-27 F	TATATCTCTCCCTCCCTGCT
26-27 R	TTCCATGTGGTTTGTGTCCTA
43-45 F	GGTCTCAAGCTCCTGTTCA
43-45 R	CTGTCTTGGTCACTGTTGT
46-47 F	CTACCCTCCTGTGTGGTAA
46-47 R	TAACTGGAGGTCTTGGAGATTCCTA
50-52 F	TGTCTAGGACCACTCCTCAATA
50-52 R	GGTCTTGAGGGTTTCTTGGATA
55-58 F	CCCATCTTCCCCTTGTC
55-58 R	TCTCAGTCTCCTCCACTC
4826Fwd (exon 100-102)	CACAGTCCTTCCTGTACC
R4821H Rev (exon 100-102)	TGCGAGAAGGAAGCGTC
HybProbe 4833, 4826 F	CACAGTCCTTCCTGTACC
HybProbe 4833, 4826 R	GCCCTTCTCCCTTCACC

APPENDIX VI

Buffer composition

50x TAE buffer (for 1000mL volume) pH 8.0

Tris base.....242 g

Glacial acetic acid.....57.1 mL

EGTA.....100 mL

MQ (deionized) water.....up to 1000 mL

10x Balanced salt solution (BSS) (For 100 mL) pH 7.3

NaCl.....8.18 g

Kcl.....0.21 g

$MgCl_2$.....0.1 g

HEPES.....2.38 g

MQ water.....up to 100 mL

*$CaCl_2$ .....0.22 g

*Glucose.....1.8 g

(* added just prior to preparing the 1x solution)

10x Ca^{2+}-free balanced salt solution (For 100 mL) pH 7.3

NaCl.....8.18 g

Kcl.....0.21 g

$MgCl_2$.....0.1 g

HEPES.....2.38 g

$MgCl_2$.....0.02 g

EGTA.....0.08 g

Glucose.....1.8 g

MQ water.....up to 100 mL